

Wave runup on fringing
reefs with paleo-stream
channels

MSc. thesis

Annouk Rey

Delft University of Technology

No man is an island

– *John Donne, 1624*

Be like the squirrel, girl

– *Little Acorns, The White Stripes, 2003*

Cover image:

From my personal art collection, chosen because I associate it with the beauty of patterns in nature, refracting waves, coral reef structures and memories to a wonderful time in Santa Cruz.

Wave runup on fringing reefs with paleo-stream channels

by

Annouk Elise Rey

In partial fulfilment of the requirements for the degree of

Master of Science
in Civil Engineering

at Delft University of Technology,
to be defended publicly on Friday August 30th, 2019 at 16:30.

Thesis committee:

Prof.dr.ir. A.J.H.M Reniers	TU Delft (chair)
Dr.ir. A.R. van Dongeren	Deltares
Dr. C.D. Storlazzi	U.S. Geological Survey, Santa Cruz CA
Dr.ir. M.A de Schipper	TU Delft
Dr. M.F.S. Tissier	TU Delft

An electronic version of this thesis is available at <http://repository.tudelft.nl/>

Abstract

Many tropical coastlines are fronted by coral reefs and are increasingly exposed to wave attack and wave-driven marine flooding. This problem demands immediate attention as safe habitability of and social and economic activity in reef-lined coastal regions are under serious threat, while these regions are known to have some of the world's highest population densities.

High runup events and flooding on coral reef-lined coasts have been subject of recent studies, and some valuable insights are gained. It was found that the recent increases in wave attack, high runup events, and coastal flooding are primarily due to high offshore water levels coinciding with high energy swell events, circumstances which will become more frequent with sea-level rise. Increasing water depth over the reef changes the hydrodynamics across the reef in such a way that larger incident-band and infra gravity-band waves reach the shoreline, causing high runup levels and flooding of the land behind the shoreline.

However, little is known about the influence of longshore variations on runup and flooding of reef-lined coasts, while most show significant longshore variations, of which shore-normal paleo-stream channels are a prevalent one. This study aims to fill in that knowledge gap by examining the influence of paleo-stream channels on runup along reef-fronted shorelines, specifically during extreme wave conditions.

With a system analysis we determine the range of naturally occurring topographies of reef-channel systems and determine a representative reef. Results of this analysis are a useful starting point for future studies on this subject.

With a parametric study using the numeric model XBeach, we show that the presence of a channel results in a strong circulation on the reef flat and significant longshore variation of runup. Depending on the geometry and forcing, runup levels are increased next to the channel or inside the channel. This impact of the channel increases for higher incident waves, lower incident wave steepness, wider channels, a narrower reef and shorter channel spacing. Longshore variation of infragravity wave height is responsible for large scale variations in runup, while setup, short waves and very low frequency wave heights cause a local increase of runup inside the channel.

Results of the parametric study are valuable as they provide insight in which locations on a coast are most vulnerable to high runup events, using only widely available data such as reef geometry and offshore wave conditions. This is relevant for prediction of coastal hazards and to guide coastal management policies. Furthermore, this study provides insights for future studies on flood risk of reef-lined coasts, as it illustrates the importance of accounting for longshore variations while schematizing a coastline to predict high runup and coastal flooding, for instance to assess when a 1D schematization is sufficient and when a 2D model is required.

Preface

This report is the result of my thesis research, the last step to completing my Master of Civil Engineering, which will earn me a diploma from the Delft University of Technology and, more importantly, the right to say “Trust me, I’m an engineer.”.

I initially planned to finish my thesis research within a modest nine months, but unfortunately life got in the way in the form of a concussion and those nine months turned into several years. And so it turned out that this thesis research was not just about learning a lot about waves, coral reefs and academic skills, but many life lessons along the way. I am very grateful for the ability of the human body to recover, and for my own persistence which enabled me to finally graduate and look forward to the bright future ahead of me.

As the wise John Donne (and later on Hugh Grant in *About a Boy*) already knew, no man is an island, and I have no doubt that I wouldn’t have made it to this point without the help and support of many.

First, I’d like to thank my thesis committee, starting with my daily supervisor Ap for offering me this interesting research subject, being patient with me and loyal to me when I had to take a break and start over, which meant the world to me. I also really appreciated your guidance during our countless meetings. I’d like to thank Curt for our many Skype sessions and welcoming me to the USGS office at Santa Cruz, sharing your vast knowledge of reefs, keeping me focused on the bigger picture of my research, and for being such a fun and inspiring person to talk to. I’d like to thank Ad Reniers for being the chair of my committee, making time in a busy schedule to talk about my progress, encouraging me to dig deeper into the physical processes. I’d also like to thank Matthieu and Marion for reading my draft chapters, giving many helpful suggestions, a lot practical tips on scientific research, and motivating me to elevate the level of my work with your positive style of giving feedback.

My gratitude goes out to Deltares for hosting me at their office, and all the people I could go to for help and advice on modeling: Robert, Kees, my predecessors Ellen, Matthijs and Stuart for being a great example, and my fellow students. I enjoyed sharing in all the knowledge Deltares has in house, the good atmosphere, and the many fun and insightful discussions at the coffee machine.

I want to thank the USGS for financing my research and offering me the chance to work on my thesis at their office in Santa Cruz, California. I spent three very special months there which I will always remember. My thanks go to Edwin Elias and his family for welcoming me and making the transition to a new country easier. To all the wonderful people I met in Santa Cruz who made me feel at home: Jerry and Claire, Karie, Sieta and Alex, thanks for taking me to the Redwoods, Halloween, whale watching, surfing, listening to coyotes and looking at the stars.

I’d like to thank my parents and family for supporting me, loving me and believing in me when I wasn’t so sure myself, my roommates for being understanding every time I didn’t clean the house when I was exhausted after studying, and my friends, especially Naomi, my Burgerlijke Kuikens and De Bloedende Vinger for support, distraction, and the occasional surprise helium balloon.

Lastly, this thesis was partially enabled by Google, Mathworks, my bike and coffee.

*Annouk Rey
Rotterdam, August 2019*

Content

—	Abstract	iv
—	Preface	v
—	Content	vi
1	Introduction	1
1.1	Introduction.....	1
1.2	Motivation	1
1.3	Goal.....	4
1.4	Research questions	4
1.5	Scope	4
1.6	Thesis outline	4
2	Literature review	5
2.1	Introduction.....	5
2.2	Introduction of relevant processes to runup and circulations on reef-lined coasts	5
2.3	Cross shore processes of reef-lined coasts.....	6
2.4	2D effects on reefs	14
3	System analysis	17
3.1	Introduction.....	17
3.2	Terminology.....	17
3.3	Oceanic forcing	18
3.4	Reef geometry.....	19
3.5	Conclusion: representative reef and forcing	21
4	Model Setup.....	24
4.1	Introduction.....	24
4.2	The XBeach model.....	24
4.3	Modeling approach.....	25
4.4	Model settings	25
4.5	Conclusion and discussion of model setup.....	31
5	Model results.....	34
5.1	Introduction.....	34
5.2	Runup results for one single simulation	34
5.3	Hydrodynamics on reef flat for one single simulation	38
5.4	Impact of different forcings and reef geometries on runup pattern	43

5.5	Contributions of frequency components to runup pattern	54
6	Discussion	61
6.1	introduction	61
6.2	implications of model schematizations	61
6.3	Research significance.....	62
7	Conclusions	64
8	Recommendations	66
—	References	68
APPENDIX A.	DIMENSIONS OF STUDIED FRINGING REEF SECTIONS WITH A CHANNEL.....	76
APPENDIX B.	EXAMPLE XBEACH INPUT FILE	78
APPENDIX C.	STATISTICAL RUNUP VALUES COMPLEMENTARY TO $RU_{2\%}$.....	82
APPENDIX D.	RUNUP PATTERNS, ORGANIZED BY GEOMETRY	84
APPENDIX E.	RUNUP PATTERNS, ORGANIZED BY FORCING	90
APPENDIX F.	CONTRIBUTIONS OF FREQUENCY COMPONENTS TO RUNUP, OVERVIEW PER GEOMETRY .	93
APPENDIX G.	CONCEPTUAL FIGURES OF THE IMPACT OF INPUT PARAMETERS TO FREQUENCY COMPONENTS OF RUNUP	104
APPENDIX H.	RUNUP SCATTERPLOTS.....	109

1

Introduction

1.1 INTRODUCTION

Many tropical coastlines are fronted by coral reefs and are increasingly exposed to wave attack and wave-driven marine flooding. This problem demands immediate attention as safe habitability of and social and economic activity in reef-lined coastal regions are under serious threat.

High runup events and flooding on coral reef-lined coasts have been subject of research for several years now. However, little is known about the influence of longshore variations on runup and flooding of these coastlines, specifically in the presence of shore-normal channels that typify most fringing reefs. This study aims to fill in that knowledge gap.

This chapter introduces the subject of runup on coral reef-lined coasts characterized by shore-normal channels. The motivation behind this study is discussed in section 1.2. Section 1.3 presents the research goal and section 1.4 the research questions. The scope is defined in section 1.5 and finally the outline for the rest of this thesis is presented in section 1.6.

1.2 MOTIVATION

1.2.1 Context

Types of reefs

Coral reefs cover one sixth of the world's coastline (Birkeland 1997), and are an important form of coastal protection due to effective wave energy dissipation. An estimated 100 million people live in coastal areas that are more or less protected by coral reefs¹, such as coral islands or coral atolls (Ferrario et al. 2014).

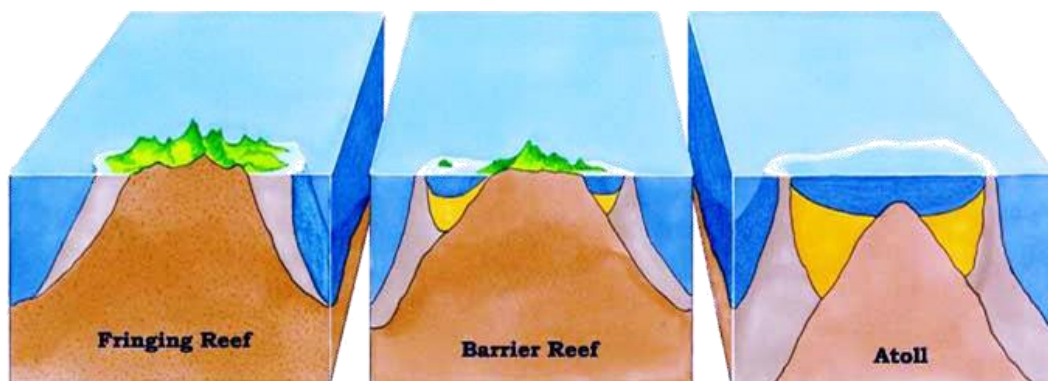


Figure 1.1, The three types of coral reefs. Source: <https://roatan.online/types-of-coral-reefs/>

¹ These coastal areas are defined by being within 10km of a shoreline that is fronted by a coral reef and having an elevation of maximum 10m above sea level.

There are three main types of coral reefs, distinguished by their morphology as first described by (Darwin 1842): fringing reefs, barrier reefs, and atoll reefs, illustrated in Figure 1.1. A fringing reef is connected to the shoreline. A barrier reef is detached from the shoreline and can enclose a lagoon. An atoll reef is a ring-shaped reef, typically containing a large number of islets, enclosing a lagoon. On the time scale of millions of years, fringing reefs may transform into barrier reefs and atoll reefs as a consequence of relative subsidence of the island and growth of the coral (Fairbridge 1975). When looking at an individual islet on an atoll, the reef resembles a fringing reef again. Fringing reefs are the most common type of reef, covering more than 50% of the global reef area (Hopley 2011). Furthermore, from a coastal management perspective, fringing reefs are most relevant due to their direct connection to the shoreline.

Protection by reefs

Fringing and atoll reefs serve as a natural coastal protection as a large part of wave energy is dissipated before reaching the shoreline. Depending on the reef geometry, reported values of wave attenuation vary from 60% up to 99% (Blacka et al. 2015; Ferrario et al. 2014).

Vulnerability of reef-lined coasts

This protection by coral reefs is important, because the consequences of flooding of land behind coral reefs are significant. Most population centers along reef-lined coasts are vulnerable due to their low elevation above sea level (Storlazzi, Elias, and Berkowitz 2015). Even population centers on larger (volcanic) islands are vulnerable: high islands with fringing reefs, such as Hawaii, Fiji and (American) Samoa and Guam, generally have the highest populations of islands in the Pacific (United Nation Population Fund 2014; “Hawaii Population. (2018-01-24).” n.d.), and the presence of steep mountains forces the majority of population and economic activity to be concentrated on a narrow strip straight behind the coastline.

More than 50% of the total population of Pacific islands lives within 1.5km of the shore (Mimura et al. 2007). This translates to high population densities, sometimes even exceeding those of Hong Kong and Singapore (Haberkorn 2008). Furthermore, nearly all airports, main roads and capital cities are situated along the coast. Locations where the reef is bisected by a channel are especially attractive for population centers, as channels provide a natural harbor, serve as easy access to deeper water for vessels, and drinking water supply through streams. Due to these favorable properties, population centers are often located adjacent to channels. For example, on on Molokai, Hawaii, the deeper channel is used to construct a harbor, and a town is located adjacent to the channel. Figure 1.2 shows examples of densely populated areas behind fringing reefs on Hawaii and Rarotonga.



Figure 1.2, High population densities near the shoreline of coasts protected by coral reefs. Oahu, Hawaii (a.) clearly shows the housing limitations due to steep mountains. Molokai, Hawaii (b.) shows a harbor in the channel, and a town behind it. Rarotonga, Cook islands (c.) shows a reef with two channels, a densely populated strip close to the shoreline, and an airport straight behind the shoreline. Source: Google Earth

Even with the protective capacity of fringing and atoll reefs, high runup levels at the shoreline and flooding are a serious risk during large swells and high offshore water levels. Flooding has occurred in the past (Hoeke et al. 2013; Quataert et al. 2015; Bosserelle et al. 2015) and will become more frequent with sea-level rise (Storlazzi et al. 2018).

1.2.2 Knowledge gaps

It is of vital importance to understand wave hydrodynamics and runup on coral reefs in order to better predict flooding.

Research is ongoing on this subject in order to understand which hydrodynamic processes lead to these high runup levels, and some valuable insights are gained about this (Quataert et al. 2015; Pearson 2016): the recent increases in wave attack, high runup events, and coastal flooding are primarily due to high offshore water levels coinciding with high energy swell events (Hoeke et al. 2013), circumstances which will become more frequent with sea-level rise (Storlazzi, Elias, and Berkowitz 2015). Increasing water depth over the reef changes the hydrodynamics across the reef in such a way that larger incident-band and infra gravity-band waves reach the shoreline, causing high runup levels and flooding of the land behind the shoreline (Quataert et al. 2015; Pearson 2016). More details on previous findings are presented in Chapter 2.

However, most previous research on runup has been based on 1D schematization, representing a uniform and straight coastline, whereas most reefs show significant variability of the bathymetry in longshore direction. Many fringing reefs are intersected by paleo-stream channels. A paleo-stream channel is the remnant of a river that was flowing down a mountain in a previous geological time. Due to relative land subsidence, the river drowned and results in a deeper part of the ocean, visible as an interruption of the coral reef. Due to their origin, paleo-stream channels are generally found on island with steep mountain gradients. Examples of reef sections with paleo-stream channels are presented in Figure 1.3.



Figure 1.3, Examples of paleo-stream channels bisecting coral reefs. Source: Google Earth.

It is expected that 2D variations on coral reef morphology lead to mean currents and circulations. These may, in turn, affect nutrient transport (Falter et al. 2004; Hench and Rosman 2013) and hence coral development. Furthermore, mean currents and processes such as diffraction and refraction change the directional wave spectrum and can affect wave-driven runup. Previous studies that have investigated alongshore variations in reefs, e.g. (Lowe et al. 2008; Gourlay 1996a; Taebi et al. 2011), usually addressed barrier reef-lagoon systems rather than fringing reefs, and focused on setup differences and flushing times rather than the response at the shoreline. Previous studies are further discussed in the next chapter.

To the best of our knowledge, no studies have been performed on the influence of paleo-stream channels on runup on fringing reef coasts, specifically during extreme wave conditions when the risk for coastal flooding and the resulting impact to coastal communities is greatest.

It is important to fill in this knowledge gap, because insights in which locations on a coast are most vulnerable to high runup events are relevant for prediction of coastal hazards and to guide coastal management policies. Next to that, the relative influence of 2D variations such as paleo-stream channels needs to be estimated in order to determine the level of detail required in field measurements and modeling studies investigating coastal hazards along coral reef-lined shorelines.

1.3 GOAL

This study will examine the influence of paleo-stream channels on runup along reef-fronted shorelines, specifically during extreme wave conditions.

1.4 RESEARCH QUESTIONS

To achieve the research goal, research questions are formulated. There is one main question, which requires the answers to several sub questions. The questions and aimed research output needed to answer the question are presented in Table 1.1.

Research question	Research output to answer question
Main question: How is runup on fringing reefs affected by paleo-stream channels?	Conclusions from analyzing numerical model results: runup patterns, contributions of frequency components to runup, and reef hydrodynamics for various forcings and reef geometry. Chapter 5
Sub question: What is the best way to schematize a reef-channel-system?	Basic reef- and channel geometry and range of variations, based on satellite image based inventory of reef-channel systems and literature. Chapter 3
Sub question: Can a conceptual model be used to understand runup on reef-channel systems	Validated numerical model with realistic runtime after model setup. Chapter 4

Table 1.1, Research questions

1.5 SCOPE

It is important to gain insight in the region of applicability of the results of the present study. Also, as this research is part of ongoing research concerning both prediction of hazards along reef-lined coastlines and ecosystem studies, it is important to distinguish which topics are part of the present study and which are not. Next to that, some processes are excluded and assumptions are made to make the research executable within a master thesis time frame. To this end, a scope is formulated.

- Type of coast: The coastline studied in the present research is representative for tropical coastlines fronted by fringing reefs characterized by paleo-stream channels, the majority of which is found in the Pacific Ocean.
- Type of 2D variations: Although a wide range of variations in bathymetry and topography occur naturally on reefs, this study will focus on paleo-stream channels. Other variations such as shoreline curvature, a longshore varying reef width and, on a smaller scale, spur and groove formations are not considered.
- Type of forcing: Waves are the only type of forcing considered. Other types of forcing such as tidal currents, wind setup, and Coriolis force are excluded from this research. Concerning the type of waves, only extreme wave conditions are considered, as the primary interest of this research are high runup events. The influence of different offshore still water levels (SWL) is not considered.
- Excluded processes: Sediment transport, morphological changes, changes in state of the coral and nutrient transport are not considered in the present study.

1.6 THESIS OUTLINE

This study can be divided into two parts, a research background study and a parametrical study using numerical simulations. The research background study covers a literature review in Chapter 2 and a system analysis to determine a representative reef-channel system in Chapter 3. The numerical modeling is discussed in Chapter 4, Model Setup, and Chapter 5, Model Results. Discussion, conclusions and recommendations are presented in Chapters 6, 7 and 8. Several appendices are included at the end of this thesis, which are referred to from the concerning chapters.

2

Literature review

2.1 INTRODUCTION

This chapter analyzes the fringing reef – paleo-stream channel system with a literature study. First, the processes relevant to runup and circulations on reef-lined coasts are introduced in section 2.2. Second, cross shore processes relevant to runup on reefs are discussed in section 2.3, ordered from offshore towards onshore. Most of past research on this subject focused on 1D schematizations. Third, 2D processes on reefs are discussed in section 2.4.

2.2 INTRODUCTION OF RELEVANT PROCESSES TO RUNUP AND CIRCULATIONS ON REEF-LINED COASTS

As waves travel from offshore towards the shoreline, they pass the fore reef and reef flat and consequently reach the beach slope and shoreline. Per location, different processes affect the waves. From offshore towards the fore reef, waves shoal until depth induced breaking occurs, resulting in a wave setup, and lower frequency harmonics are generated. On the reef flat, the wave spectrum deforms further, with dissipation of mainly the higher frequencies of incoming waves, and sometimes amplification of the lower frequencies (Cheriton, Storlazzi, and Rosenberger 2016; Pomeroy, Lowe, et al. 2012). Figure 2.1 presents the relevant cross shore wave processes on reefs, which have been studied in 1D schematizations, e.g. Quataert et al. (2015). Due to the presence of the channel, a flow circulation occurs with net onshore flow over the reef flat and a return current through the channel, and refraction and diffraction occur. At the shoreline, the remaining waves lead to runup. In the following sections, these processes are discussed in further detail. Figure 2.2 shows the 2D processes that are relevant to reef-channel systems in the present study, in addition to the 1D hydrodynamics.

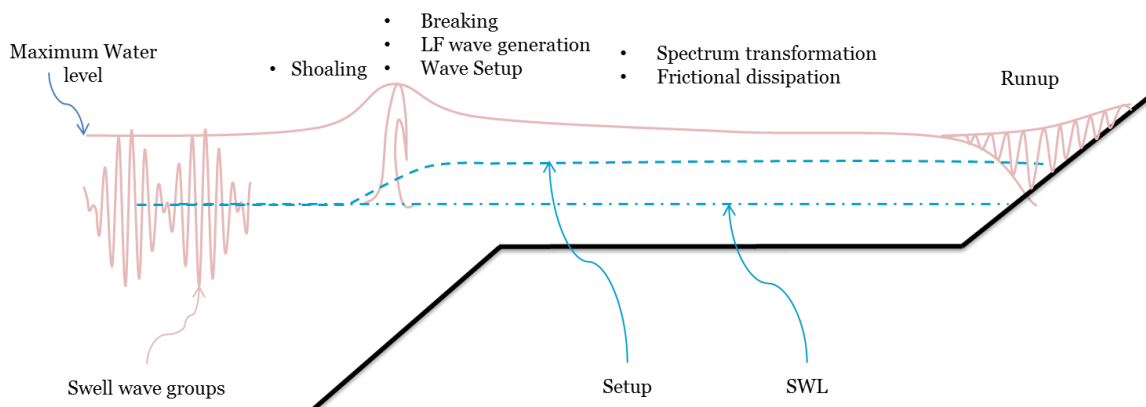


Figure 2.1, Cross shore wave processes on a reef flat, shoaling, wave breaking, setup, long wave generation, spectrum transformation, frictional dissipation and runup

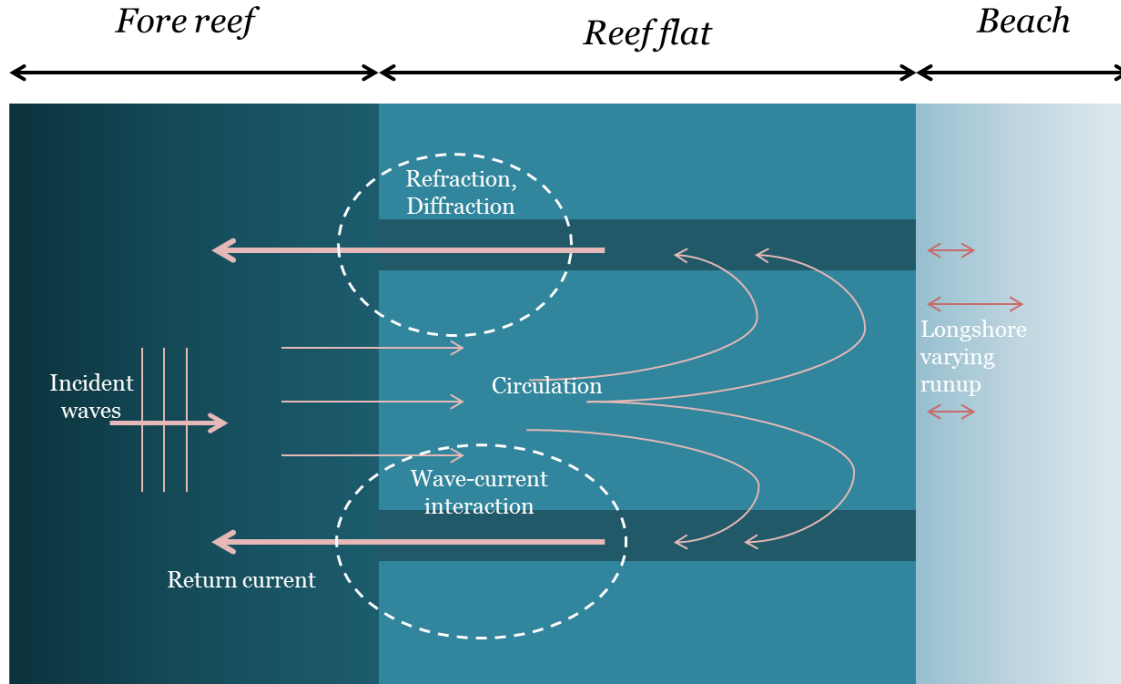


Figure 2.2, Top view of wave and current processes on a reef-channel system, such as reef circulation, refraction, diffraction, a return current in the channel, wave current interaction, and a longshore varying runup. This figure excludes processes that might be relevant for 2D variations but that are outside the scope of the present study, such as shoreline curvature, oblique incidence and directional spreading of waves.

2.3 CROSS SHORE PROCESSES OF REEF-LINED COASTS

2.3.1 Shoaling

As the water depth decreases on the steep fore reef, waves slow down while keeping their energy. This results in an increase of the wave height known as shoaling. The difference in wave amplitude scales with the square root of the ratio in wave group celerities (Eq. 2.1):

$$a_2 = \sqrt{\frac{c_{g,1}}{c_{g,2}}} a_1 \quad \text{Eq. 2.1}$$

In which a_n denotes the wave amplitudes and $c_{g,n}$ denotes the wave group celerity, computed from the wave number k and depth h as in Eq. 2.2 and Eq. 2.3.

$$c_g = \left(\frac{1}{2} \left(1 + \frac{2kh}{\sinh(2kh)} \right) \right) * c \quad \text{Eq. 2.2}$$

$$c = \sqrt{\frac{g}{k} \tanh(kh)} \quad \text{Eq. 2.3}$$

Higher wave harmonics are generated in the shoaling process, steepening the wave peaks and flattening the wave troughs (Eldeberky 1996; Young 1989). Without dissipation, shoaling theoretically leads to an infinitely high wave height, but in reality wave breaking limits the wave height.

2.3.2 Breaking

Wave breaking is an important mechanism for dissipation of wave energy. On sandy beaches, it usually is the dominant energy dissipation mechanism, while on fringing reefs either bottom friction or wave breaking can be dominant, depending on geometry and bottom roughness. On

the steep fore reef however, wave breaking is always dominant. Breaking can be either wave steepness induced, or depth induced. Steepness induced breaking occurs when a wave becomes too steep to be stable and usually occurs on deep water. For swell waves on fore reefs, steepness induced breaking does not occur, and breaking is depth induced. In shallow water, the breaker limit γ is used to relate the wave height at which breaking occurs to the water depth following Eq. 2.4:

$$\gamma = \frac{H}{h} \quad \text{Eq. 2.4}$$

Solitary wave theory dictates a breaker index of $\gamma = 0.78$ (Longuet-Higgins 1974). However, for irregular waves on a sloping bed, the breaker index varies over a wider range.

On a mild slope such as found on sandy beaches, $\gamma = 0.55$ usually is applied, but this breaker limit is generally much higher on fringing reefs due to the steep fore reef and rapid shoaling, with reported γ values even exceeding the solitary wave limit. Vetter et al. (2010) reported values found on a fringing reef varying between 0.9 and 1.1, using H_b , the wave height at breaking, increasing with incident wave height. Furthermore, the breaking limit was found to be dependent on the slope (Young 1989) by being higher for higher slopes. Blacka et al. (2015) supports this using physical wave flume modeling, stating waves at steep reef faces remain unbroken until they are very close to the reef crest, then shoal rapidly and break over a short distance across the reef crest, resulting in $\gamma = 0.8$.

The depth dependence of wave breaking is most distinct for saturated conditions, when all waves break (Costa et al. 2016). The use of h in formulation of γ indicates wave breaking is both modulated by tidal elevation as by a varying wave height within a wave group. As the wave height varies over a wave group, the breakpoint moves between deeper and shallower locations within a wave group, known as breakpoint excursion (Symonds, Huntley, and Bowen 1982). For longshore non-uniform forcing or geometries, the breakpoint varies over the longshore as well, causing 2D effects.

Summarizing wave breaking on reefs, energy dissipation by breaking on reefs is mostly dependent on the relative submergence $\gamma = H/h$ and fore reef slope, indicating that for higher water levels and steep fore reefs a larger percentage of incident wave energy protrudes over the reef flat.

2.3.3 Setup

Setup is the mean elevation of the water level compared to still water level (SWL), and influences the water depth on the reef, and therefore affects wave propagation and dissipation, and resonant time scale on the reef. Furthermore, currents can result from water level gradients due to longshore non-uniform setup. Therefore, it is important to understand setup on reefs. There are three sources of setup: wind, barometric, and wave setup.

Wind setup

Wind setup on fringing reefs is usually negligible due to the very narrow continental shelf of most reef coasts: large water depths are reached near the shore (Shimozono et al. 2015; Smithers and Hoeke 2014; Damlamian et al. 2015). However, wind setup might play a role on reefs in an embayment, where the water depth is limited and the wind pushes the water into the bay (Tajima, Gunasekara, et al. 2016). Furthermore, Lentz et al. (2016) found that for platform reefs in the Red Sea, wind was an important driver of longshore current while cross shore current was dominated by wave setup. Demirbilek, Nwogu, and Ward (2007) performed a laboratory study in which the effect of wind setup, wave setup, and a combination was studied. It was found that the setup over

the reef is enhanced under combined wind-wave conditions as compared to a linear superposition of wind-only and wave-only setup, presumably due to increased roughness of the sea surface caused by waves. In cases where wind setup is not negligible, it should be accounted for combined with wave setup, not as an isolated elevation in water level.

Barometric setup

Barometric setup is a result of low atmospheric pressures, caused by tropical storms and cyclones. Usually, the swell waves most important for flooding of fringing reefs are found outside of the region of influence of barometric setup (Smithers and Hoeke 2014).

Wave setup

Wave setup is the most important source of setup on fringing reefs. Wave setup on reefs was first described during a field and desktop study by Munk and Sargent (1948), who found a wave setup of 45 cm at Bikini Atoll. Since then, it has been studied extensively (i.e. Tait 1972; Seelig 1983; Gourlay 1996a; Gourlay and Colleter 2005; Vetter et al. 2010; Becker, Merrifield, and Ford 2014). Wave setup is caused by the cross shore gradient in radiation stress caused by breaking waves on the fore reef, which is compensated by a water level gradient (Longuet-Higgins and Stewart 1962; Symonds, Huntley, and Bowen 1982). This setup is dependent on incoming wave height, and found to be 10% to 20% of it, e.g. (Tait 1972; Gourlay 1996a; Hearn 1999). Furthermore, increasing the still water depth over the reef decreases setup until the water depth becomes so large that waves cease to break at the fore reef. Gourlay (1996a) observed a minimum threshold value of $H_i / h_{reef} = 0.4$, in which H_i is the incident wave height, or, accounting for shoaling, $H_{reef} / h_{reef} = 0.55$, for setup to occur. This depth dependence of setup implies it decreases with higher tidal elevation and sea level rise, as described by (Becker, Merrifield, and Ford 2014). In 1D schematizations without mean currents, the wave setup is often regarded as constant between the landward end of the surf zone and shoreline. However, (Jago, Kench, and Brander 2007) used field measurements under moderate wave conditions on a fringing reef at Lady Elliot Island to show that the cross shore location of maximum setup varies with sea level elevation. At low tide the highest setup is found at the reef edge, while at medium tide a dual setup system occurs at both reef edge and shoreline, and at high tide the dominant setup is found at the shoreline.

Throughout the years, various expressions to estimate wave setup have been presented.

Tait (1972) applied the theory for setup on plane beaches to the Bikini Atoll observations of Munk and Sargent (1948), and suggested the following formula Eq. 2.5 to estimate setup:

$$\bar{\eta}_r = \frac{\gamma^2 h_b}{16} + \left[\frac{1}{1 + 8/3\gamma^2} \right] (h_b - h_r) \quad \text{Eq. 2.5}$$

In which $\bar{\eta}_r$ is the setup on the reef, h_b is the still water depth at the point of breaking, and h_r is the still water depth on the reef flat, H_b is the breaker height and $\gamma = H_b / h_b$. From this relationship, maximum setup is found for $h_r = 0$, indicating an offshore mean water level equal to the reef flat level, and setup reduces to zero when the waves cease to break on the reef. The reef face slope is implicit in this relation through the parameter γ , which depends on the slope. Based on the conservative assumption that waves lose all their momentum while breaking on a very steep reef face, Eq. 2.5 reduces to the simpler expression Eq. 2.6:

$$\bar{\eta}_r = \frac{3}{16} \gamma H_i \quad \text{Eq. 2.6}$$

Gourlay (1996a, 1996b) performed a laboratory experiment of an idealized reef under regular wave forcing and compared it with various field data and states the setup is a relation between two dimensionless parameters as in Eq. 2.7 and Eq. 2.8:

$$\text{Relative setup: } \bar{\eta}_r / T \sqrt{gH_o} \quad \text{Eq. 2.7}$$

$$\text{Submergence: } (\bar{\eta}_r + h_r) / H_o \quad \text{Eq. 2.8}$$

Using a combination of energy and momentum concepts an implicit formula (Eq. 2.9) to calculate wave setup for idealized reefs was derived:

$$\frac{\bar{\eta}_r}{T \sqrt{gH_o}} = \frac{3}{64\pi} K_p \left[1 - K_R^2 - 4\pi\gamma^2 \cdot \left(\frac{\bar{\eta}_r + h_r}{H_o} \right)^2 \cdot \frac{1}{T} \sqrt{\frac{\bar{\eta}_r + h_r}{g}} \right] \times \left(\frac{H_o}{\bar{\eta}_r + h_r} \right)^{3/2} \quad \text{Eq. 2.9}$$

In which K_p is the reef profile factor, accounting for the various dissipation mechanisms over the reef profile and K_R is a wave reflection factor.

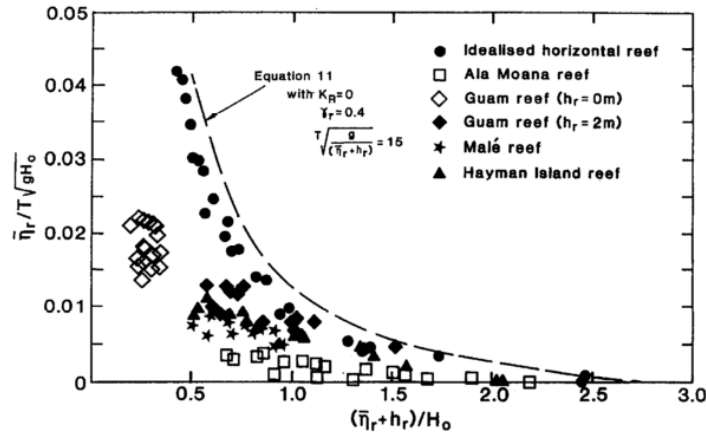


Figure 2.3, Relative setup as a function of reef submergence, Source: (Gourlay 1996b)

For natural reefs, setup is usually slightly lower than for the idealized situation this formula was based upon. Moreover, when water is able to escape on the leeward side of the reef edge (platform reef) or laterally, in the case of channels, setup is reduced further by an amount at least equal to the velocity head of the wave-generated flow across the reef, $U^2/2g$. This reduction in setup was confirmed by Gourlay and Colleter (2005).

The difference between monochromatic versus irregular waves which are more likely to occur in nature was described by Seelig and Asce (1983): random waves of a given offshore significant wave height and period produce lower setup compared to monochromatic waves of the same wave height and period, which can be explained as an irregular wave group contains less energy than a monochromatic wave field of the same wave height.

Summarizing setup on reefs: wave setup is the dominant source of setup on reefs. Setup is found to be increasing for increasing incident wave height and period, and decreasing for increasing reef submergence, largest for smooth, steep reef faces and situations without reflection. For longshore non-uniform coasts setup is generally lower than for an idealized 1D situation.

2.3.4 Long wave generation

After breaking on the fore reef, waves propagate shoreward over the reef flat. Here, the wave spectrum changes shape: longer waves are generated and energy is dissipated by bottom friction.

In the hydrodynamics on coral reefs, the wave spectrum can be divided into different components: incident short waves and low frequency (LF) waves, which can be subdivided into infra gravity (IG) and very low frequency (VLF) waves. The frequency bands as determined by Quataert et al. (2015) are used, defined as in Table 2.1.

Short waves	Low frequency (LF) waves	
Sea swell (SS) 0.04-0.2 Hz	Infra Gravity (IG) 0.004-0.04 Hz	Very Low Frequency (VLF) 0.001-0.004 Hz

Table 2.1, Definition of different wave components of the wave spectrum.

Multiple studies have confirmed the importance of low frequency waves on water levels and runup on fringing reefs, e.g. recent field studies by Cheriton, Storlazzi, and Rosenberger 2016; Pomeroy, Lowe, et al. (2012); Péquignet, Becker, and Merrifield (2014). Both IG and VLF waves contribute to a slow time-varying water elevation near the shoreline, known as surf beat. There are two main generation mechanisms for these long waves.

The first generation mechanism is the shoaling of wave groups creating a bound long wave with a wave length on the wave group scale (Foda and Mei 1981; Schaffer and Svendsen 1988). These bound long waves can be released during the breaking process of the short waves in the surf zone. If that happens a free long wave occurs (Battjes et al. 2004).

The second generation mechanism of long waves is breakpoint forcing. The varying wave height within a wave group causes the waves to break at different depths and thus cross shore locations. This oscillating breakpoint excursion generates long waves (Symonds, Huntley, and Bowen 1982). This mechanism is more efficient when the breakpoint excursion is small, as it assumes a nodal structure of the standing wave pattern, which requires a breakpoint excursion smaller than the distance between a node and anti-node of a free standing wave with the frequency of the generated long wave f_{LF} (Baldock and Huntley 2002). Baldock (2012) developed the surf beat similarity parameter $\xi_{SURFBEAT}$ based on the normalized bed slope parameter β (Battjes et al. 2004) and the square root of the short wave steepness. This parameter allows fast assessment of the type of long wave generation.

Because of the steep fore reef slope and hence relatively small breakpoint excursions, the breakpoint mechanism is likely to occur at coral reefs. Indeed, it was found that breakpoint forcing is the dominant generation mechanism of long waves at Ningaloo reef Australia (Pomeroy, Lowe, et al. 2012) and Roi-Namur (Gawehn 2015).

For both generation mechanisms, the groupiness of the incident waves is important. As remotely generated swell waves have a narrower spectrum than locally generated sea state waves, the groupiness is stronger and hence swell waves are more efficient in generating LF waves on reefs.

2.3.5 Wave transformation along the reef flat

The development of the various spectrum components from the reef crest towards the shoreline is found to depend on the reef geometry, offshore forcing and water level. Processes such as frictional dissipation, wave amplification, and resonance play a role.

Dissipation

Waves continue breaking on the reef flat for some distance, until sufficient energy is dissipated and the waves reach a stable height for $\gamma < 0.55$. Blacka et al. (2015) states the extent of the surf zone is less than one quarter of the deep water wave length, in line with findings of Nwogu and

Demirbilek (2010). Furthermore, bottom friction occurs. Short waves are found to decay towards the shoreline, but this dissipation is strongly dependent on water depth on the reef flat (Péquignet et al. 2011). Larger depths reduce the dissipation, allowing more short wave energy to reach the shoreline. Dissipation of the long wave energy occurs at a much lower rate than short waves.

Van Dongeren et al. (2013) and Quataert et al. (2015) used the XBeach model to reproduce and investigate the hydrodynamics across the Ningaloo Reef and Roi-Namur. Van Dongeren et al. (2013) found that the IG wave heights vary for different water depths at the reef due to differences in rates of friction-related IG wave damping. Quataert et al. (2015) concluded that both the geometrical parameters as well as friction on the flat reef are important for the wave hydrodynamics and that sea level rise will increase the amplification of LF waves further. The differences between the hydrodynamics on the different reefs are mainly attributed to differences in frictional dissipation (Péquignet et al. 2011). For all studies the influence of LF waves is growing in onshore direction and dominant at the shoreline.

Resonance

A fringing reef can be schematized as a half open basin, of which the fundamental resonant period T_{res} is given as in Eq. 2.10:

$$T_{res} = \frac{4L}{\sqrt{gh}} \quad \text{Eq. 2.10}$$

In which L is the width of the reef flat, and h is the water depth on the reef flat, including setup. Under normal circumstances, the resonant period does not coincide with incident or IG wave time scales. However, under high and long swell waves, resonance may occur. This was the case at Guam, where Péquignet et al. (2009) found a standing wave character. Under moderate wave conditions, the infra gravity wave heights slightly decayed towards the shoreline. However, during high energy swell conditions the water level on the reef increased significantly causing the eigen frequency of the reef to decrease with a factor two, enabling resonance on the reef flat and increasing wave heights towards the shoreline. Gawehn et al. (2016) and Cheriton, Storlazzi, and Rosenberger (2016) also found resonance and cross-reef standing waves at Roi-Namur, with amplification of infra gravity and very low frequency waves towards the shoreline, indicating resonant behavior under extreme wave conditions.

Summarizing wave transformation on reefs, different frequency components show different rates of dissipation along the reef flat, depending on reef geometry and water level. The wave spectrum deforms, with increasing relative importance of LF waves shoreward. At the inner reef flat, LF waves are dominant in most cases. Under high energy wave conditions, resonance may occur.

2.3.6 Runup

Runup is an important parameter used to describe the water levels at the shoreline. It is generally used in coastal studies to describe or estimate extreme water levels and in predicting coastal inundation. Runup is defined by Holman (1986) as the vertical excursion of the water level at the shoreline relative to the still water level. For engineering applications usually high runup levels are more of interest than lower ones, and the runup level that is exceeded by 2% of the waves is commonly used to describe runup, known as $Ru_{2\%}$.

Most past research on runup concerned sandy beaches or man-made structures such as dikes and breakwaters (Van Gent 2001). Runup on coral reefs has only been subject of research for a few years (Quataert et al. 2015; Pearson 2016). Furthermore, most runup studies concerned 1D schematizations rather than more realistic longshore non-uniform situations.

Runup components

Runup can be divided into two components (Holman 1986): the time-averaged setup at the waterline, and a time-varying water level variation of this mean setup, called swash. Like the wave spectrum, swash is divided into short waves (S_{inc} , incident swash) and LF waves (S_{LF} , IG swash) frequency bands. Stockdon et al. (2006) quantified runup as the sum of these components as presented in Eq. 2.11 and Figure 2.4:

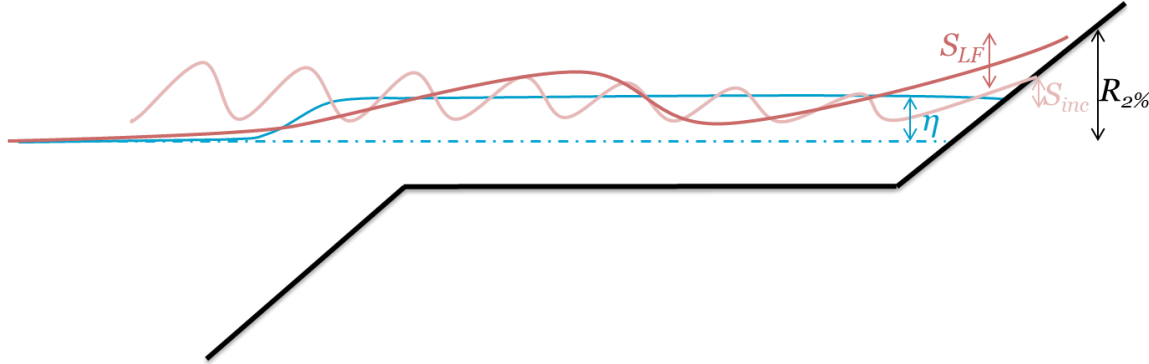


Figure 2.4, Runup decomposed into components. The total runup is a combination of setup and incident and LF swash at the waterline. Picture after Pearson (2016).

$$Ru_{2\%} = \eta + \frac{1}{2} \sqrt{S_{inc}^2 + S_{LF}^2} \quad \text{Eq. 2.11}$$

Runup dependence

Hunt (1959) stated runup scales linearly with the Iribarren number or surf similarity parameter ξ (Battjes 1974) which describes the relation between the steepness of the incoming waves and the slope of the structure or beach, represented by i_{beach} as in Eq. 2.12:

$$\frac{Ru_{2\%}}{H_{mo}} = \xi, \text{ with } \xi = \frac{i_{beach}}{\sqrt{H_{mo} / L_o}} \quad \text{Eq. 2.12}$$

This indicates higher runup levels for a larger relative steepness. Furthermore, runup varies with still water level, indicating a tidal modulation and changes with sea level rise (Becker, Merrifield, and Ford 2014; Beetham et al. 2016). The two components of runup show different responses (Merrifield et al. 2014). While wave setup decreases for an increasing SWL, more wave energy protrudes over the reef flat and hence the swash component increases. The combination of swash and setup responses leads to a weak increase of runup for increasing SWL. Regarding swash, IG waves were found to be the dominant contribution from field data analysis on Roi Namur (Cheriton, Storlazzi, and Rosenberger 2016) and a laboratory reef study (Nwogu and Demirebilek 2010). However, by numerical modeling of Roi Namur by Gawehn et al. (2016) and Quataert et al. (2015) it is found that incident wave energy still has a significant contribution to swash and is not negligible while determining runup. Guza and Feddersen (2012) found that on sandy beaches, the IG component of runup increases for a larger frequency spread of incident waves, but decreases for larger directional spread.

Several empirical formulations to predict runup are found in literature, developed for either sandy beaches (Stockdon et al. 2006), dikes (Van Gent 2001) and coral reefs (Blacka et al. 2015; Merrifield et al. 2014). Pearson (2016) compared runup predictions by these formulations with runup values from numerical modeling of a vast range of 1D reefs. All formulations represent runup or extreme water levels as a function of H_s (albeit defined at different locations) and L_o or T_p , supplemented with empirical constants, foreshore slope or beach. In general, Pearson (2016)

found scatter to be large between predicted runup values and modeled values for all formulations. For the formulae by Stockdon et al. (2006) and Van Gent (2001), the scatter is presumably because these formulae are not designed for reef applications. The formulae by Merrifield et al. (2014) and Blacka et al. (2015) were both derived from a limited range of geometries, and do not include any geometrical parameters in the calculation of runup, which might be the cause of the scatter observed by Pearson (2016). This indicates that reef geometry parameters may have a significant influence on runup.

Pearson et al. (2017) studied the influence of the different geometrical parameters on runup, distinguishing the contributions of setup and swash components, based on a large number of numerical simulations, presented in Figure 2.5. The results show that runup increases for increasing offshore water level and wave height and steeper beach and forereef slopes, and decreases with increasing wave steepness, roughness and reef width, which is in line with findings of Quataert et al. (2015) and Shimozono et al. (2015). The strongest dependence of runup was found to be on offshore forcing, as the above empirical relations suggest, followed by reef width and, slightly less important, forereef slope. Friction and beach slope appear to be less important.

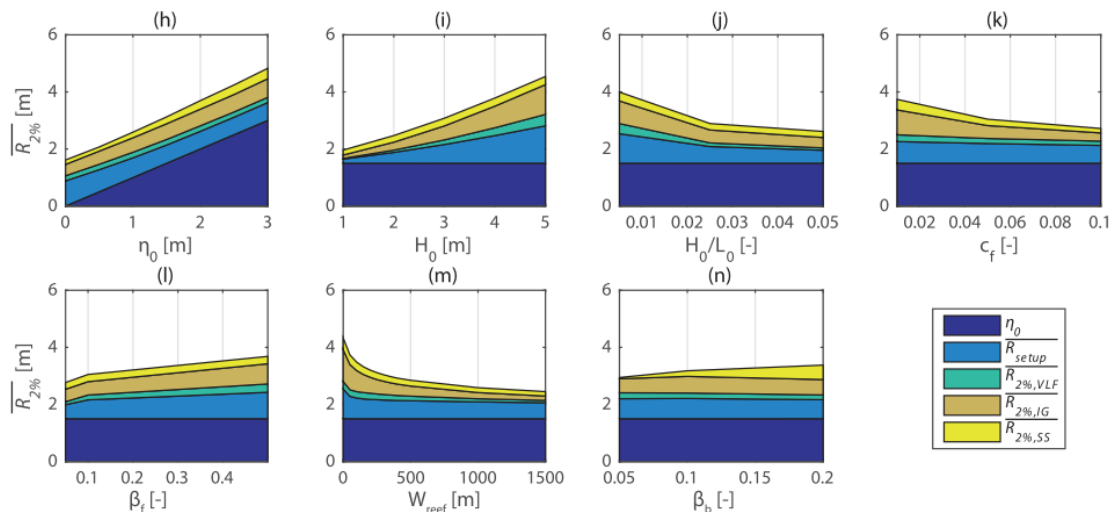


Figure 2.5, Runup results on coral reefs as a function of the parameters SWL (h), offshore wave height (i), offshore wave steepness (j), roughness (k), forereef slope (l), reef width (m), and beach slope (n). Contributions of still water level, setup, and different frequency components of swash are distinguished by color. Source: (Pearson et al. 2017)

Link to field data

The importance of offshore conditions and reef width is convenient as offshore wave and water level statistics are generally known (Storlazzi et al. 2015) and reef width is easily estimated from satellite images, while the less influential roughness and slope conditions are generally not known and more difficult to measure. Field measurements of runup data on reef lined coasts are scarce, especially during extreme conditions, but Pearson et al. (2017) found a strong correlation between extreme water levels at the inner reef flat ($\eta_{2\%}$), which are more commonly measured in the field and runup levels, with runup values $\pm 29\%$ higher than $\eta_{2\%}$.

Summarizing runup on reefs, runup depends strongly on offshore forcing (wave height and period and SWL), and reef width, while other geometrical parameters and friction are less influential.

2.4 2D EFFECTS ON REEFS

The presence of a channel bisecting a reef leads to various 2D wave and circulation processes, such as refraction, diffraction, circulation over the reef and a return current through the channel, and is therefore expected to affect runup. These processes are discussed below. First, previous studies on longshore variations of runup are discussed. Second, processes which are expected to be important to explain longshore variations of runup are discussed.

2.4.1 2D variation of runup

As most runup studies have been based on 1D schematizations, little is known about longshore variations in runup. Two studies that did mention longshore variability in the context of runup on reefs are the following:

First, Gelfenbaum et al. (2011) studied the inundation after a tsunami on the fringing reef of Tutuila, American Samoa using a Delft3D numerical model, and found the presence of a channel increased the nearshore wave height and inundation levels compared to a situation without a channel. This increase in wave height is largest just landward of the channel, and the effect of a channel was largest if the channel occurs within an embayment, which is very common in nature. While this research concerned a tsunami wave rather than the swell waves of the present study and the used numerical model did not incorporate complex wave hydrodynamics, the observed increase in inundation heights suggests a channel can locally increase runup heights.

Second, Smith, Hesser, and Smith (2012) studied hydrodynamics and runup on reefs with a laboratory study of longshore non-uniform reefs. They stress the dominance of LF waves towards the inner reef flat and for runup, with increasing influence of incident waves for higher SWL, which is in line with the findings from 1D reef studies. Longshore varying wave patterns were attributed to the longshore varying bathymetry, wave-wave interactions, refraction and reflection. In tests with a channel, waves in the shoaling region showed greater heights than without a channel, possibly due to wave-current interaction. Differences in runup with and without a channel are not elaborated upon.

A third study on longshore varying runup, albeit on sandy beaches rather than reef environments is performed by Senechal (2017), which studied longshore variability of runup on a sandy beach with a bar in France. Runup energy was found to vary by a factor 4 between different cross sections, while wave data in the surf zone did not show such variability. Observations suggest that wave transformation processes such as dissipation, harmonic release, and wave-current interaction are responsible for this 2D variation of runup. However, no clear causal relations are found yet. Although sandy beaches are different from reef environments, the main drivers for 2D variations in runup may be similar.

2.4.2 Refraction and diffraction

Refraction is the phenomenon where waves change direction due to differences in phase speed along the wave crest (Holthuijsen 2011). As in shallow water the phase speed of waves c is depth dependent, the wave crest moves faster in deeper water than in shallow water. This occurs for oblique incident waves, or for longshore non-uniform topographies, or in the presence of a current. Refraction can be described with Snell's Law (Eq. 2.13):

$$\frac{\sin \theta}{c} = \text{constant} \quad \text{Eq. 2.13}$$

In which θ is the angle between the wave ray and the normal to the depth contours. Due to conservation of energy between two wave rays, refraction can focus wave energy on locations where wave rays approach each other, and defocus energy where wave rays deviate from each other. This focusing of wave energy can locally increase runup.

Diffraction is the phenomenon where the wave amplitude is not constant along a wave crest, and wave energy propagates not only in the direction of incident waves, but also in lateral direction. It is particularly strong along the shadow line behind obstacles such as islands, breakwaters or headlands (Holthuijsen 2011).

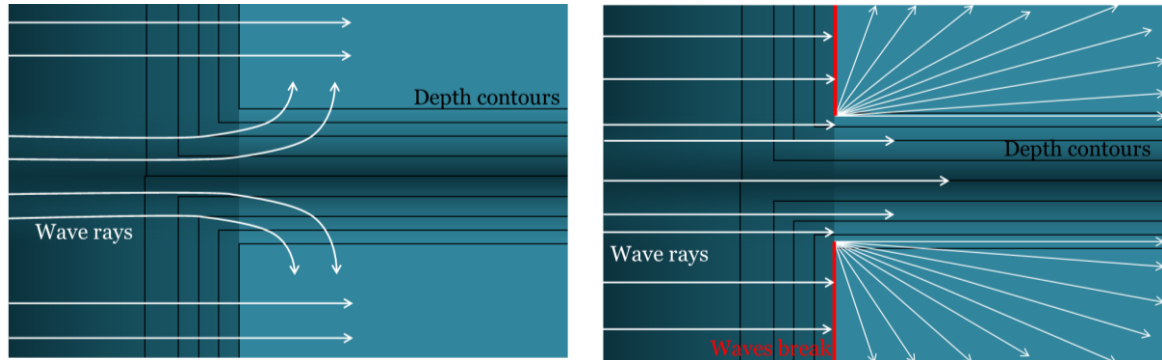


Figure 2.6, Examples of refraction and diffraction on reefs with a channel. The white arrows indicate wave rays, and the black lines are depth contours. Left: refraction, wave rays bend towards shallower zones. Right: diffraction, as waves break on the reef crest as indicated by the red lines, wave energy translates from the channel to the reef flat. Both refraction and diffraction lead to energy transport in longshore direction, and make the wave pattern 2D.

Figure 2.6 shows examples of refraction and diffraction on reef-channel systems. On reef-channel systems, refraction may occur due to the depth differences between the channel and the reef flat, and due to the return current in the channel. Diffraction may occur due to depth induced breaking on the fore reef, and the absence of breaking in the channel, causing large wave amplitude gradients in longshore direction. As a result, shore normal waves transform into a more complicated 2D wave pattern, with waves directed from the channel towards the reef flat coinciding with the shore normal incident waves. Refraction was shown to have a significant effect on wave transformation in reef environments (Young 1989; Hardy and Young 1996; Harris et al. 2015), and was suggested to be one of the factors responsible for longshore differences in runup on sandy beaches (Senechal 2017). Hoeke, Storlazzi, and Ridd (2011) identified diffraction as an important process in reef-bay systems regarding wave transformation. After a flooding event in Matarinao Bay, the Philippines, Tajima, Shimozono, et al. (2016) studied a coastline with a fringing reef and a bay, and found refraction combined with diffraction resulted in focusing of wave energy just outside the bay, responsible for large runup and flooding right next to the bay, and lower runup heights in the bay.

2.4.3 Circulations

A circulation is expected to occur due to the channel. Although mean currents on reefs have been studied in the past, most studies concerned reef lagoon systems, rather than fringing reefs, or focused on flushing times /nutrient uptake rather than the response at the shoreline. To the best of our knowledge, no circulation study on a fringing reefs with a channel is available. To better understand the circulation, the analogy with sandy beaches with bars where circulations and rip currents are observed might be of interest.

From past findings on coral reefs, circulations are found to be generated by three mechanisms:

First, a wave-driven flow based on the radiation stress approach (Longuet-Higgins and Stewart 1962) was mentioned in several researches (Symonds, Black, and Young 1995; Lowe et al. 2008; Taebi et al. 2011; Hearn 1999). This theory states that incident waves break and transfer their momentum into a mean setup of the water surface at the reef crest. Variations in bathymetry lead to variations in setup, hence water level gradients. This drives a mean current, of which the resulting bottom friction balances with the water level gradient (Lentz et al. 2016). In the presence

of a channel the flow is onshore directed over the reef flat and offshore through the channel (Lowe et al. 2008). Circulation velocities increase with increasing wave height and period and decreasing water depth over the reef flat (Gourlay 1996a). Observed velocities of the circulation current are generally in the order of 0.5m/s (Gourlay and Colleter 2005; Lowe et al. 2009). Lowe, Hart, and Pattiaratchi (2010) studied a reef-lagoon-channel system, and found the dimensions of the channel are limiting for the magnitude of the return current.

The current scales with incident wave height. This flow also varies on tidal frequencies due to tidal modulations of wave setup, and ebb-and flood currents over the reef (Taebi et al. 2011). This is an indication that these currents may decrease with rapid sea level rise, as the influence of setup will decrease. Hoeke, Storlazzi, and Ridd (2011, 2013) found that at Hanalei bay, the flow pattern varied largely between different wave conditions.

Second, very low frequency oscillations may be driven by breakpoint forcing. The breakpoint excursion that generates low frequency waves may not only vary in time but also in space for a longshore varying bathymetry.

Third, circulations may be driven by spurs and grooves (SAG) formations, alternating shore-normal ridges of coral called spurs and sediment patches called grooves, generally located offshore of the surf zone (Storlazzi, Logan, and Field 2003). SAG formations have been modeled and their varying bed shear stresses were found to cause a circulation pattern of counter-rotating circulation cells, driven by the imbalance between the pressure gradient and nonlinear wave terms following from different bed shear stresses (Rogers et al. 2016). The circulations are enhanced by spur-normal waves, increased wave height, weak alongshore currents, increased spur height and decreased bottom drag (Leal Campos Fonseca da Silva 2017). Rogers et al. (2015) researched the SAG formations in a field work at Palmyra atoll and found that the circulations driven by the SAG formations were very weak (around 1 cm/s) with offshore flow over the spurs and onshore flow over the grooves.

Of the three mentioned generation mechanisms of circulations, wave breaking and setup differences are dominant (Lowe et al. 2008). The mentioned mean flow patterns influence both the mean water level and waves across the reef (Van Dongeren et al. 2013), and therefore it is expected that they have an effect on runup.

2.4.4 Analogy with rip currents

The return current through the channel is found to show an analogy with rip currents on barred sandy beaches (Nielsen, Brander, and Hughes 2001; Bellotti 2004; Haller, Dalrymple, and Svendsen 2002). In these studies it was suggested that the friction associated with the return flow can have a restricting effect on the magnitude of the rip current. Reniers et al. (2007) observed a sandy beach with shore-connected shoals intersected by rip channels, and remarked VLF motions with frequencies of less than 0.004 Hz, which became stronger near the rip channel. Mean cross-shore flow velocities of the rip current were generally around 0.5-1 m/s maximum for a forcing of $H = 1\text{m}$. On barred sandy beaches, offshore flow velocities are found to scale with the longshore gradient in wave setup (Nielsen, Brander, and Hughes 2001), and is maximum when the surf zone is saturated and all incident waves break (Moulton et al. 2017). Furthermore it is remarked that the rip currents show instabilities outside of the surf zone due to wave-current interaction (Haller and Dalrymple 2001; Yu and Slinn 2003).

Summarizing 2D effects on reefs, circulations on reefs may have several causes, of which setup differences are the most important driver. Diffraction and refraction turn the wave pattern into a more complicated and 2D one. The return current through the channel can transform the waves through wave-current interaction. Little is still known on how a longshore varying coast affects the longshore runup pattern.

3

System analysis

3.1 INTRODUCTION

This chapter presents a system analysis, in which a representative geometry of fringing reef-paleo-stream channel systems is determined, as well as representative oceanic forcing, using data from literature and Google Earth. This is necessary to set up a representative generic numerical model to study reef-channel systems, which will be done in the next chapter. The result of this chapter is a representative reef and forcing, which answers one of the research questions.

First, the terminology of different parameters used to schematize a reef is presented in section 3.2. Second, the range of oceanic forcings that occurs in regions with reef-channel systems examined in section 3.3. From this a representative forcing is determined. Third, the range of naturally occurring geometries of reef-channel-systems is examined in section 3.4, and a representative geometry is determined in section 3.5.

3.2 TERMINOLOGY

A typical fringing reef consist of a steep and rough fore reef, a smoother horizontal reef flat around or slightly below mean sea level, and a steep beach slope. The reef is intersected by one or several paleo-stream channels.

The terminology of geometric parameters that are used to schematize the reef-channel system are defined in Table 3.1 and illustrated in Figure 3.1.

Parameter	Definition
W_r [m]	Reef flat width, distance between the reef crest and the beach toe.
W_c [m]	Channel width
spacing [m]	Channel spacing, or the length of a reef section, distance between two channels.
i_{fore} [-]	Slope of the fore reef, defined as the vertical difference in elevation over 1m horizontally.
i_{beach} [-]	Slope of the beach, defined as the vertical difference in elevation over 1m horizontally.
H_s [m]	Significant wave height.
T_p [s]	Peak period.
s [-]	Wave steepness, defined as the ratio between wave height and wave length.
SWL [m]	Still water level, $SWL=0$ by definition.
h_o [m]	Still water depth on the reef flat. Difference between the reef flat level and the still water level.

Table 3.1, terminology of reef geometry and forcing

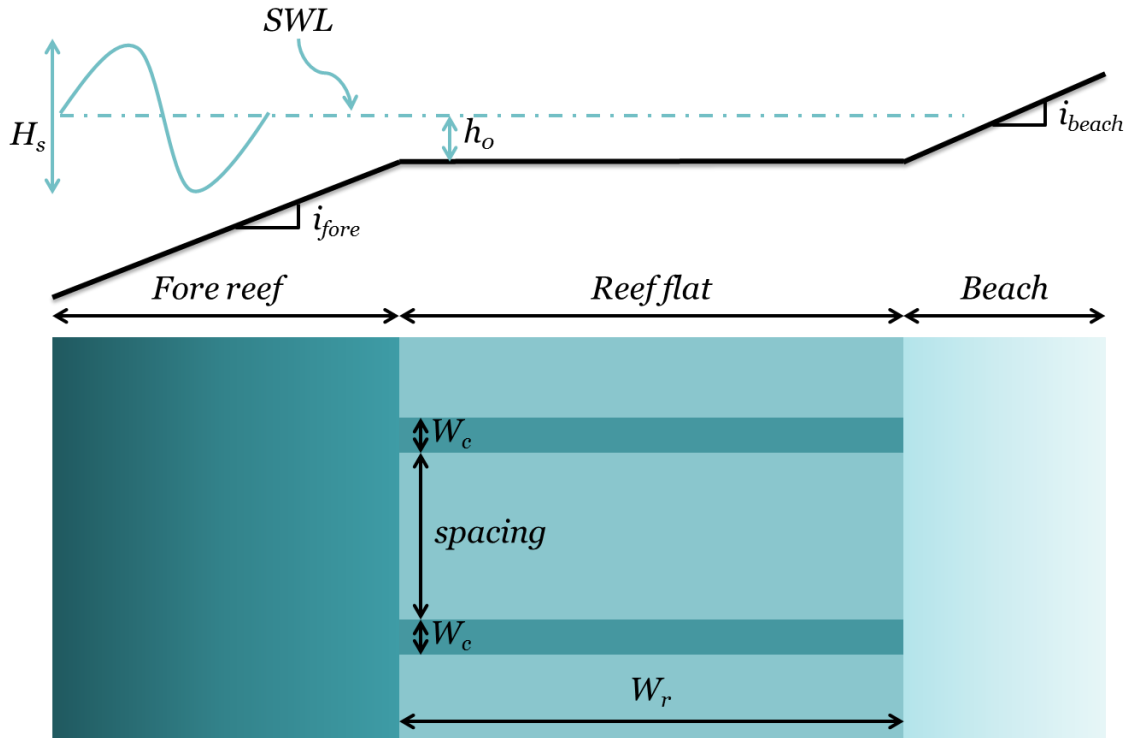


Figure 3.1, Terminology of reef geometry and forcing. Cross section view (top), and top view (bottom).

3.3 OCEANIC FORCING

Wave conditions

Most fringing reefs are exposed to both episodic tropical cyclones and large swell events, but the latter are responsible for the majority of past high runup events and flooding of reef lined coasts (Hoeke et al. 2013; Storlazzi et al. 2015). Concerning return intervals, the primary interest of this study is not the weather extreme that occurs once in a lifetime, but episodic events that occur approximately yearly and are a regular nuisance to inhabitants of coastal regions protected by fringing reefs. Therefore, yearly maxima of swell conditions will be used as the forcing in this study.

To determine the yearly maximum swell event, and thus the representative wave conditions, a report made available by USGS was used, which presents both hindcasts of wave statistics of the past 30 years for different locations in the Western Pacific, as well as predictions for the future (Storlazzi et al. 2015).

Hindcast conditions that occur 5 percent of the time during the month with the highest swell waves, usually January, are presented in Table 3.2. The averaged 2-yearly and 5-yearly maximum significant wave heights are also given to illustrate the range of occurring extreme conditions. The corresponding wave steepness s was calculated from the wave height and period, calculated as in Eq. 3.1.

$$s = \frac{H_s}{L_o}, \text{ with } L_o = \frac{g}{2\pi} T_p^2 \quad \text{Eq. 3.1}$$

In which L_o is the deep water wavelength. Predictions are that over the coming century wave heights may slightly increase or decrease compared to hindcast values, depending on the climate scenarios. However, these variations are small compared to the variations between the different return periods from Table 3.2 and are therefore not considered further.

	Top 5% conditions during most energetic month		2-Yearly maximum	5-Yearly maximum
	H_s	Steepness s	H_s	H_s
Average	4,8	0,022	6,9	7,6
Stdev	1,1	0,005	1,6	1,8
Max	8,1	0,030	11,2	12,2
Min	3,5	0,010	4,3	4,8

Table 3.2, Summary of hindcast wave conditions in the Pacific (Storlazzi et al. 2015).

Offshore water level

The still water level (SWL) is defined at 0 m, so the depth of the reef flat will be chosen to obtain a representative submergence of the reef flat for still water h_0 . The subscript 0 indicates the reef flat submergence is taken under still water conditions, and does not include wave setup. SWL is difficult to obtain from literature, as values in literature are usually measured on the reef flat while subjected to wave forcing and therefore do include setup (so h rather than h_0). Furthermore, they are taken during various tidal elevations. An overview of reef flat water depth observations at different locations is presented in Table 3.3. The average h is around 1m depth, which corresponds with a slightly lower h_0 . The still water depth can vary per location up to several meters due to different tidal elevations and sea level rise.

Location	Reference	Average h
Ningaloo Reef, Australia	(Zhang et al. 2012; Taebi et al. 2011; Pomeroy, van Dongeren, et al. 2012)	1,5 m
Moorea, French Polynesia	(Gattuso et al. 1993)	1,4 m
Heron Island, Great Barrier Reef, Australia	(Gourlay and Colleter 2005)	1,5 m
Hanalei Bay, Hawaii	(Hoeke, Storlazzi, and Ridd 2013)	2 m
New Caledonia	(Bonneton et al. 2007)	0,8 m
Lady Elliott island, Australia	(Jago, Kench, and Brander 2007)	0,5 m
Funafuti Atoll	(Beetham et al. 2016)	0,3 m
CMI Reef Flat, Marshall Islands	(Becker, Merrifield, and Ford 2014)	0,8 m
Roi Namur, Marshall Islands	(Becker, Merrifield, and Ford 2014)	0,8 m
Ipan, Guam	(Becker, Merrifield, and Ford 2014)	0,5 m
Fiji	(Bosselle et al. 2015)	1,5 m
Average		1 m

Table 3.3, Values of reef flat submergence found in literature

3.4 REEF GEOMETRY

To gain insight in the range of values for reef width, channel width and channel spacing, satellite imagery from Google Earth is analyzed. To determine the range of occurring slopes of fore reef and beach, data from literature are used.

3.4.1 Horizontal reef and channel dimensions

A total of 70 reef sections in the Pacific Ocean with a channel were analyzed, of which the locations are presented in Figure 3.2. For every analyzed section, measured dimensions of the reef and channel are presented in Appendix A. The results are summarized in Figure 3.3 and Table 3.4.

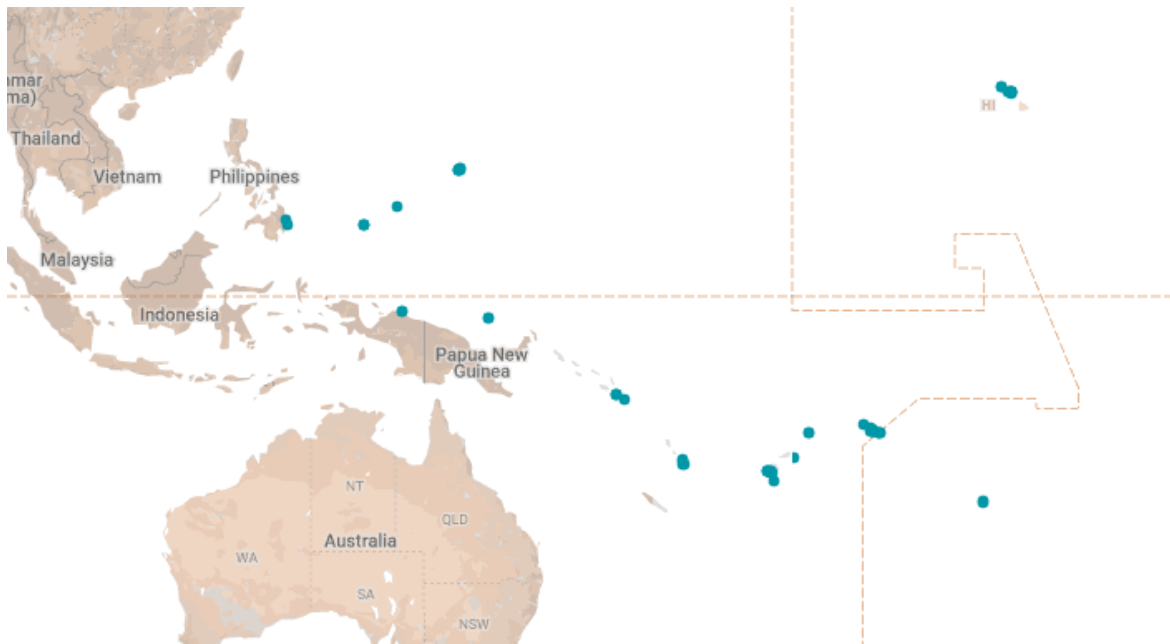


Figure 3.2, Locations of analyzed reef sections with a paleo-stream channel. The blue dots indicate one or several analyzed reef sections.

For every reef section reef width, channel width, channel spacing and channel angle are determined. Reef width is measured next to the channel, perpendicular to the coastline. Channel width is the average channel width of the channel, perpendicular to the channel axis. The channel spacing was measured on the two reef sections on both sides of the channel. In some cases it was not possible to measure the channel spacing due to the curvature of the island or the absence of a reef section on one side of the channel, in which case no value was noted. In other cases the spacing was very large due to the absence of a second channel, in those cases the spacing is marked as infinite. Both cases are excluded from calculation of the average and other statistics. The channel angle defined as the angle between the channel axis and the perpendicular to the coastline.

For every analyzed section, measured dimensions of the reef and channel are presented in Appendix A. The results are summarized in Table 3.4 and Figure 3.3.

Statistic	Reef width [m]	Channel width [m]	Channel spacing [m]	Channel angle [deg.]
Average	493	138	1441	7
Stdev	286	116	1349	9
Max	1400	600	6600	50
Min	50	30	100	0

Table 3.4, Summary of reef dimensions from reef geometry study based on Google Earth imagery data, statistic values.

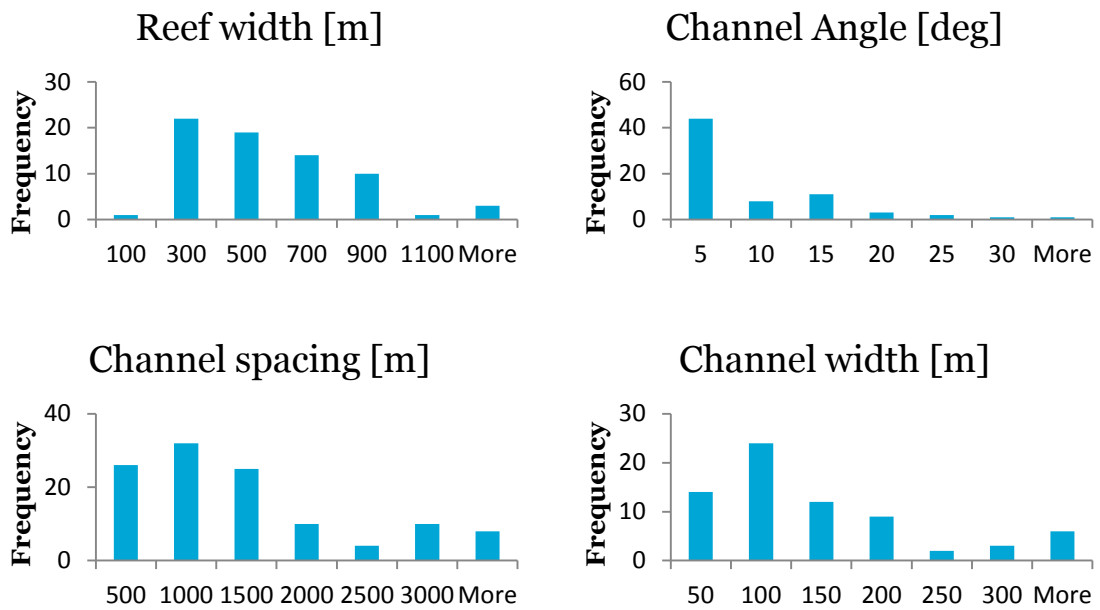


Figure 3.3, Histograms summarizing results of reef geometry analysis, based on Google Earth imagery data. The bin range is indicated by the numbers below. For instance, the bin with reef width 300 contains reefs the widths 100-300m.

3.4.2 Slopes of fore reef, beach and channel

Typical values for fore reef slope and beach slope were found by comparing different field studies, presented in Figure 3.4. It was not possible to retrieve reliable data on the water depths in the channel. Due to the terrestrial origin of the channels, it is assumed that the channels have the same slope as the adjacent land above the shoreline.

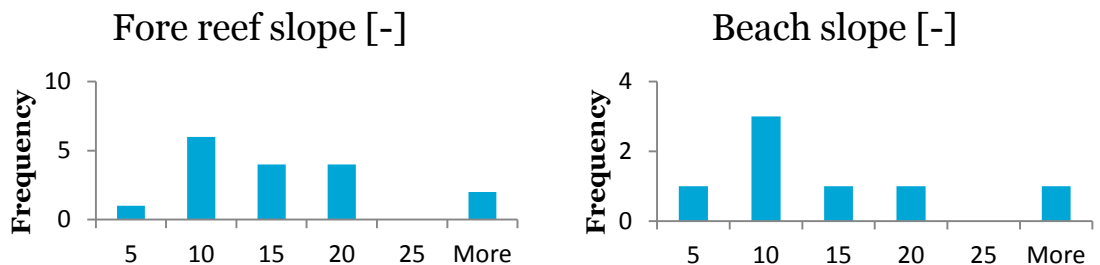


Figure 3.4, Summary of values of fore reef slope and beach slope found in literature, all values are given as the horizontal distance in which the vertical difference is 1m. Sources: (Zhang et al. 2011, 2012; Pomeroy, Lowe, et al. 2012; Hench, Leichter, and Monismith 2008; Bonneton et al. 2007; Hoeke, Storlazzi, and Ridd 2011; Storlazzi, Presto, and Logan 2009; Pomeroy, van Dongeren, et al. 2012; Buckley et al. 2015; Jago, Kench, and Brander 2007; Beetham et al. 2016; Becker, Merrifield, and Ford 2014; Gelfenbaum et al. 2011; Quataert 2015; Blacka et al. 2015)

3.5 CONCLUSION: REPRESENTATIVE REEF AND FORCING

From examining of data from literature and Google Earth, natural ranges of geometry and forcing are determined. The range of topography and forcing values used in the model are based on this. Motivation of the selected values for each parameter is presented below. The representative values are used in the baseline geometry, and the variations in simulations are based on the naturally occurring range of forcings and reef geometries. At the end of this section a summary and overview figure are presented.

Wave forcing

For the baseline scenario a significant wave height of 5m will be applied with a steepness of 0.02, corresponding to a peak period of 12.8s. In the simulations, variations in significant wave height will be in the range of 3-7 m, corresponding to the yearly maximum wave height plus and minus two standard deviations, covering 95% of naturally occurring values. Variation in wave steepness will be in the range of 0.01-0.03, corresponding to the maximum and minimum observed values. For simplicity reasons, in the baseline scenario the waves will approach the coast perpendicular with no directional spreading.

Still water level

Runup is largest for large reef submergence, but circulations are driven largely by setup differences, which are largest when the reef submergence is small. To gain insight in both circulations and runup, the baseline scenario will have a SWL of 1m above the reef flat. This parameter will not be varied between simulations.

Reef width

Most reefs have a reef width of approximately 300m, which will be the value in the baseline scenario. However, the standard deviation is significant. Therefore, reef width will be varied from 100 to 1000m between simulations.

Channel width

Most channels have a width of approximately 100m, which will be the value in the baseline scenario. Channel width will be varied from 50 to 300m between simulations

Channel spacing

The channel spacing was measured on the two reef sections on both sides of the channel. In some cases it was not possible to measure the channel spacing due to the curvature of the island or the absence of a reef section on one side of the channel, in which case no value was noted. In other cases the spacing was very large due to the absence of a second channel, in those cases the spacing is marked as infinite. Both cases are excluded from calculation of the average and other statistics. Most spacings are in the order of 1000m, which will be used as the baseline value. Again, the standard deviation is large, spacings will be varied from 300 to 2000m between simulations.

Channel angle

In most cases, the channel is perpendicular to the coastline, or less than five degrees. To keep the baseline scenario simple, the channel will be perpendicular to the coastline.

Slopes

Based on the most common values, in the reference scenario both the fore reef and the beach slopes will have values of 1 in 10, meaning 1 vertical : 10 horizontal. Inside the channel, the beach slope will be extended below the waterline, so 1 in 10 as well.

The values of the different parameters in the baseline scenario are displayed in Table 3.5, and visualized in Figure 3.5.

Parameter	Value
Offshore forcing	
H_s	5 m
Wave steepness s	0.02, giving $T_p = 12.8$ s
Offshore water level above reef flat	1 m
Wave approach angle	Perpendicular to the coast
Reef geometry	
Reef width	300 m
Dimensionless channel width	0,2
Dimensionless channel spacing	2
Fore reef slope	1:10
Beach slope	1:10
Channel slope	1:10

Table 3.5, List of parameter values as will be applied in the baseline scenario

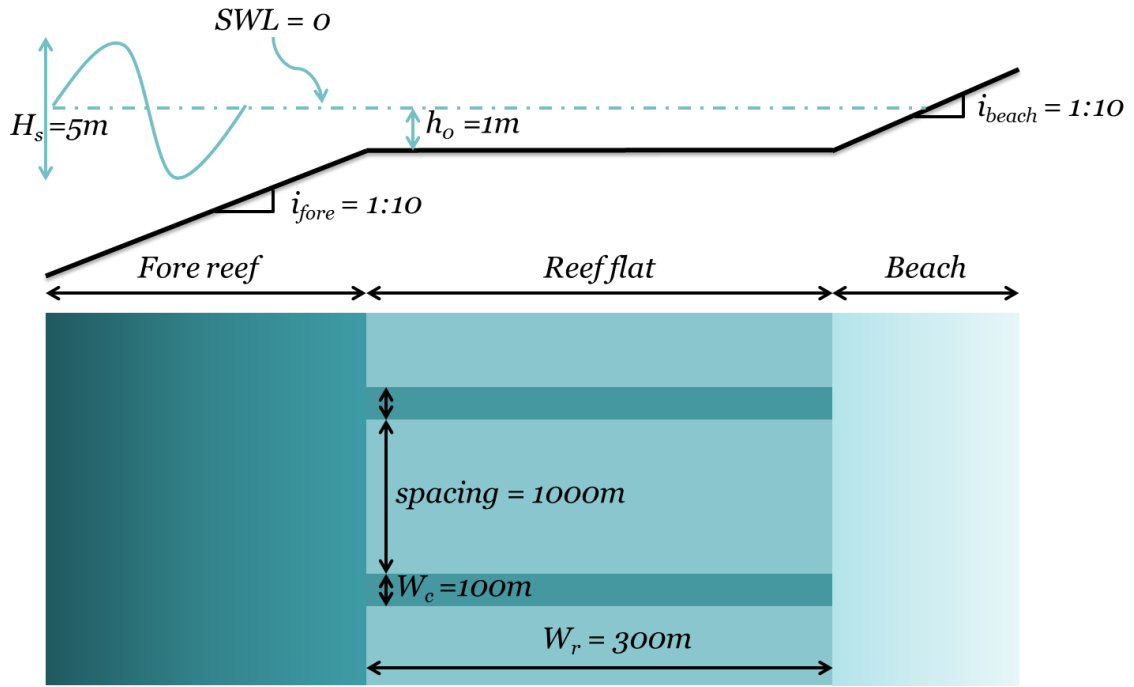


Figure 3.5, Reef geometry with values as will be applied in the baseline scenario. Top: cross section, bottom: top view. The offshore is on the left and the beach is on the right.

4

Model Setup

4.1 INTRODUCTION

To understand the influence of longshore variations in reef geometry on wave hydrodynamics and runup, a two dimensional (2D) numerical model is used. The XBeach Non Hydrostatic model (Roelvink et al. 2018) was chosen for this purpose. This chapter discusses the setup of this model. First, a brief description of the XBeach Model is given in section 4.2. Next, the modeling approach and settings, and the stages of the model setup are discussed in section 4.3 and section 4.4. Finally, the conclusions and discussion of the model setup, including an overview of the performed simulations, is presented in section 4.5.

4.2 THE XBEACH MODEL

XBeach is a process-based, depth averaged numerical model, which includes a number of hydrodynamic processes such as short and long wave transformation, wave-induced setup, unsteady currents and overwash (Roelvink et al. 2009, 2018). It was originally developed to simulate hydrodynamic and morphodynamic processes on sandy coasts during storm events. Later on it has been applied to a wider range of modeling situations, such as gravel coasts (McCall et al. 2015) and vegetated coasts (Van Rooijen et al. 2015). The XBeach model has successfully been applied to coral reef environments in numerous studies, e.g. (Quataert et al. 2015; Gawehn et al. 2016; Van Dongeren et al. 2013; Pearson 2016; Pomeroy, van Dongeren, et al. 2012). For an elaborate description of the XBeach model and the used equations one is referred to the user manual (Roelvink et al. n.d.).

XBeach has two modes, the phase-averaged XBeach Surf Beat (XB SB) and XBeach Non Hydrostatic (XB NH, the latter being phase resolving (Smit et al. 2010)). In XB NH the wave field is resolved on the timescale of individual waves, and the model is capable of resolving the non-linear evolution of the wave field, wave-current interaction and wave breaking in the surf zone accurately (Zijlema and Stelling 2008). There are other extensions of the XBeach models in development: XBeach NonH+, in which a reduced second layer is added to the vertical to improve wave dispersion. The XB NH+ model was extended with the addition of a porous in-canopy model, specifically for coral reef applications by (De Ridder 2018) This study showed promising results. However, the development of XB NH+ model, its first application to a coral reef situation (Klaver 2018), and the development of the in-canopy model were parallel in time to the present study. No validated precedent study on coral reefs was available at the time of the model simulations. Therefore, for the present study only XB SB and XB NH are considered.

XB NH solves the free surface flow based on the Navier-Stokes equations, under the assumptions of incompressible, homogeneous, and Newtonian flow, leading to the following simplified Navier-Stokes equations in Cartesian coordinates presented in Eq. 4.1:

$$\frac{\partial \mathbf{u}}{\partial t} + \nabla(\mathbf{u} \otimes \mathbf{u}) = -\frac{1}{\rho} \nabla P + \mathbf{g} + \nabla * T \quad \text{Eq. 4.1}$$

In which $\mathbf{u} = [u(x, t), v(x, t), w(x, t)]$ is the velocity vector, $P(x, t)$ is the pressure, $\mathbf{g} = [0, 0, -g]$ is the gravitational body force, and T is the deviatoric viscous stress tensor, a higher order component.

The numerical discretization in XB NH is a combination of the non-hydrostatic model by (Zijlema and Stelling 2008), and a flux limited variant of the scheme by Maccormack (1969). It is momentum conservative and second order accurate in time and space, and allows for accurate modeling of wave breaking without a separate breaking model.

Because the non-hydrostatic mode solves both long and short waves on the individual wave scale, it is more accurate regarding individual wave breaking and short wave runup than the hydrostatic mode. However, it is computationally more expensive, and the grid resolution that needs to be higher.

Although the computational demand of a 2D model is already high, it is necessary to use the computationally more expensive XB NH, as the primary focus of this thesis is on runup, and it was shown by (Quataert 2015), that to accurately reproduce wave runup on coral reefs, short wave processes cannot be ignored and a phase resolving model is required.

4.3 MODELING APPROACH

As variations in the alongshore geometry of coral reefs are the core of this research, a 2D model is required. A large number of XB NH simulations is performed, in which the geometry parameters reef width (W_r), channel width (W_c), channel spacing are varied, with the goal to compare the runup, circulation and wave hydrodynamic results for different geometries and forcings. All simulations are based on the geometry of the baseline scenario, determined as described in the previous chapter.

4.4 MODEL SETTINGS

In this section the model input files and settings are presented. For all parameters that are not mentioned, the XBeach default values are applied.

4.4.1 Model domain and orientation

For the baseline scenario the most simplified version of a reef-channel system is chosen: a straight reef section with a channel in the middle. The x direction is the cross shore direction and positive onshore, the offshore boundary is located at $x=0\text{m}$ by definition. The y direction is the longshore direction. The lateral boundaries are on the southern and northern end of the model domain, as displayed in Figure 4.1.

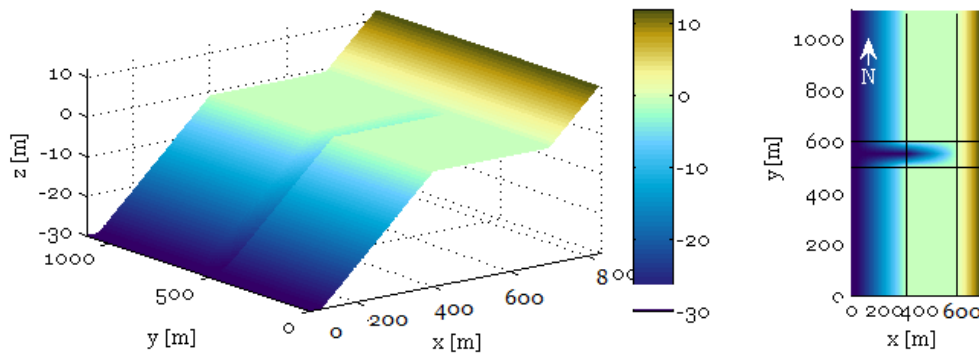


Figure 4.1, Model domain and bathymetry, 3D view (left) and top view (right)

4.4.2 Bathymetry and grid

In the baseline scenario, the reef has a width of 300m, with a channel of 100m wide, and a channel spacing of 1000m. Cyclic boundary conditions (explained in the next paragraph) are applied on the lateral boundaries, which translate to a 100m wide channel in the the middle of the grid, with an adjacent reef flat of 500m long on both sides. For simplicity reasons, the channel has a triangular cross section. At the offshore boundary, the grid is extended to a depth of 30m followed by 20 horizontal grid cells. At the shoreward boundary the model is extended to +12m with a slope of 1V:10H, to account for very high runup levels. Cross sections of the schematized reef bathymetry are presented in Figure 4.2.

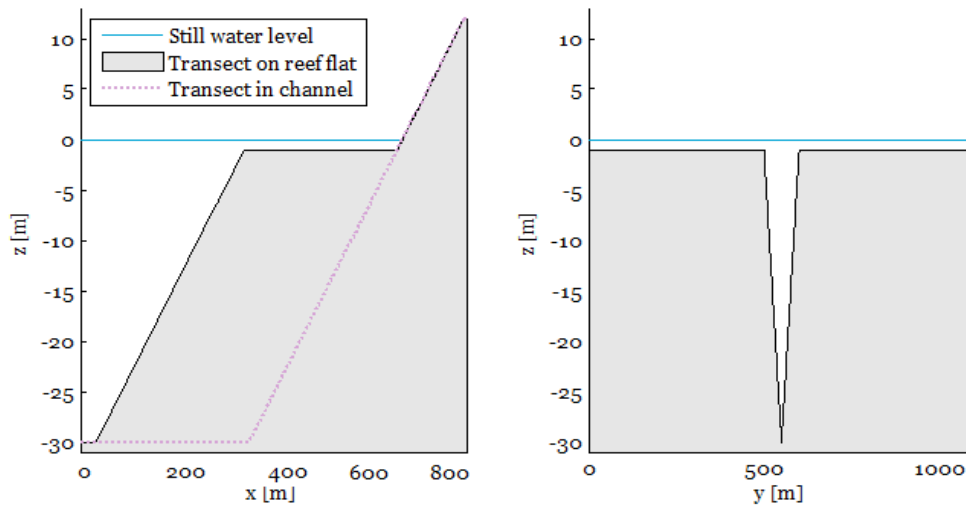


Figure 4.2, cross shore reef transect (left) and longshore cross section of the reef flat (right).

A rectangular grid is applied. The longshore grid resolution varies between 1m in the channel to 4m near the boundaries. To account for the cyclic boundary condition which will be discussed in the next paragraph, 3 rows of cells are added at the northern end of the grid, $y=1100\text{m}$ for the baseline scenario. The cross shore grid size is calculated with the CFL condition, using a maximum resolution of 0.5m at the shoreline (corresponding with a 0.05m vertical resolution for a beach slope of 1:10) and a minimum resolution of 1.5m further offshore. With a beach slope of 1:10 the vertical resolution is 5 cm at the shoreline. A maximum smoothness, defined as the ratio between cell sizes of two adjacent cells of 1.05 is applied. The grid resolution is displayed in Figure 4.3.

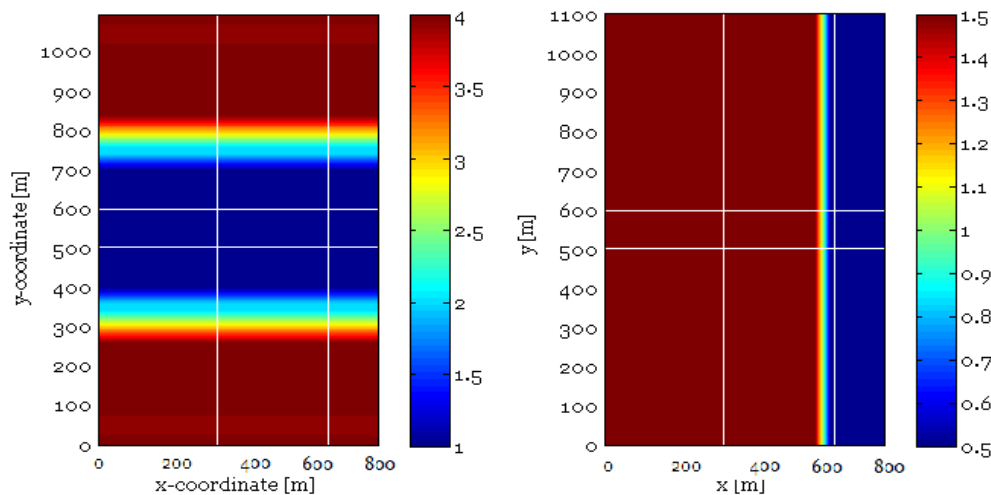


Figure 4.3, Longshore (left) and cross shore (right) distributions of the grid cell size in meter.

4.4.3 Boundary conditions

At the offshore boundary the boundary condition “nonH_1D” is applied, which is the default boundary condition for XB NH. At the shoreline a wall boundary is applied. The lateral boundaries are cyclic, which means XBeach treats the two lateral boundary regions as if they are physically connected. Waves and flow that exit the model through one boundary will be copied to the other side. Cyclic boundaries have the advantage that there are no shadow zones. The grid virtually repeats itself, representing an endless series of reef sections and many equidistant channels.

4.4.4 Parameter settings

The processes sediment transport and morphology are disabled. The non-hydrostatic mode is used (keyword nonh =1) and the short wave action balance is disabled (keyword swave =0). Bottom friction is accounted for by use of the friction coefficient c_f , which is associated with both the mean currents and long period (infra gravity) waves in both XB SB and XB NH. For the rough fore reef a c_f of 0.04 is applied, and for the smoother reef flat and beach c_f has the value of 0.002, based on the c_f values used in 2D XBeach reef studies by (Van Dongeren et al. 2013) and (Storz et al. 2018). An example of the params.txt file which dictates the model settings and desired output is presented in Appendix B.

4.4.5 Forcing

The wave forcing applied to the model is a Jonswap spectrum, based on which XBeach generates offshore time series of water level which are applied at the boundary.

In the baseline scenario $H_s = 5\text{m}$ and $T_p = 12.8\text{s}$. The waves approach the coast perpendicular and there is no directional spreading. The offshore water level is the reference level, so the tidal elevation is 0m, corresponding with a still water depth on the reef flat of 1m, and is constant over the entire simulation. Table 4.1 displays the input values of the Jonswap type input file. From the boundary condition input file XBeach calculates water level time series of the given duration corresponding with the applied Jonswap spectrum. The XBeach input parameter “random” is set to 0, indicating there is no randomness in the way XBeach translates the Jonswap spectrum to a time series. All time series derived from the same Jonswap spectrum will be identical. These time series will be applied consecutively at the offshore boundary.

H_{mo} [m]	T_p [s]	Mainang [deg.]	Gammajsp [s]	s [-]	Duration [s]	Dtbc [s]
5.0	12.8	270	3.333	100000	3600	1.0

Table 4.1, Input parameters of the Jonswap boundary condition file. Dtbc indicates the time step used for the calculations of the boundary condition at the offshore boundary, in this case 1s.

4.4.6 Simulation time

The simulated time is the sum of two parts: the spinup time and the time required for the runup results to be independent of the runtime. A long simulation of 18 hours was run to determine the required simulated time. For the baseline scenario, the total required simulated time is 4 hours.

First, the spinup time is determined. After the spinup time, the circulation over the reef and through the channel needs to be fully developed. To evaluate this, the total discharge through the channels, which is an indicator for the occurring circulation, and the maximum and minimum discharge occurring in the model domain are calculated, averaged over 100s intervals, displayed in Figure 4.4. After approximately 1000s the discharge pattern appears to reach a dynamic equilibrium. As the spinup time may vary for different reef geometries and wave forcings, a conservative value of 1500s is applied. For all simulations, it is verified that the assumed spinup time is sufficient.

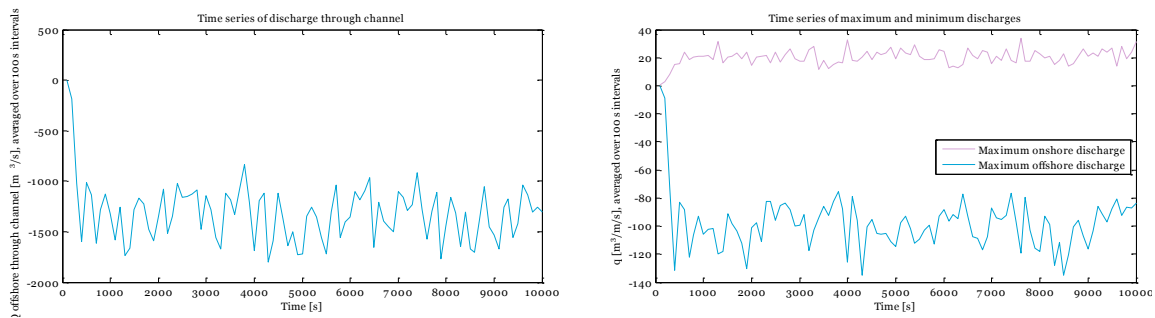


Figure 4.4, Time series of total discharge through channel (left) and maximum and minimum discharge occurring in the model domain (right), time averaged over 100s intervals

The second factor influencing the total simulated time is the time required for the runup results to be independent of the runtime. As the $Ru_{2\%}$, defined as the average of the highest 2% of waves, is an important parameter to analyze the runup, it is required to have a large number of waves reaching the coastline during the simulation. It is common practice to calculate the $Ru_{2\%}$ over 1000 waves, so the $Ru_{2\%}$ is the average of the 20 highest waves. For a wave period of 12.8s, this requires a simulation time of 3.5 hours. In order to investigate the dependence of the $Ru_{2\%}$ value on the simulation time, we perform a simulation with a duration of 18 hours, and the alongshore results of $Ru_{2\%}$ are compared for different time intervals, as presented in Figure 4.5. After 1 hour simulated time, the runup results are very irregular, because the $Ru_{2\%}$ is averaged over only a few waves. After 5 hours, corresponding with slightly less than 1500 waves, most of the larger undulations have evened out. The alongshore $Ru_{2\%}$ is still not completely identical to the 16 hour simulation graph, so the $Ru_{2\%}$ results are still dependent on the simulation time. However, the resemblance is significant and most irregularities due to coincidental high waves are averaged out.

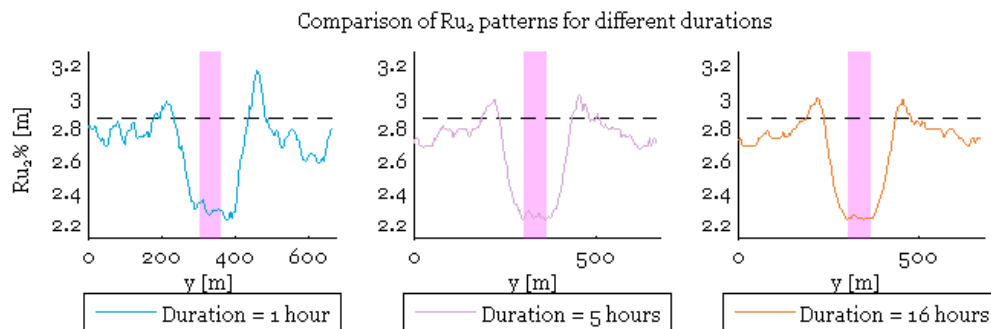


Figure 4.5, Comparison of runup patterns for different simulation times. The three graphs represent simulation times of 1, 3, and 16 hours. The black dashed line represents the reference runup for a reef without a channel. The pink rectangle indicates the location

Figure 4.6, shows the development of the $Ru_{2\%}$ characteristics over time. In the top figure, the maximum values of the northern and southern half of the model domain are very different after only a few hours of simulation, but reach their equilibrium value after 5-6 hours. The mean absolute difference of $Ru_{2\%}$ between two adjacent cells is plotted in the bottom figure of Figure 4.6, as a measure for the size of the undulations in the longshore runup pattern. The longshore smoothness reaches an equilibrium after 12 hours of simulation. After 6 hours, the difference with the equilibrium value is less than 20%, meaning that most of the undulations have damped out, decreasing the influence of occasional high waves on the $Ru_{2\%}$.

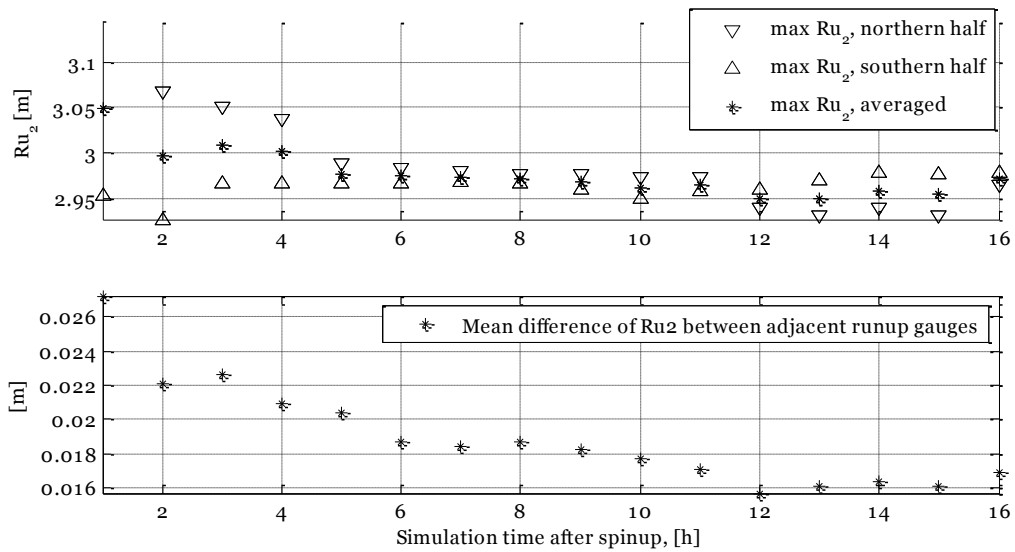


Figure 4.6, Comparison of $Ru_{2\%}$ for different simulation durations. The top figure displays the peak $Ru_{2\%}$ values of the northern and southern half and the averaged value. The bottom figure displays the mean absolute difference of $Ru_{2\%}$ between two adjacent runup gauges.

Ideally the model would be run for a larger duration, but due to the high computational demand of the 2D XBeach model this is not feasible. Therefore a balance between ideal results and acceptable runtime is found at a simulated time containing 1500 waves, corresponding with a simulation time of slightly less than 6 hours for a T_p of 12.8s.

4.4.7 Model output

Model output exists of global output and point output. Global output is generated for every grid cell every 500s interval. Point output generates a 0.5s interval time series at strategic locations in the model domain. Cross shore locations of output points are: the offshore boundary, the last point of a water depth of 30m, midway on the fore reef at 15m depth, 20m in front of the reef crest, at the reef crest, 20m behind the reef crest, midway on the reef flat, and at the beach toe. Long and cross shore locations of the output points are presented in Figure 4.7. To generate runup output, runup gauges register the instantaneous runup level at 0.5s intervals. Runup gauges are placed along the entire shoreline, at 2m intervals within 120m of the channel, and at 4m intervals along the remaining shoreline.

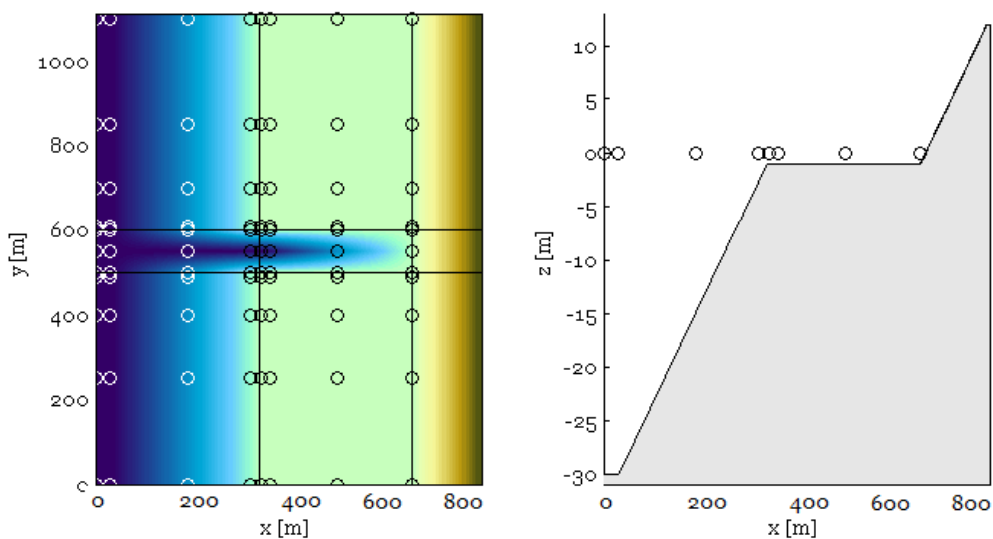


Figure 4.7, Locations of point output indicated by circles, top view (left) and cross shore view (right).

4.4.8 Model performance

Due to the symmetrical nature of the bathymetry, theoretically all model output should be perfectly symmetrical. However, all model results during model setup showed various levels of asymmetry, most noticeable in the plume generated by the outflow through the channel. This plume was not directed perpendicular to the reef crest, but showed slight deviations, either to the south or to the north. These asymmetries are supposedly due to inherent instabilities in the flow, numerical round of errors in the grid, the order in which hydrodynamics in grid cells are computed.

During the model setup, simulations with multiple channels were performed and compared to single channel runs, which theoretically should be identical due to the cyclic boundary condition. The differences between single and multiple channel runs were indeed small, and as the required computation time is smaller for a single channel, all simulations are performed with a single channel.

To further assess the asymmetry in results, various model runs were performed to see for which settings the asymmetry is lowest. The asymmetry was found to be slightly lower for runs with a larger channel spacing to increase the distance between channel and longshore boundary, Increasing the distance between the offshore boundary and the reef did not significantly improve the symmetry.

Two examples of asymmetry are presented below. First, Figure 4.8 displays two simulations, between which the only difference is the addition of the 3 extra grid cells in longshore direction, required for the cyclic boundary condition. These 3 extra cells, adding a width of 12 meters to the model domain, change the direction of the channel plume. The direction of the discharge plume is varies between the two simulations, indicating that the asymmetry in model asymmetry results is sensitive to small variations in the grid definition.

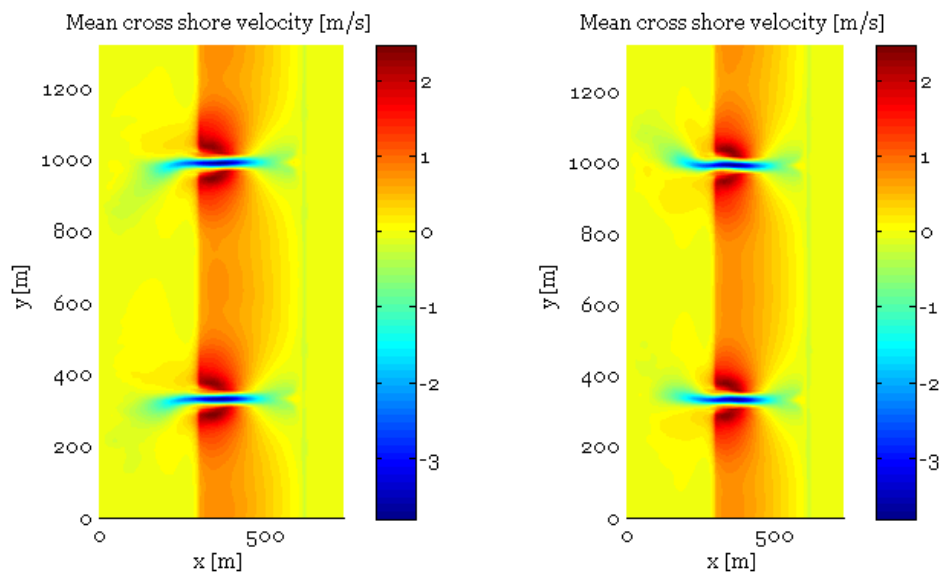


Figure 4.8, Comparison of mean cross shore velocity for two model runs. Both had two channels, and were forced with identical boundary conditions: $H_s = 5\text{m}$ and $T_p = 12.8\text{s}$ for a short simulated time of 2 hours. The first simulation (test071) was ran without 3 paste cells for cyclic boundary (left), while the second one (test072) was ran with 3 paste cells for the cyclic boundary (right)

Second, simulations with non-equidistant channels the channel plumes were deflected slightly in the direction of the shortest reef section, as displayed in Figure 4.9.

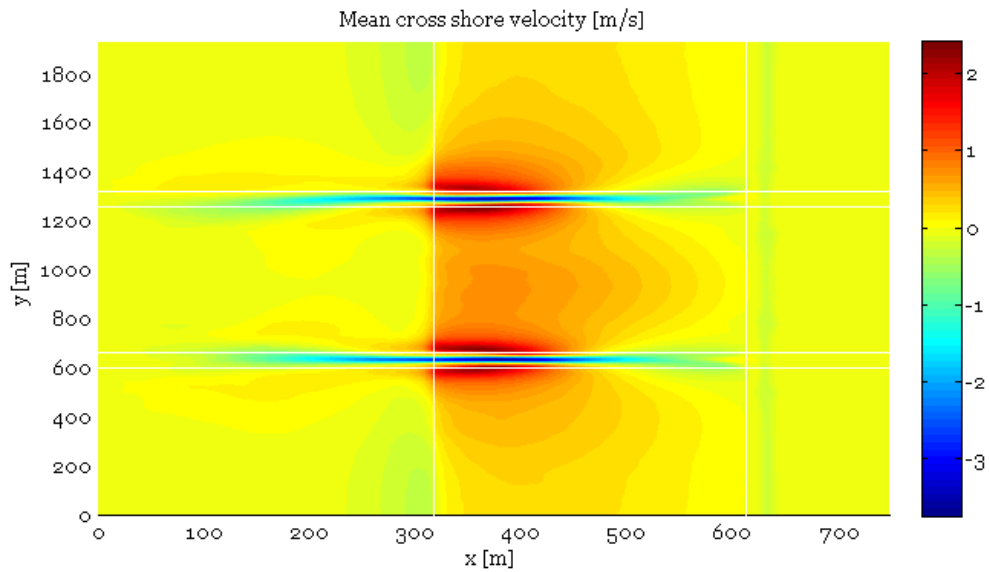


Figure 4.9, Asymmetry for a model run with non-equidistant channels, in this case the channel spacings are 1200m over the lateral boundary and 600m in the middle of the reef. Data from run o85

The largest factor contributing to the model symmetry was found to be the simulated time. In the 18 hour run that was performed to evaluate the spinup time, it was found that the channel plume changed direction on a time scale of several hours. This is possibly a result of instability of the outflow through the channel similar to rip current instabilities on sandy beaches, e.g. (Kennedy and Zhang 2008).

When averaged over a large number of hours, the alternating direction of the plume evens out to a shore-normal one, and the results for runup and flow velocities become symmetrical. However, it is not feasible to run every simulation for 18 hours due to the high computational demand of the 2D XBeach model. Therefore, small asymmetries are accepted. In the analysis of model results, north and south output will be averaged, to approach the dynamic equilibrium values of a very long run.

Concluding, even though the model was setup to be perfectly symmetrical, during the model setup it was found that both the runup results and the flow velocities show some asymmetry in longshore direction. This is probably caused by a combination of numerical round-off errors and flow instability of the offshore directed flow through the channel, which partially evens out after a long runtime. To fully explain this asymmetry, further research is required.

For the present study, it would be ideal to run every simulation for a large number of hours, in which the flow fluctuations would even out over time and give symmetrical results. However, as stated before that is not realistic due to the large computational demand of the 2D model. Still, even with small asymmetries, the model results can provide insights in runup and circulation patterns.

4.5 CONCLUSION AND DISCUSSION OF MODEL SETUP

To assess the impact of paleo-stream channels in fringing reefs on runup, a numerical model, XBeach Non Hystostatic was used to run 135 simulations. In the model setup a balance between computational demand (simulated time per simulation and number of simulations) and perfect, symmetrical results was achieved. To the purpose of the present study, it is concluded that the model performed satisfactorily and is valid.

This section presents an overview of the model simulations and some discussion points of the model setup.

4.5.1 Overview of model simulations

With the results of the model setup and the settings as described above, a total of 135 simulations are performed, a combination of 9 different forcing scenarios, presented in Table 4.2, each applied to 15 reef geometries, presented in Table 4.3.

For the forcing scenario's 3 different significant wave heights are used, each for 3 different wave steepnesses s , corresponding with the range of steepness of swell waves found in nature, determined in section 3.5 in the previous chapter.

H_s [m]	s [-]	T_p [s]
3	0.01	13.9
	0.02	9.8
	0.03	8.0
5	0.01	17.9
	0.02	12.8
	0.03	10.3
7	0.01	21.2
	0.02	15.0
	0.03	12.2

Table 4.2, Overview of forcings that are used in the model simulations.

Each forcing is applied to 15 different geometries: 4 reference scenarios (runs of reef sections with a given reef width, without a channel), the baseline geometry, 4 variations in channel width W_c , 3 variations in reef width W_r , and 3 variations in channel spacing,

Geometry variation	W_c [m]	W_r [m]	Spacing [m]
1 (ref)	0	100	No channel
2 (ref)	0	300	No channel
3 (ref)	0	500	No channel
4 (ref)	0	1000	No channel
5 (baseline)	100	300	1000
6	50	300	1000
7	70	300	1000
8	200	300	1000
9	300	300	1000
10	100	100	1000
11	100	500	1000
12	100	1000	1000
13	100	300	300
14	100	300	600
15	100	300	2000

Table 4.3, Overview of geometries that are used in the model simulations.

4.5.2 Model validation

It is common practice to calibrate and validate a numerical model to field or laboratory data. However, to the best of our knowledge no suitable data are available for this study: no runup or hydrodynamic data are available for coral reefs sections with channels. However, two factors mitigate the need to calibrate the numerical model on measured data. First, the goal of this conceptual study is not to replicate one case study perfectly, but instead to gain general insights in how the longshore runup pattern varies in the presence of a paleo-stream channel in the reef depending on the local reef geometry and forcing and to relate these patterns to dimensionless parameters. In other words, the focus of this study is not to find exact quantitative values for runup heights or currents, but to identify and understand qualitative spatial patterns. Second, as stated before, XB NH has been applied numerous times for 1D and 2D modeling studies, e.g. (Quataert et al. 2015; Gawehn et al. 2016; Pearson 2016; Storlazzi et al. 2018). In those studies,

the model was calibrated and validated against measured data, and performed satisfactorily, so XB NH has proven its applicability to coral reef studies. The latter makes us confident that we can employ the model to explore the effects of paleo-stream channels in reef in a conceptual study.

4.5.3 Selection of wave forcings

A side note on the selection of forcings should be made. At first simulations were performed for $H_s=1$ as well, but results were not reliable as they showed non-physical damping. The wave heights decayed very fast after entering the model at the offshore boundary. This error is attributed to the combination of short waves, with a deep offshore boundary (30m), resulting in a too high kh value, which ideally should be below 1-1.5 but were way above this limit. Reruns with adapted bottom depths showed large asymmetry, of which the cause is not clear. To stay focused on the main research goal, and not lose a lot of time trying to get the $H_s=1$ m runs right; it is decided to discard these runs from analysis of the model results. This is justified because the focus of this study is on extreme conditions, which are more around $H_s = 5-7$ m.

4.5.4 H_s versus H_{m0}

In analyzing the model results, it was found that at the offshore boundary there was a difference between H_s , the wave height dictated by the model settings and H_{m0} , the calculated wave height, which was 10-20% larger than H_s at the offshore boundary. A similar difference was also observed in results of previous XBeach simulations (Pearson 2016). It is unclear what is the causing this discrepancy between dictated and actual wave height in the XBeach model. This is not further examined in this study. In the next chapter, model results are sometimes linked to H_s , and sometimes against $H_{m0,offshore}$.

5

Model results

5.1 INTRODUCTION

To examine the response of runup and other hydrodynamic processes to varying offshore wave forcing and reef geometries, 135 XBeach model simulations are performed. Results are analyzed for runup and reef hydrodynamics. First, the analysis on individual simulations is presented using one example simulation in section 5.2 for runup and section 5.3 for reef hydrodynamics. Results for the remaining simulations are presented in Appendix D and Appendix E. Per simulation several relevant parameters are defined and used in section 5.4 to compare different simulations and assess the influence of varying forcing and reef geometry on runup and circulation. To better understand what drives runup differences, the contribution of different frequency components to runup is discussed in section 5.5.

5.2 RUNUP RESULTS FOR ONE SINGLE SIMULATION

Results for single simulations are processed to gain insight in the alongshore variations in runup. The longshore runup pattern is described both using several relevant parameters, which will be used to compare different simulations later on. The results are presented here for one simulation, for the other simulations results are presented in Appendix D and Appendix E.

The example simulation has the default geometry: $W_c=100\text{m}$, $\text{spacing}=1000\text{m}$ and $W_r=300\text{m}$, and a forcing² of $H_s = 7\text{m}$ and $s=0.02$. This simulation is selected as the most representative, as the runup pattern shows properties which are also found in many other simulations.

5.2.1 Model output

Runup heights are determined by the XBeach model by tracking the water level in the most shoreward wet cell of a cross shore transect, using virtual runup gauges. Runup gauges are implemented along the entire shoreline, with a longshore resolution varying between 4 meters mid reef flat and 2 meters in proximity of the channel. Every runup gauge generates a runup time series with intervals of 0.5s. These time series are further analyzed: runup points are identified and for every runup gauge as presented in Figure 5.1. $Ru_{2\%}$, defined as the runup level which is exceeded by the highest 2% of the waves, is determined along the entire shoreline. For completeness, $Ru_{5\%}$, $Ru_{10\%}$, maximum runup and minimum rundown are also determined and presented in Appendix C. These other runup values largely show the same pattern, but the vertical range and difference with the reference level may vary. As $Ru_{2\%}$ is the most common value to represent runup in coastal science, this will be used in further analysis.

² As stated in the previous chapter, it was found that there is a difference between the dictated wave height H_s and the calculated wave height H_{m0} in the XBeach model: at the offshore boundary H_{m0} is 10-20% larger than H_s , so 9m instead of 7m for the presented run. In the analysis of results, H_{m0} is used in the analysis of the frequency components to runup and wave height on the reef flat, and H_s is used in comparison of the runup pattern and in the scatterplots.

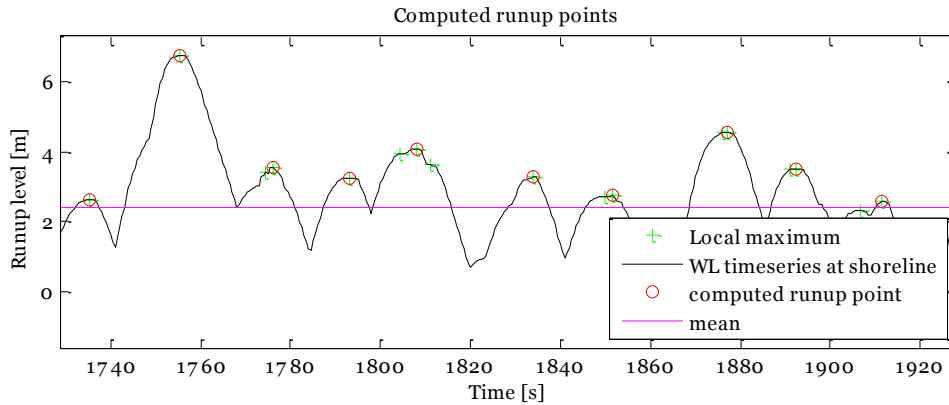


Figure 5.1, Determination of individual wave runup levels from the water level time series at the shoreline (black solid line). All local maxima (green markers) are determined from the time series. Maxima of individual waves are distinguished as runup points (red circles), based on T_p . From these runup levels, $Ru_{2\%}$ is determined as the value that is exceeded by the highest 2% individual runup levels. Similarly, $Ru_{5\%}$, $Ru_{10\%}$ are determined, as well as the maximum runup level and the minimum rundown level.

5.2.2 Longshore runup patterns

$Ru_{2\%}$

The longshore varying runup is found by plotting the $Ru_{2\%}$ against its longshore coordinate. Figure 5.2 shows the longshore $Ru_{2\%}$, a smoothed line and the reference runup without a channel.

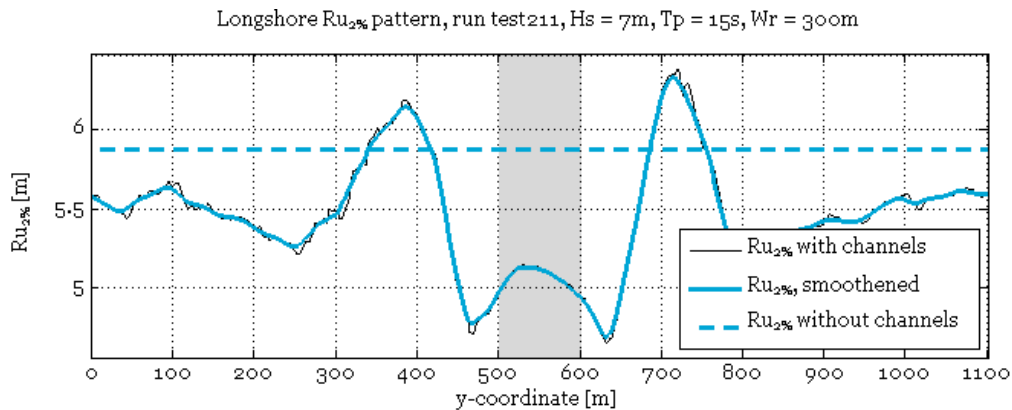


Figure 5.2, Alongshore runup pattern. $Ru_{2\%}$ values are plotted against the alongshore coordinate. The black line shows the runup model output. This line shows a lot of small wiggles, which are of minor interest compared to the large scale variations along the reef flat and channel. The solid blue line shows a smoothed runup line where the small wiggles are removed. The dashed line shows the $Ru_{2\%}$ of the reference runup: $Ru_{2\%}$ of a 2D reef with similar geometry but without a channel, under identical forcing. The grey area marks the location of the channel.

Figure 5.2 is used to describe the runup pattern. The following things can be noted:

- There is longshore variability in $Ru_{2\%}$, with a range of 1.5m or 20% of H_s .
- The highest runup (longshore runup peak) is higher than in the reference run, and the lowest runup (trough in runup) is lower than in the reference run.
- Peaks are about 120 meters away from the channel edge.
- Minima are found right next to channel edges.
- There is a local runup maximum in the channel
- There is some asymmetry, northern and southern halves show slightly different runup patterns.
- Small wiggles are present, even after smoothing of the runup pattern

- Runup slowly approaches reference runup towards mid reef, but this value is not reached

5.2.3 Relative longshore runup pattern

For a more quantitative analysis and to enable the comparison of different simulations, runup is presented in a different form, as the relative longshore runup pattern. Two new parameters are applied: $Ru_{2\%}^*$, and y^* , defined in Table 5.1:

Parameter	Definition
$Ru_{2\%}^*$	Relative $Ru_{2\%}$, defined as the difference between $Ru_{2\%}$ and the reference $Ru_{2\%}$ from the corresponding reference simulation without a channel.
y^*	Relative y-coordinate, defined as the distance from the edge of the channel in meters. Positive values indicate locations on the reef flat, and negative values indicate locations in the channel. The use of y^* enables the northern and southern model half to be mirrored over each other, and their average to be used in further analysis.

Table 5.1, Definitions of $Ru_{2\%}^*$ and y^* , used in further runup analysis

From the averaged pattern peak zones are determined, defined as zones in which the runup is higher than in the reference scenario. For this simulation, there is only one peak zone. In these zones, the channel increases the risk of coastal flooding for the given forcing. In each peak zone the peak $Ru_{2\%}^*$ is determined, as well as its y^* location. Also, for each simulation the minimum $Ru_{2\%}^*$ and the mid reef $Ru_{2\%}^*$, defined as the average of the 10 gauges in the middle of the reef flat, are determined. These statistical values are used to compare results from different simulations. Figure 5.3 presents the relative longshore runup pattern.

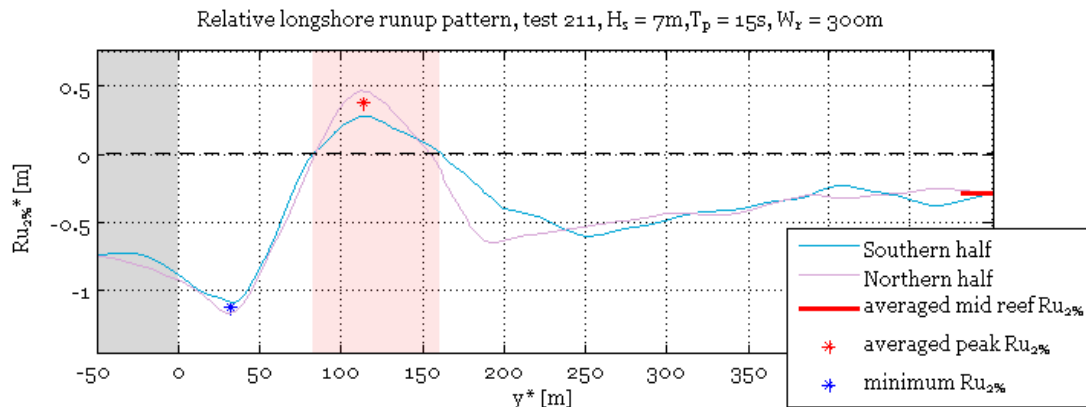


Figure 5.3, Relative longshore runup pattern: $Ru_{2\%}^*$ as a function of y^* . Northern and Southern halves are plotted over each other and the average of those is used to determine significant values. High runup zones where $Ru_{2\%}$ exceeds the reference $Ru_{2\%}$ are indicated by the red patch. For every zone the peak $Ru_{2\%}^*$ is indicated by a red asterisk. The lowest $Ru_{2\%}^*$ is indicated by the blue asterisk. The mid reef runup is marked by a horizontal red line. The channel is marked by a grey patch.

From the relative longshore runup pattern, the following things can be noted:

- One high runup zone is present, located 80-160m from the channel edge.
- Northern and southern halves differ from each other up to 20 cm, but the general trends are similar, and the average of these two halves is regarded as representative for the whole model domain.
- The peak $Ru_{2\%}^* = 0.37m$, which is 5% of H_s .
- The minimum $Ru_{2\%}^*$ is $-1.15m$ or 15% of H_s lower than the reference runup
- The mid reef $Ru_{2\%}^*$ is $0.3m$ or 5% of H_s lower than the reference runup

Summarizing: three statistical values are determined for further analysis: the peak $Ru_{2\%}^*$, minimum $Ru_{2\%}^*$, and mid reef $Ru_{2\%}^*$. The vertical range between peak and minimum $Ru_{2\%}^*$ is 20% of H_s .

5.2.4 Runup contributions of frequency components

To better understand which wave processes are responsible for longshore runup differences, the influence of different frequency components to runup is assessed. For each runup gauge the vertical runup signal is split into four different water level time series according to the frequency: setup, SS (0.04-0.2 Hz), IG (0.004-0.04 Hz) and VLF (0.001-0.004 Hz), presented on the right in Figure 5.4. From these time series the wave height of every frequency component is calculated using the variance of the water level time series as in Eq. 5.1, which is normalized against the H_{m0} at the offshore boundary presented on the left in Figure 5.4. Again, this figure presents only one simulation, all other simulations are presented in Appendix F.

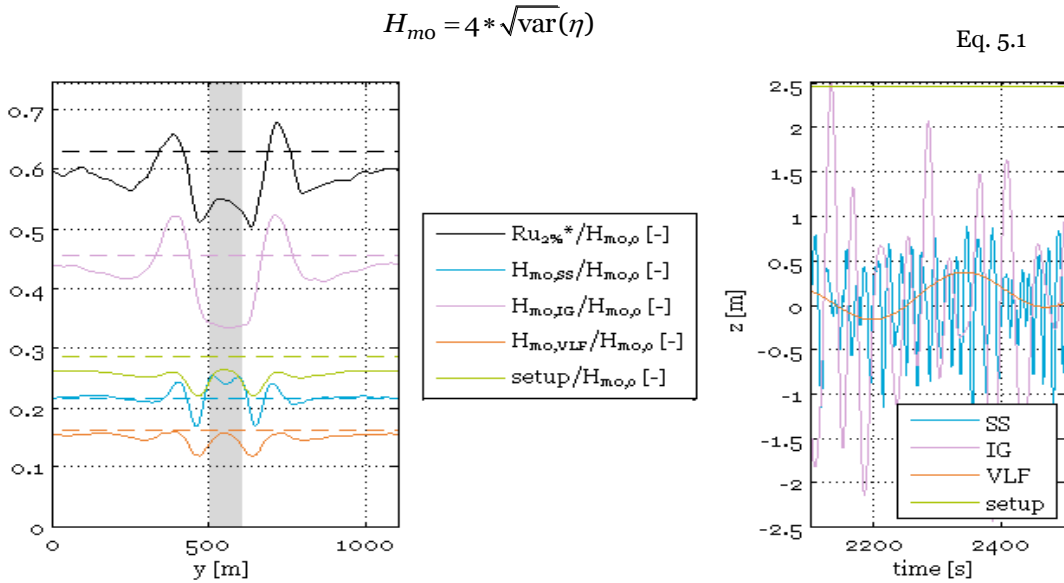


Figure 5.4, Left: Longshore varying runup (black) split into frequency components: setup (green), SS (blue), IG (pink), and VLF (orange), presented as the fraction of the incoming waves by normalizing with $H_{m0,offshore}$ at the offshore boundary. The dashed lines in corresponding colors show the frequency components in the reference run without a channel. The grey patch indicates the location of the channel. Right: the time series of these different frequency components, taken at mid reef at the shoreline.

Regarding the contributions to runup of the different frequency components, the following things can be noted.

- IG waves are dominant at the shoreline, with a magnitude up to 50% of the offshore H_{m0} , which is approximately double the contribution of the other components. The peaks align with the runup peaks, but the local runup increase in the channel is not present in the IG wave heights. The vertical range is similar to the runup range.
- In this simulation, setup is the second largest contributor to runup. The channel decreases the shoreline setup globally, as it is lower than in the reference run. The setup peaks next to the channel align with runup peaks, and also show a peak inside the channel which is present in the runup pattern, but not in the IG pattern.
- $H_{m0,VLF}$ is approximately half the setup, with a similar longshore pattern
- $H_{m0,SS}$ only varies from the reference scenario in the vicinity of the channel. There are peaks just inside the channel.

5.2.5 Conclusion: runup pattern for one single simulation

Three statistical values are determined for further analysis: the peak $Ru_{2\%}^*$, minimum $Ru_{2\%}^*$, and mid reef $Ru_{2\%}^*$. There is longshore variation in runup in the presence of a channel: the vertical range between peak and minimum $Ru_{2\%}^*$ is 20% of H_s .

For this simulation there is a decrease in runup in the vicinity of the channel, with a small increase inside the channel, a peak next to the channel, and a gradual approach of the reference runup towards mid reef. Of the contributions of the different frequency components, $H_{m0,IG}$ is dominant for the large scale runup pattern compared to the other components. However, the other frequency components are responsible for the local increase in runup in the channel.

$Ru_{2\%}$ is up to 70% of incident wave height, which is in the range of runup values observed by (Demirbilek, Nwogu, and Ward 2007), where $Ru_{2\%}$ was found to be 45-100% of $H_{m0,offshore}$.

The longshore variation of 20% of H_s is slightly smaller than longshore runup variation on a sandy beach as identified by Senechal (2017), who found horizontal runup to vary over the longshore between 40-100m, corresponding to 0.8-2m in the vertical for H_s of 2m.

The importance of the IG component to runup is in line with findings from 1D reef studies, e.g. (Cheriton, Storlazzi, and Rosenberger 2016; Pearson 2016; Quataert et al. 2015). While IG wave heights of 50% of $H_{m0,offshore}$ seem high, comparable values were observed by (Pearson 2016), where the IG wave height at the inner reef flat was found to be up to 90% of the incident wave height, albeit not more than 55% for most cases. Furthermore, it should be noted that IG wave heights are likely to be overestimated, as only shore-normal waves without directional spreading are applied, a simplification which is known to overestimate IG wave heights (Veldt 2019; Sand 1982).

5.3 HYDRODYNAMICS ON REEF FLAT FOR ONE SINGLE SIMULATION

Longshore variations in runup might be the results of the hydrodynamics on the reef flat changing due to the presence of a channel. Therefore, wave heights, setup and velocities on the reef flat are examined in this section. The numerical model reports water level and flow velocities in every cell in 100s intervals, giving mean, maxima, minima and the variance, which are used to determine the mean setup, wave height and velocities.

5.3.1 Instantaneous water level

To gain insight in how waves translate over the reef, Figure 5.5 shows the instantaneous water level after about an hour of simulated time.

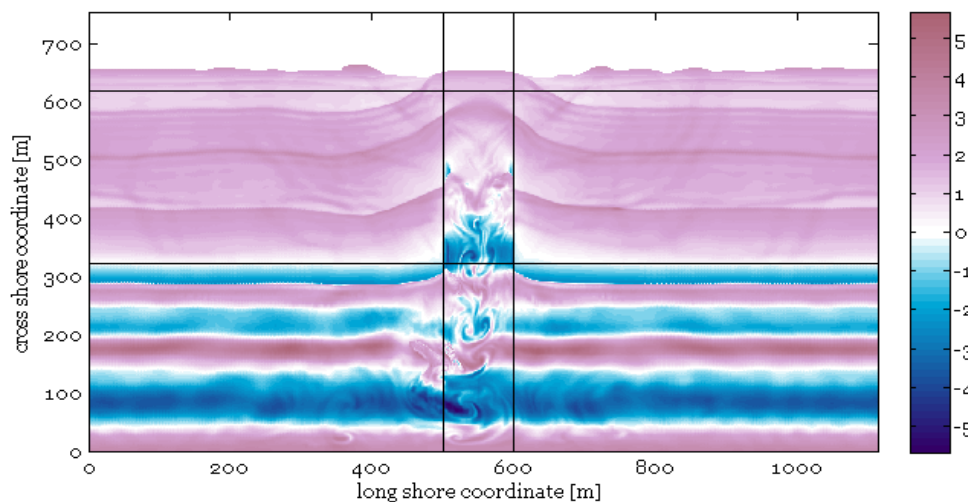


Figure 5.5, Top view of instantaneous water level after 4001s. Blue indicates the water level is lower than SWL, and pink indicates the water level is higher than SWL. The black lines mark the locations of the reef crest, beach toe, and channel.

From Figure 5.5 it can be noted that:

- Wave crests are shore normal at the offshore boundary, but in the vicinity of the channel the wave crests change direction, directed from the channel towards the reef flat, indicating diffraction and refraction.
- The return current contains eddies, indicating wave-current interaction. The return current deflects to the left, an asymmetry which was shown to change direction on the timescale of hours during model setup, and to average out over the duration of the model simulation.
- There are reflected wave crests which appear to originate from the channel at the shoreline and propagate in a semi-circle over the reef flat.
- The instantaneous runup level varies along the shoreline, with an instantaneous maximum 100m from the channel edge.

5.3.2 Wave height

Mean wave height H_{m0} is calculated from the variance of the water level as in Eq. 5.1. The influence of the channel is assessed by subtracting H_{m0} from H_{m0} in the reference run without a channel (H_{m0}^*).

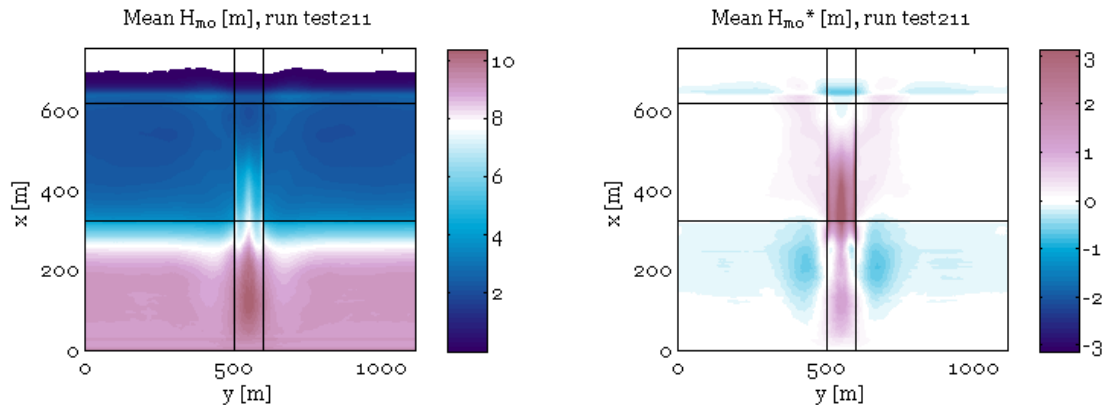


Figure 5.6, Top view of wave height in the entire model domain. Mean wave height H_{m0} (left), and mean relative wave height H_{m0}^* (right). In the right figure, pink indicates the wave height is larger than in the reference case, and blue indicates a decrease compared to the reference case.

From top views of H_{m0} and H_{m0}^* , presented in Figure 5.6 the following things can be noted:

- Wave height is largest offshore from the channel, in line with the channel as a result of wave-current interaction.
- Waves break in front of the reef crest, and continue to decrease towards the shoreline.
- There is a high longshore gradient of wave height in the channel,
- Comparing simulations with and without a channel, the differences are from -3 to +3m, indicating the channel has large influence on wave propagation. There is a relative increase inside the channel and a decrease offshore next to the channel. On the reef flat, the difference is small, but at the shoreline there is a pattern of decrease mid reef and in the channel, and increase next to the channel, aligned with the runup peaks.

5.3.3 Setup

The mean setup (η_{mean}) is calculated as the mean water level over the entire simulation, and the influence of the channel is assessed by subtracting the setup from the reference run without a channel (η_{mean}^*), as shown in Figure 5.7.

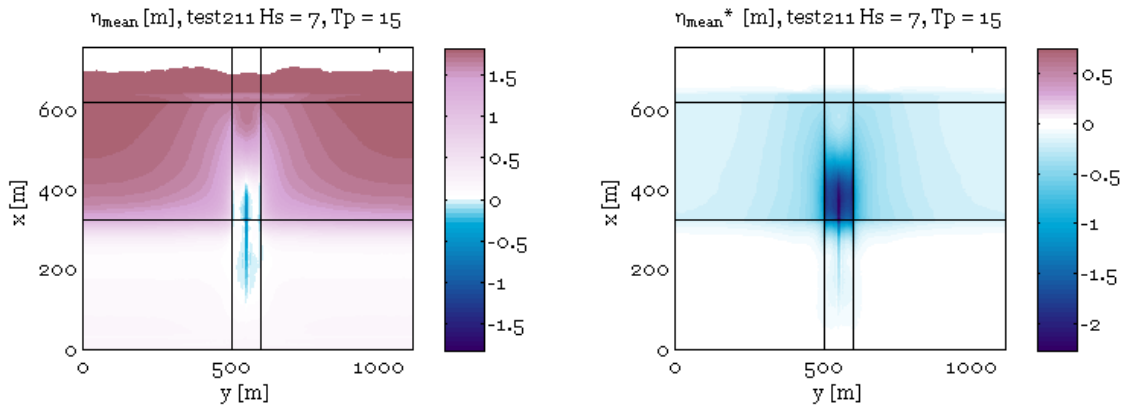


Figure 5.7, Top view of setup in the entire model domain. Left: mean setup. Right: mean setup relative to the reference level, the pink zones indicate a positive value, and the blue ones a negative one. In this figure, offshore is on the bottom at $x=0$ m, and the shoreline on the top.

Regarding setup, the following things can be noted:

- Similar to in 1D schematizations, wave forcing causes setup on the reef flat up to 1.5m.
- In the channel, in the vicinity of the reef crest, η_{mean} is lower than the SWL, Near the shoreline, the setup is positive, decreasing from mid reef towards the channel
- The channel globally decreases setup, up to 2 meters. The difference is strongest in the channel near the reef crest, and decreases with increasing distance from the channel.
- Setup increases cross-shore from the reef crest towards the beach toe, and longshore from the channel towards the mid reef.
- There is a steep water level gradient on the channel edges.

5.3.4 Flow pattern

The strong gradients in wave height and setup are hypothesized to be a result of the circulation on the reef flat. Therefore the flow pattern is studied, using cross shore and longshore velocities presented in Figure 5.8 as well as the vorticity pattern, which indicates in what locations the rotation and circulation of the flow is strongest, calculated as in Eq. 5.2, and the circulation pattern, presented in Figure 5.9. Furthermore, the flow velocity in the channel is related to wave-current interaction. Therefore, the maximum time-averaged offshore directed velocity in the channel is determined and used in the comparison of simulations in the next section.

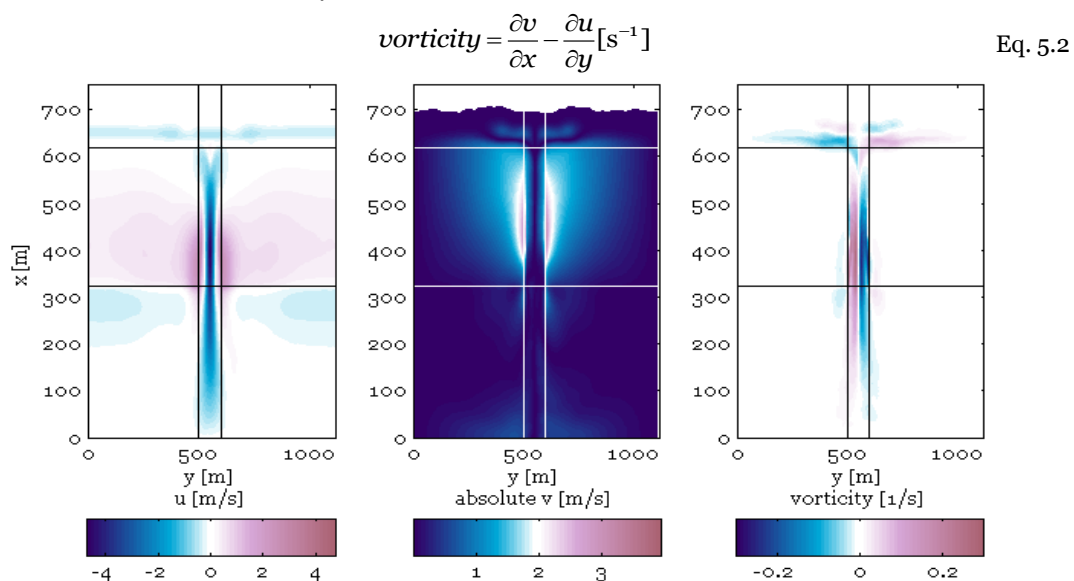


Figure 5.8, Top view of time averaged velocities and vorticity. Left: mean velocity in cross shore direction (u). Middle: mean velocity in longshore direction (v). Right: mean vorticity.

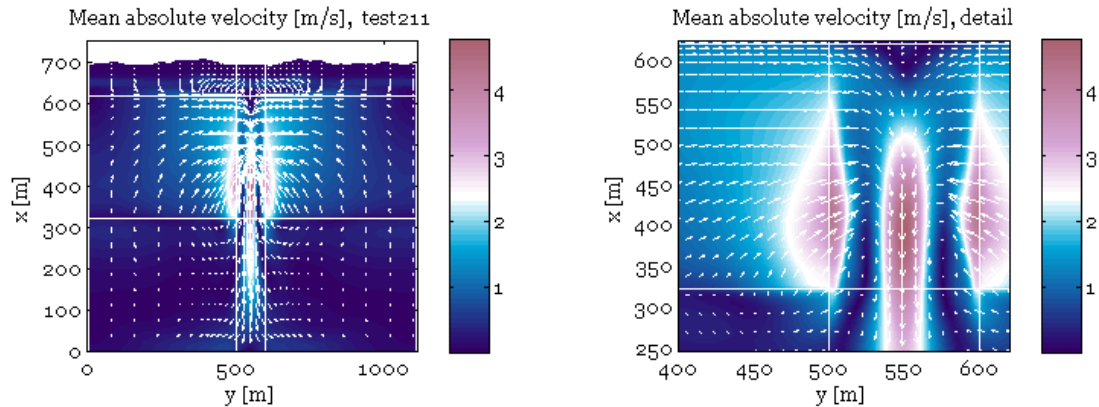


Figure 5.9, Flow circulation pattern, absolute velocity and direction arrows, presented for full model domain (left), and detail of the channel and part of the reef flat (right).

Regarding the flow pattern, the following things can be noted:

- There is a circulation pattern on the reef flat: flow is directed onshore on the reef flat, and offshore in the channel.
- The return current is strong and reaches mean velocities of up to 4 m/s in the center of channel. The channel plume extends far offshore.
- Onshore velocities are largest in the vicinity of the channel, on the shoreward half of the reef flat, where they reach up to 3 m/s. 100m Away from the channel, maximum cross shore velocities have decreased to 0,7m/s.
- Longshore flow from mid reef towards the channel, and reach values of 4 m/s at the channel edge
- Vorticity has the shape of the letter T, being confined to the shoreline, channel, and channel plume. Maxima are 0.27 s^{-1} .
- At the shoreline, flow is dominantly directed towards the channel, but as vorticity is high at the shoreline, 2D effects are present.
- Mid reef, flow is dominantly cross shore, directed onshore. Near the channel, strong gradients in magnitude and direction occur.
- Overall flow velocities are large, exceeding 1 m/s on nearly half of the reef flat.

5.3.5 Channel discharge patterns

To further examine the circulation pattern, the discharge pattern, presented on the left in Figure 5.10 is plotted. Pink indicates a net onshore flow and blue a net offshore flow. Two circles indicate the location of maximum and minimum discharge. Furthermore, to enable comparison of different forcings and geometries, the magnitude of the flow circulation is quantified by the total discharge through the channel, presented on the right in Figure 5.10. The parameter Q_{offshore} is introduced for this, determined by integrating all offshore directed discharge along the reef crest. Q_{offshore} is negative by definition. From the discharge pattern the following things can be noted:

- On the reef flat discharge is onshore directed, varying from 0-6 $\text{m}^3/\text{m/s}$
- Both the maximum and minimum discharge are found in the channel, indicating gradients are strong. Discharge ranges from -120 to +14 $\text{m}^3/\text{m/s}$.
- Offshore discharge is an order of magnitude larger than onshore discharge, it occurs only in a narrow zone in the middle of the channel.
- Total offshore discharge is nearly 2800 m^3/s .

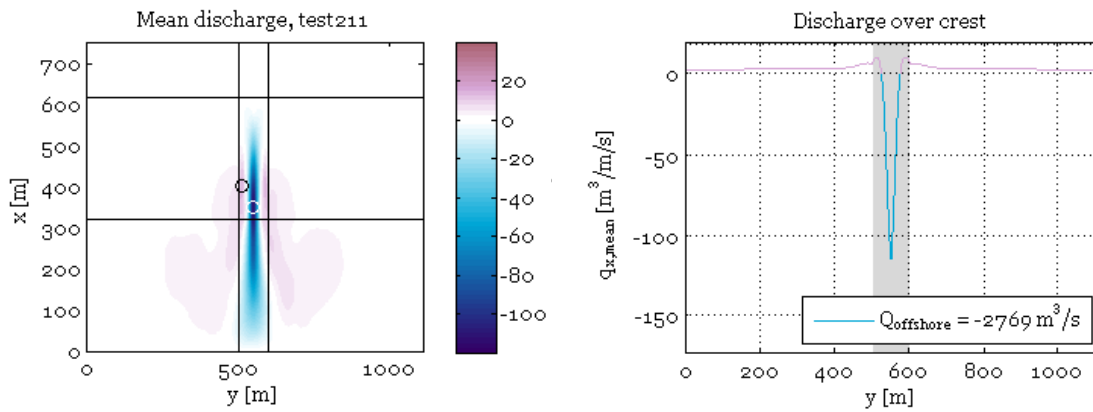


Figure 5.10, Cross shore discharge [$\text{m}^3/\text{m}/\text{s}$], positive onshore. Left: top view. Pink indicates onshore directed, and blue indicates offshore directed. The black circle marks the location of the maximum discharge (onshore directed), and the white circle marks the location of the minimum discharge (offshore directed). Right: discharge over the reef crest. The total offshore directed discharge is calculated by integrating over the entire zone with offshore discharge.

5.3.6 Link between reef hydrodynamics and runup

To examine the relation between reef hydrodynamics and runup, the longshore runup pattern is compared to wave height and setup on three locations on the reef flat in Figure 5.11.

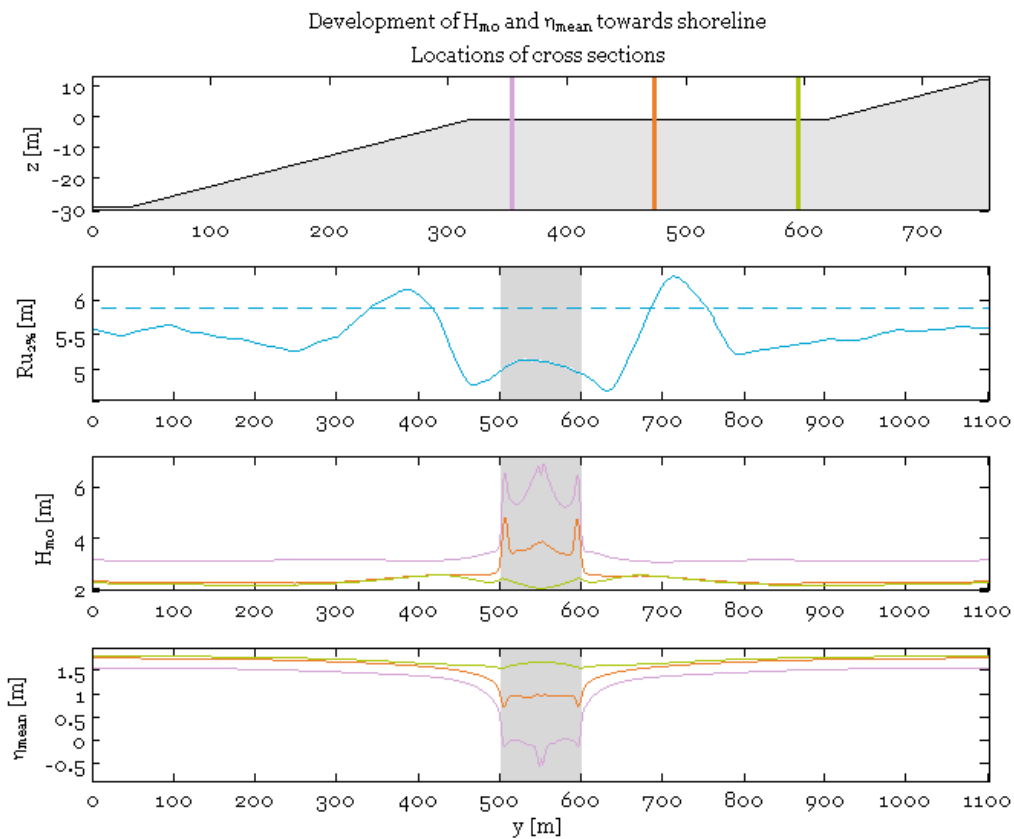


Figure 5.11, Development of H_{m0} and η_{mean} towards shoreline. Three cross sections are shown, respectively 10%, 50% and 90% between reef crest and beach toe (270, 150 and 30 meters from the beach toe), as illustrated in the top figure by the pink, orange and green line. The second figure shows the runup pattern at the shoreline for comparison. The third figure shows the wave height development, and the fourth shows the development of mean water level towards the shoreline.

From Figure 5.11 the following things can be noted:

- H_{m0} is found to decrease towards the shoreline, while η_{mean} increases. This is in line with radiation stress theory.

- Variation of H_{m0} and η_{mean} is most notable within 100 meters from the channel, while the runup pattern shows strong variation for double the distance.
- Both H_{m0} and η_{mean} show sharp gradients around the channel edge.
- The cross section closest to the beach toe shows the best correspondence with the runup pattern. The increase in runup inside the channel aligns with the peak in setup of the green line. Wave height shows a small peak 70 meters from the channel, but this does not align with the runup peaks.

5.3.7 Conclusion and discussion hydrodynamic on reef for one single simulation

The channel strongly influences setup and wave height on the reef flat and in the channel and generates a circulation. Gradients of water level, wave height and flow velocity are all very strong in the vicinity of the channel. Setup increases towards the shoreline and towards mid reef. Differences in wave height are most notable on the fore reef, in the channel and at the shoreline. The flow pattern is strongly 2D, showing a circulation with net onshore flow on the reef flat and a strong return current in the channel, with large velocities and vorticity in the vicinity of the channel. The cross-shore discharge is positive throughout most of the model domain and offshore only in a narrow zone in the channel, resulting in an order of magnitude difference. H_{m0} and η_{mean} 30 meters away from the beach toe show increasing correspondence with the runup pattern, but still there are significant differences.

Setup is larger away from the channel and minimum where the return current is strongest. This suggests the channel acts as a drain of the reef flat, attracting flow and causing strong water level gradients. The flow velocities in the circulation reduce the setup on the reef flat by an amount at least equal to the velocity head of the wave-generated flow across the reef following Bernoulli's law, as was also found by Gourlay and Colleter (2005). Still, the reduction of setup due to the presence of the channel seems very large, and there are local peaks in setup next to the channel, which are not explained by this. Possibly this is the results of the momentum carried away through the return current combined with WCI, diffraction and refraction in the channel.

Wave heights are found to be highest offshore of the channel. As the return current extends to far offshore of the channel, shoaling due to WCI is likely the cause of these high wave heights. Traveling shoreward through the channel, waves bend from the channel towards the reef flat, presumably due to refraction and diffraction. Strong gradients of water level, flow velocity and high vorticity in this zone may also play a role. At the shoreline, a large part of the wave energy has translated to the zone next to the channel, with corresponding increased runup.

The strength of the return current indicates that momentum is carried away through the channel, the momentum balance is no longer cross shore but 2D and setup is decreased, resulting in lower runup levels around the center of the reef flat.

It should be noted that the strong gradients near the channel are an indicator that 3D effects may occur on real reefs, which are not reproduced by the depth averaged model representation.

As there are significant differences between the patterns of H_{m0} and setup 30m from the shoreline, it is likely that there are other factors of influence on runup than solely setup and wave height, such as wave direction.

5.4 IMPACT OF DIFFERENT FORCINGS AND REEF GEOMETRIES ON RUNUP PATTERN

To compare different simulations and assess the influence of varying forcing and geometry on runup, overview figures are made for each geometry containing every forcing, and, vice versa, for each forcing containing every geometry. Again, the comparisons for the baseline geometry and

for one forcing are presented in this section, for the other geometries and forcings the overview figures are presented in Appendix D and Appendix E.

5.4.1 Impact of varying forcing on longshore runup patterns

The impact of forcing on longshore runup patterns is assessed by plotting all variations in forcing for the same fixed geometry, as in Figure 5.12, which presents an overview of the longshore runup for all simulations with the baseline geometry.

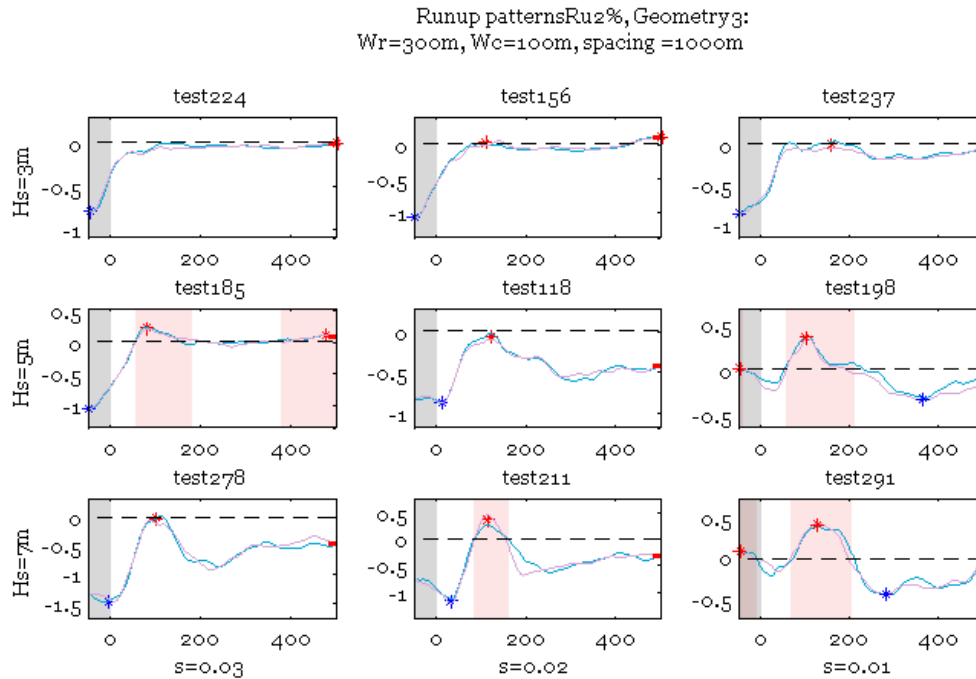


Figure 5.12, Longshore runup overview for all simulations with the baseline geometry: $W_c = 100\text{m}$, $W_r = 300\text{m}$, $\text{spacing} = 1000\text{m}$. Nine different forcings are presented: H_s increases from top to bottom, and wave steepness decreases from left to right, so the wave length increases from left to right. The x-axis of each graph represents y^* , and the y-axis represents $Ru_{2\%}^*$. The grey shading marks the location of the channel (negative values of y^*), and the red shading marks high runup zones where the runup is higher than the reference runup without a channel.

For this geometry, the following can be noted regarding the runup pattern:

- There is significant variation in shape of runup pattern for varying forcing.
- The range of runup, defined as the difference between the highest peak and the minimum, varies for different forcings on the same geometry. It is minimum 68 cm and maximum 150 cm, which is about 20% of H_s .
- For $H_s = 3\text{m}$ there are clear troughs in the channel, but no pronounced peaks on the reef flat
- All runs except for $H_s=3\text{m}$, $s=0.03$ show a peak at $y^* = 80\text{-}125\text{m}$
- The five runs with the longest period show a local peak in the channel.
- The $Ru_{2\%}^*$ at mid reef varies between 0 and -0.5m .
- The location of the lowest runup varies; while it lies inside or right next to the channel for 7 of the 9 forcings, it is located at 1/4-1/3 of the reef flat for the two longest waves with $s=0.01$

Complete overviews of the other geometries are presented in Appendix D. Table 5.2 presents the findings for varying forcings regarding the runup pattern.

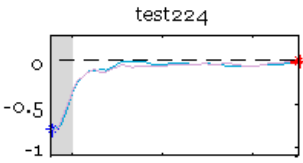
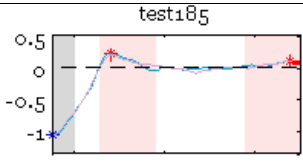
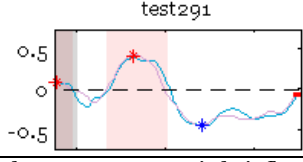
Variation in forcing	Example runup pattern
<p>Small and short waves The two forcings with the lowest ($H_s = 3\text{m}$) and shortest waves don't show the significant peak in runup next to the channel, runup just decreases from mid reef towards the channel.</p>	
<p>Middle forcings Middle forcings ($H_s = 5\text{m}$) show the most common runup pattern with the three components as described above,</p>	
<p>High and long waves The two forcings with the highest and longest waves ($H_s = 7\text{m}$) show a different runup pattern, more showing a dual runup system with one inside the channel and a second one next to the channel</p>	

Table 5.2, Findings from comparison of the results for different forcings. The runup pattern is briefly discussed per forcing, and representative runup patterns are displayed as an example.

5.4.2 Impact of reef geometry on longshore runup patterns

The impact of reef geometry on longshore runup patterns is assessed by comparing runup patterns with identical forcings but varying geometries, of which overview figures are presented in Appendix E. From this comparison it is concluded that runup patterns vary strongly for different geometries. Most intermediate geometries show approximately the same pattern with (1) a minimum inside or right next to the channel, (2) a peak next to the channel, next to which $Ru_{2\%}^*$ drops again, (3) a gradual approach of the reference runup without a channel towards the mid reef, and (4) a local peak inside the channel. The last characteristic is present in only part of the simulations. Variations in both geometry and forcing change one or more of these characteristics:

- For small and short waves the runup pattern does not show a clear peak, just a decrease in runup towards the channel
- Long waves and wide channels both result in a dual peak system with a second peak inside the channel.
- Narrow reefs make the runup pattern more alternating and irregular, while wide reefs decrease runup compared to the reference runup without a channel
- Short channel spacings move the runup peak towards mid reef, while for long spacings the longshore runup variation stays restricted to the vicinity of the channel.
- The largest peaks occur in the channel, for wide channels and high and long waves. Peaks are largest as the channel takes up a large fraction of the total shoreline and when the incident wave period is closer to the resonant period of the reef.

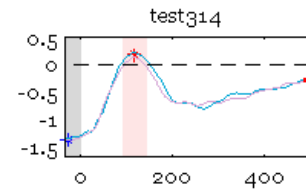
Table 5.2 presents the findings for variations in geometry regarding the runup pattern.

Variation in geometry

Narrower channel:

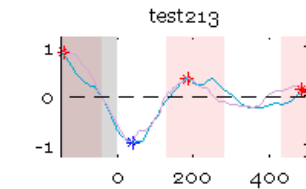
The two geometries with the narrowest channel, 50 and 70m (geometry 1 and 2) show similar runup patterns, with a clear trough in and next to the channel, one runup peak zone about 90-150m from the channel, next to which the runup decreases again and gradually approaches the reference runup towards the mid reef. Mid reef runup is still lower than reference runup. While the shape of this pattern is similar for these geometries, the value of peak runup is dependent on the forcings, and the range of runup (difference between maximum and minimum) varies from 0.55m to 1.98m.

Example runup pattern



Wider channel:

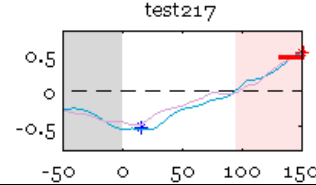
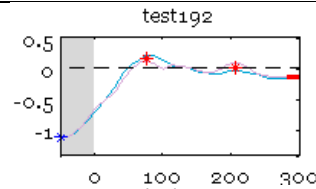
When the channel becomes wider, 200 or 300m (geometries 4 and 5), the runup pattern shows a dual set of peaks, with one peak in the channel, and one on the reef flat. The peak on the channel becomes more dominant for longer waves and a wider channel. The maximum occurring peak is 2.5m above the reference runup, so the channel increases runup with 35% of H_s . The peak runup on the reef flat can be up to 1m above the reference runup, and the location is further from the channel compared to narrower channel geometries, ranging 140-240m from the channel. Mid reef runup approaches or exceeds the reference runup, up to 0.3m. For the 300m channel, $Ru_{2\%}^* > 0$ on over half of the reef flat.



Short channel spacing:

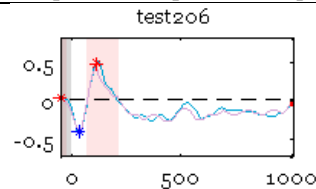
When the spacing between channels is decreased to 600m (geometry 10), the peak runup shifts further towards mid reef, but generally remains 100-150m from the reef crest. For most forcings, the typical trough-peak pattern remains, albeit less distinct.

When the channel spacing is decreased further to only 300m (geometry 9), the pattern is again clearly different, runup is increasing towards the mid reef, peaking at mid reef, with $Ru_{2\%}^*$ going as high as 1 m or 15% of H_s .



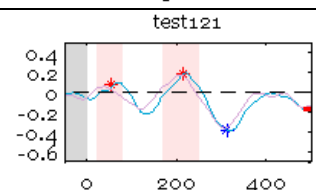
Long channel spacing

When the channel spacing is increased to 2000m (geometry 11), variation in the runup patterns is restricted to the first 300m of the reef flat with $Ru_{2\%}^*$ up to 0.51m. On the rest of the reef flat runup slightly below the reference runup,



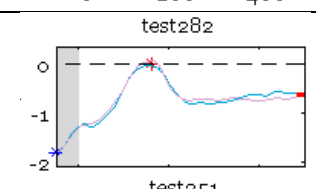
Narrow reef:

For a narrow reef, with only 100m between reef crest and beach toe (geometry 6), the runup pattern is very irregular. There is not one clear peak zone, but $Ru_{2\%}^*$ is alternately positive and negative. Both maximum and minimum runup locations are found along the entire model domain. While the shape of the runup pattern is most irregular of all geometries, the vertical range is the smallest of all geometries, of only 0.27-1m.



Wider reef:

When the reef is wider, 500m (geometry 7), the runup pattern again shows a trough in the channel, a peak at 120-175m from the channel, but in this case the runup barely exceeds the reference runup, with maximum $Ru_{2\%}^* \approx 0$. Except for the two longest wave runs, $Ru_{2\%}^* < 0$ globally, with a minimum of -1.8m.



When the reef is extremely wide, 1000m (geometry 8), runup is again globally lower than reference runup, with the exception of the longest wave run. Maxima are -0.25 to -0.45m. Also, there is no distinct peak, but rather a clear trough in the channel which decreases towards mid reef. Minima get as low as -1.4m

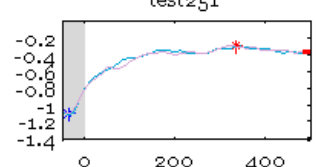


Table 5.3, Findings from comparisons of the results per geometry. The runup pattern is briefly discussed per geometry, and representative runup patterns are displayed as an example.

5.4.3 Conclusions: runup pattern for all simulations

The findings of the previous section on varying runup patterns for varying forcing and geometry, as stated in Table 5.2 and Table 5.3 are presented in a conceptual figure that illustrates the general runup pattern for a reef-system, and what impact of each parameter has on this pattern, presented in Figure 5.13. This conceptual figure illustrates the conclusions regarding the longshore varying runup pattern.

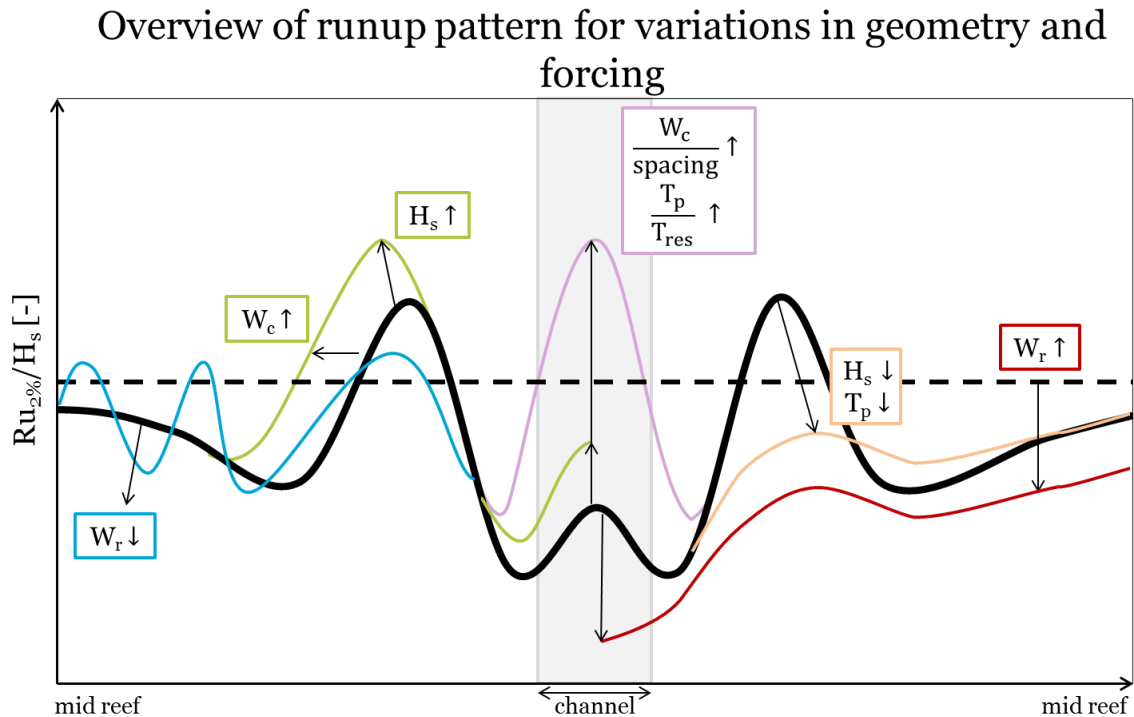


Figure 5.13, Overview of runup pattern for variations in geometry and forcing. The solid black line shows the general longshore runup pattern for a reef with a channel, and the dashed line represents the reference line for a case without a channel. The colored lines illustrate the influence of variations of forcing and reef geometry.

This conceptual figure illustrates the conclusions regarding the longshore varying runup pattern:

Both geometry and forcing affect the longshore runup pattern in the presence of a channel. In general $Ru_{2\%}^$ maxima are positive and $Ru_{2\%}^*$ are negative (relative to the reference scenario without a channel).*

In general: the runup pattern shows 4 characteristics: (1) a minimum inside or right next to the channel, (2) a peak next to the channel, next to which $Ru_{2\%}^$ drops again, (3) a gradual approach of the reference runup without a channel towards the mid reef, and (4) a local peak inside the channel. The last characteristic is present in only part of the simulations. Variations in both geometry and forcing change one or more of these characteristics:*

- *For small and short waves the runup pattern does not show a clear peak, just a decrease in runup towards the channel*
- *Long waves and wide channels both result in a dual peak system with a second peak inside the channel.*
- *Narrow reefs make the runup pattern more alternating and irregular, while wide reefs decrease runup compared to the reference runup without a channel*
- *Short channel spacings move the runup peak towards mid reef, while for long spacings the longshore runup variation stays restricted to the vicinity of the channel.*
- *The largest peaks occur in the channel, for wide channels and high and long waves. Peaks are largest as the channel takes up a large fraction of the total shoreline and when the incident wave period is closer to the resonant period of the reef.*

5.4.4 Runup maxima and minima distribution

To find patterns in the runup and assess the influence of varying parameters, scatterplots are made, in which minima and maxima of each simulation are plotted. Next to the overall maximum, the maximum for each peak zone is plotted. Some scatterplots are presented and discussed below, but for a more complete overview, one is referred to Appendix H.

Runup versus input parameters

To assess the influence of the input parameters, the maximum $Ru_{2\%}$ of every simulation is plotted against the five input parameters W_c , W_r , spacing, H_s and wave steepness in Figure 5.14. The subfigures of W_c , W_r and spacing show only the selection of simulations for which the subjected parameter is varied, so variations of W_r are excluded from the scatterplot of W_c etc. Runup maxima are higher for scenarios with higher H_s , a lower steepness, very short channel spacing, a narrower reef, and wider channels. Both H_s as steepness have a large influence on $Ru_{2\%}$. Of geometry, channel width W_c has the strongest influence on $Ru_{2\%}$.

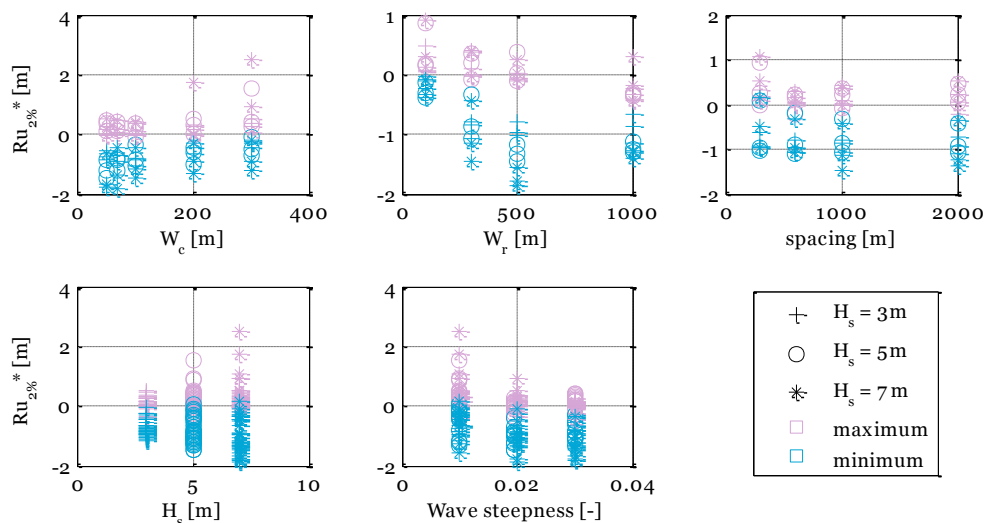


Figure 5.14, $Ru_{2\%}^*$ for different input parameters: varying geometrical parameters (top row), and forcing parameters (bottom row). The marker shapes indicate the significant wave height.

Runup maxima versus the peak locations

To see if runup $Ru_{2\%}^*$ peaks are located on a fixed location from the channel edge, $Ru_{2\%}^*$ maxima are plotted against their distance from the channel edge y^* in Figure 5.15.

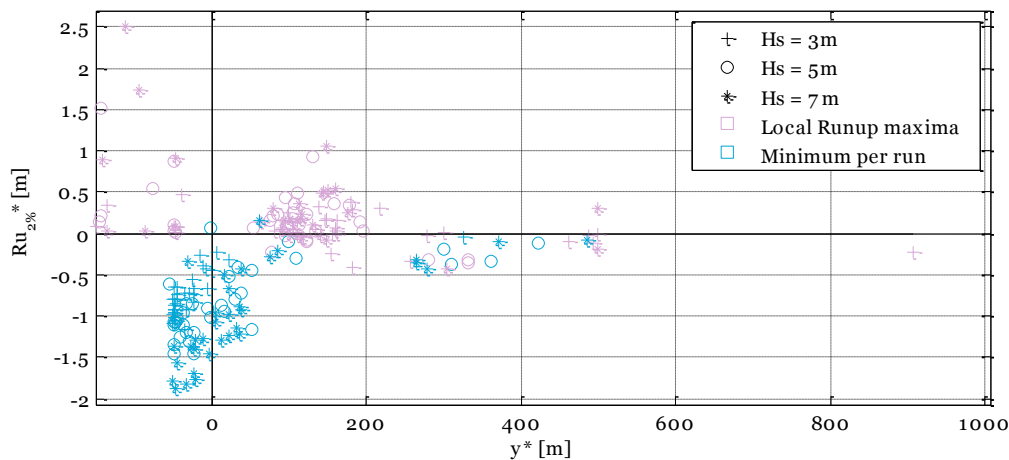


Figure 5.15: Runup scatterplot. $Ru_{2\%}^*$ values are plotted against y^* . Different marker shapes represent different significant wave heights. For each run, the overall maximum $Ru_{2\%}^*$ is plotted, as well as the maximum $Ru_{2\%}^*$ in each peak zone, and the global minimum $Ru_{2\%}^*$.

From Figure 5.15, the following things can be noted: there are three zones with high runup values occurring: 1) Inside the channel, originating from runs with wide channels or high and long waves, 2) 80-200m from the channel, for most simulations and 3) 500m from the channel, corresponding to mid reef peaks for most simulations.

- Generally, higher waves result in higher $Ru_{2\%}^*$
- Most simulations (90%) have a maximum of $Ru_{2\%}^* < 0.5m$. Of the highest 10%, the majority is found in the channel, and originates from simulations with very long offshore wave lengths and/or a wide channel.
- Minimum $Ru_{2\%}^*$ is mostly restricted to 70m within the edge of the channel, and decrease with increasing wave height.

Runup versus dimensionless parameters

As the previous section showed $Ru_{2\%}^*$ is highest for high H_s and long waves, the influence of L_0 and H_s is further assessed in Figure 5.16, a dimensionless scatterplot. $Ru_{2\%}^*$ is presented as a fraction of the offshore wave height, and the longshore coordinate is related to the offshore wave length. The influence of the wave length is made visible by the color of the markers.

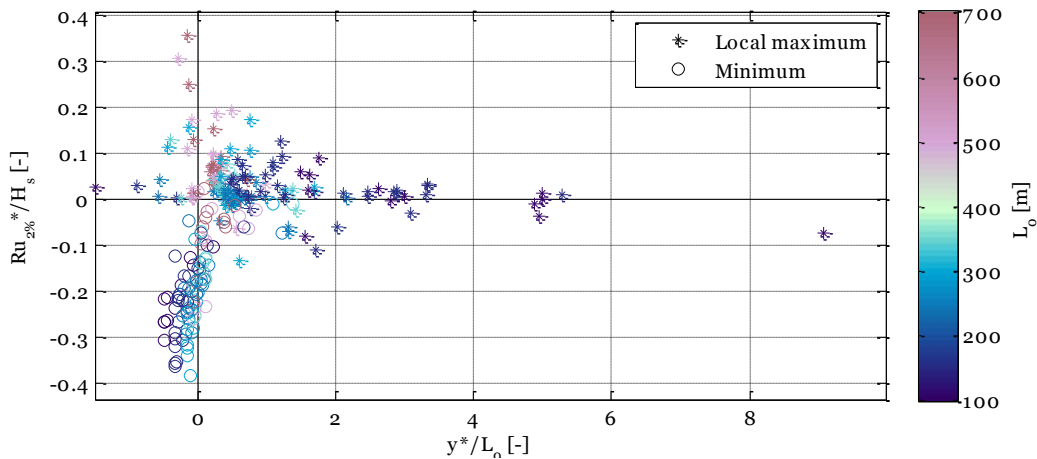


Figure 5.16, Dimensionless runup scatterplot. Runup is divided by H_s and y^* is divided by L_0 . Maxima are marked by an asterisk, and minima by a circle. The color of the markers represents the offshore wave length.

From Figure 5.16 it can be noted wave length has a large influence on both the location and magnitude of $Ru_{2\%}^*$:

- Runup peaks are found within 2 wave lengths of the channel, of which the highest ones stay within one wave length of the channel.
- Longer waves increase the maximum runup, not only absolutely, but also relative to H_s . $Ru_{2\%}^*$ is generally less than 10% of H_s for shorter waves ($L_0 < 250m$), while it reaches up to 40% of H_s for longer waves.
- Minima of shorter waves are found in the channel, while minima of longer waves are found on the reef flat.

It is expected that the channel has a stronger influence on runup when the channel makes up a larger percentage of the total shoreline. The influence of a channel is also expected to increase when the time scale of the forcing approaches the resonant time scale of the reef flat. To test this hypothesis runup is plotted against two dimensionless parameters $W_c/spacing$ and T_p/T_{res} in Figure 5.17 and Figure 5.18. The resonant timescale is estimated using Eq. 5.3 based on Eq. 2.10, in which the water depth on the reef is the still water depth plus setup, estimated as 10% of the incident wave height (Tait 1972):

$$T_{res} = \frac{4L}{\sqrt{gh}} = \frac{4L}{\sqrt{g\left(h_o + \frac{H_s}{10}\right)}} \quad \text{Eq. 5.3}$$

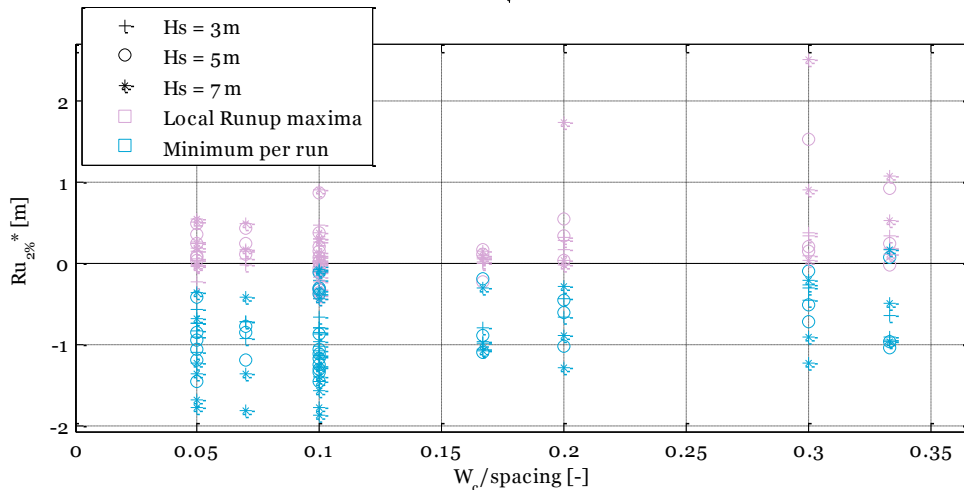


Figure 5.17, Runup plotted against the fraction of the shoreline that consists of channel: $W_c/\text{spacing}$

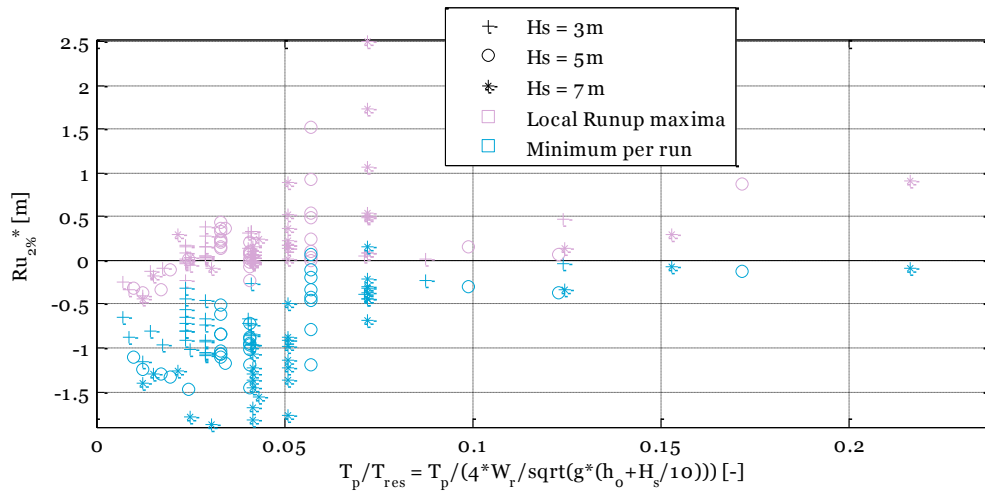


Figure 5.18, Runup plotted against the forcing timescale divided by the first order resonant timescale: T_p/T_{res}

$Ru_{2\%}^*$ increases as the channel makes up a larger part of the shoreline, but there is significant scatter (Figure 5.17), and initially increases as the timescale of the forcing approaches the timescale of the first order resonant period (Figure 5.18). There is a break of this trend line at $T_p/T_{res}=0.08$, after which runup increases again. When looking into the markers right from this trend break, these markers originate from simulations with a narrow reef $W_r=100\text{m}$.

To obtain a dimensionless parameter that includes all input parameters, the above two parameters are multiplied and presented in Figure 5.19. While scatter is still present, there is a clear trend visible: $Ru_{2\%}^*$ as a fraction of H_s increases for increasing $\frac{W_c}{\text{spacing}} * \frac{T_p}{T_{res}}$.

For lower values of $\frac{W_c}{\text{spacing}} * \frac{T_p}{T_{res}}$, $Ru_{2\%}^*$ shows a scatter up to $Ru_{2\%}^* = 0.1 * H_s$. Minimum $Ru_{2\%}^*/H_s$ also

shows scatter, but here too an upward trend is visible for increasing $\frac{W_c}{\text{spacing}} * \frac{T_p}{T_{res}}$.

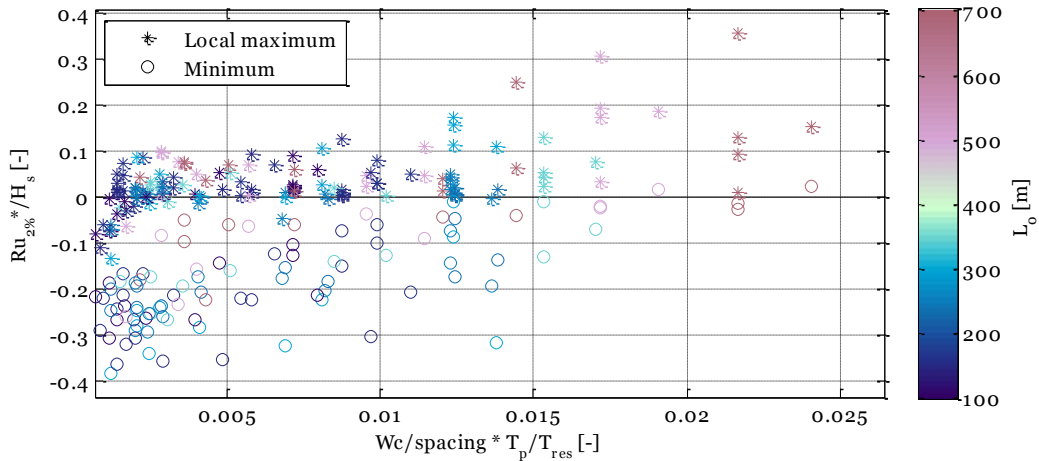


Figure 5.19, Dimensionless runup scatterplot, $Ru_{2\%}^*/H_s$ versus $W_c/spacing * T_p/T_{res}$. The star markers indicate maxima and the circle markers minima. The color of the markers corresponds with offshore wave length.

5.4.5 Conclusion and discussion: runup maxima

Runup peaks increase for higher waves, lower wave steepness, shorter channel spacing, narrower reefs and wider channels. Next to absolute $Ru_{2\%}^$, the normalized $Ru_{2\%}^*/H_s$ increases too.*

Of geometry, channel width has the strongest influence on $Ru_{2\%}^$. Of forcing, offshore wave length is the best indicator for high ratios of $Ru_{2\%}^*/H_s$.*

The location of the peaks is either within the channel (for wide channels and long waves) or relatively close to the channel (200 m, or 2 wavelengths)

Combining parameters, runup is found to increase as the channel makes up a larger part of the reef, and as the period of the forcing approaches the resonant period of the reef. However, there is scatter: $Ru_{2\%}^$ shows scatter up to 10% of H_s for low values of $W_c/spacing * T_p/T_{res}$.*

For most simulations runup is highest on the reef flat. In that case, $Ru_{2\%}^*$ is generally up to 10% of H_s . However, the highest maxima $Ru_{2\%}^*$ are all found inside of the channel and originate from simulations with very wide channels and/or very long waves. In those cases $Ru_{2\%}^*$ is up to 40% of H_s . This indicates there are two categories of extreme runup levels: inside the channel and on the reef flat.

From the available data, runup shows an increasing trend for increasing $W_c/spacing * T_p/T_{res}$. This is in line with expectations, as when the channel takes up a large part of the reef, the situation is expected to approach a situation without a reef in the center of the channel. Furthermore, as the forcing period approaches the resonant period of the reef, shoreline response also increases (Pomeroy, van Dongeren, et al. 2012).

Concerning resonance, all incoming wave periods are much shorter than the resonant period of the reef: $T_p/T_{res} \ll 1$ for most simulations, indicating the simulations are not in the resonant period of the reef. However, the generated infra gravity wave periods are an order of magnitude longer and may well be around the resonant period of the reef. Further analysis of the IG waves is recommended to check if resonance occurs and whether this explains the extreme runup values.

Furthermore, it should be noted that there are only few data points in the region of extreme $Ru_{2\%}^*$, only 10% of the $Ru_{2\%}^*$ maxima exceed 15% of H_s . Furthermore, there is quite some scatter between these data points. Future simulations with the range of conditions that lead to extreme runup response could improve the accuracy in describing this trend.

5.4.6 Impact of geometry and forcing on flow circulation and return current

The total offshore discharge and the maximum time averaged offshore velocity in the channel ($u_{\text{mean,offshore,max}}$) are used as a measure for the reef circulation and return current. The impact of varying forcing and geometry on the discharge and flow velocity is presented in Figure 5.20 and Figure 5.21. Again, the scatterplot for one geometrical parameter contains only variations of this parameter and not the others. From these figures the following things can be noted:

- The discharge varies from -250 to -4750 m^3/s between simulations, equivalent to mean discharges of the rivers Meuse to double the Rhine discharge.
- Of the geometrical parameters, reef width has the most influence on discharge, the largest 10% discharges all have a reef width of 500 or 1000m.
- Circulation becomes slightly stronger for increasing channel spacing, but seems to cease to increase for larger spacings.
- Discharge increases with wave height, and decreases with increasing wave steepness.
- $u_{\text{mean,offshore,max}}$ varies from -1.5 to -5m/s. It mostly shows the same response to input parameters as the discharge, except that flow velocities increase for narrower channels, and the increase in velocity for wide reefs is not as strong as for the discharge.

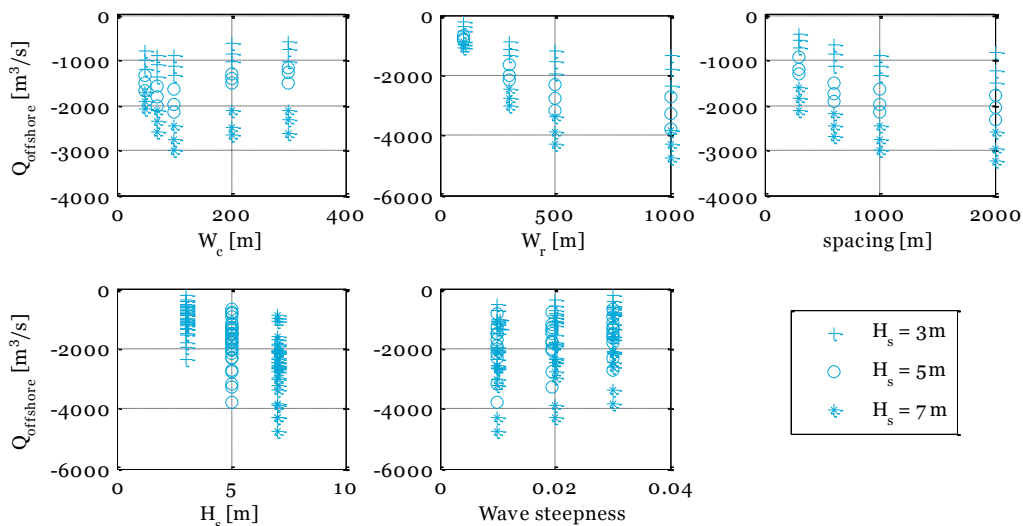


Figure 5.20, Offshore discharge for different input parameters: varying geometrical parameters (top row), and forcing parameters (bottom row). The marker shapes indicate the significant wave height.

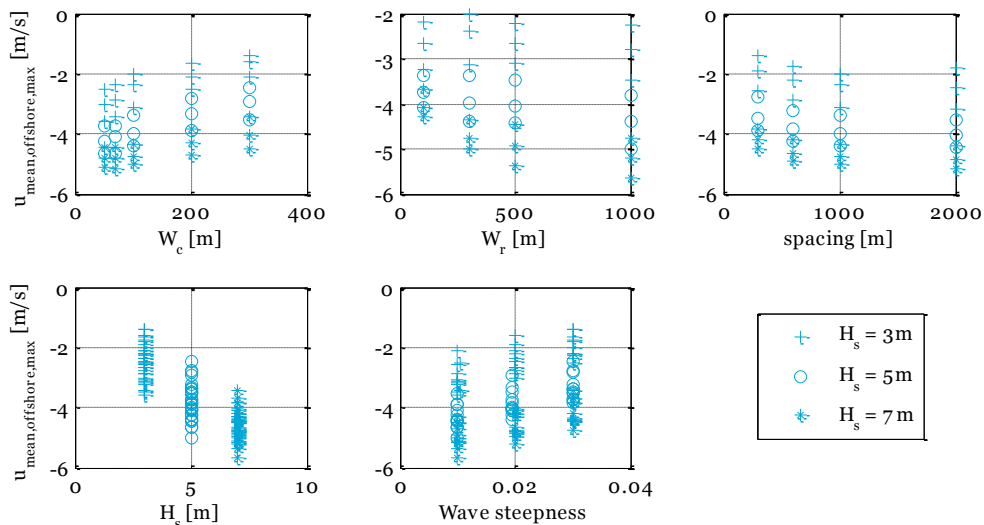


Figure 5.21, The maximum time-averaged offshore directed velocity for different input parameters: varying geometrical parameters (top row), and forcing parameters (bottom row). The marker shapes indicate the significant wave height.

$Ru_{2\%}^*$ is plotted against offshore discharge in Figure 5.22 and against $u_{\text{mean,offshore,max}}$ in Figure 5.23. Initially, runup maxima seem to scale with increasing discharge, but for discharges exceeding 2700 m^3/s (mainly the 500 and 1000m W_r), no such relation is present. $Ru_{2\%}^*$ minima are found to decrease with increasing discharge. This might be a result of the return current lowering the water level in the channel. $Ru_{2\%}^*$ increases with increasing flow velocities, but there is some scatter of the results.

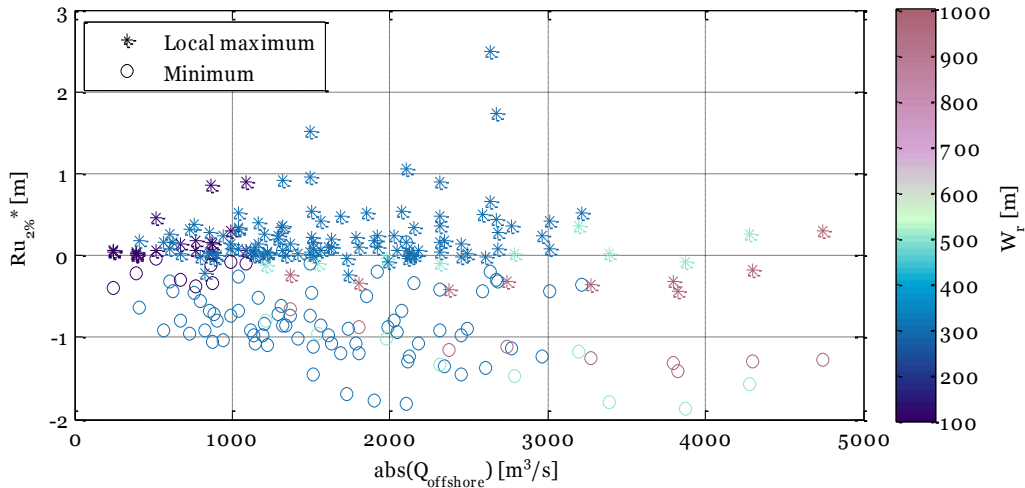


Figure 5.22, $Ru_{2\%}^*$ versus discharge. The different marker colors indicate the reef width W_r . Asterisks indicate local maxima and circles indicate minima in $Ru_{2\%}^*$.

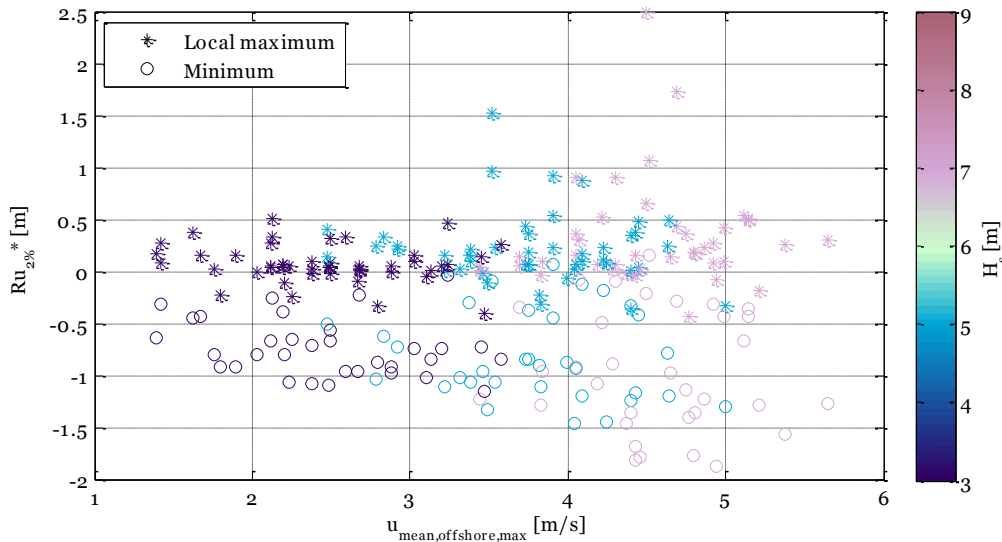


Figure 5.23, $Ru_{2\%}^*$ versus $u_{\text{mean,offshore,max}}$. The different marker colors indicate varying H_s . Asterisks indicate local maxima and circles indicate minima in $Ru_{2\%}^*$.

5.4.7 Conclusion and discussion: circulation and return current versus runup

Reef circulation increases for higher waves, lower wave steepness, and an increasing reef width. For low to moderate reef widths up to 300m, there seems to be a positive relation between channel discharge and $Ru_{2\%}^$, but for larger reef widths, no such relation is present. The flow velocities in the channel show a positive correlation with $Ru_{2\%}^*$ maxima, but there is some scatter.*

Runup and channel discharge both increase for higher and longer incoming waves, but the response to variations in geometry is very different. While $Ru_{2\%}^*$ is most sensitive to channel width, the channel discharge is most sensitive to reef width and maximum for wide reefs, in which case runup values are lowered. This indicates that for wide reefs, when the wave driven flow on

the reef has more time to reach the channel, more mass and momentum exits through the channel which leads to lower runup at the shoreline.

The channel width has little influence on the magnitude of the discharge of the return current. This suggests that for the simulated geometries, the flow carrying capacity of the channel is larger than the actual generated flow. This is in contrast with the reef-lagoon-channel study by (Lowe, Hart, and Pattiaratchi 2010) which found the channel was a restricting factor for the circulation through the channel. Possibly a channel with a more limited depth would have a restricting effect on the circulation. The flow velocities do increase for smaller channel cross sections, which is linked to stronger WCI.

The circulation becomes slightly stronger for increasing channel spacing, but seems to cease to increase for larger spacings. Whether there is a spacing between 1000 and 2000m for which circulation is largest cannot be concluded from this dataset due to insufficient data points. Although there are only few data points for larger spacings, results are in line with previous research on rip current spacing on sandy beaches (Svendsen, Haas, and Zhao 2001), where it was found that rip currents are not affected by neighboring channels when the channel spacing is more than eight times the channel width. As the distance to a channel is large, the water flows back through undertow rather than through the channel. Eight times the channel width translates to 800m in the present study, and indeed the velocities don't seem to increase further for larger spacings.

Channel discharge and flow velocity in the channel are positively correlated, as shown in Figure 5.24, but the discharge but the discharge shows a stronger increase for wider reefs than the maximum velocity. It is uncertain why this occurs, perhaps the flow is better distributed over the channel cross section for wider reefs. While channel width does not affect the discharge, flow velocity does increase for narrower channels, so the same flow goes through a smaller cross section. This also indicates that the for the channel geometries applied in the present study, the flow carrying capacity of the channel is not a restricting factor for the magnitude of the circulation, contrary to the reef-channel-lagoon systems studied by Lowe, Hart, and Pattiaratchi (2010).

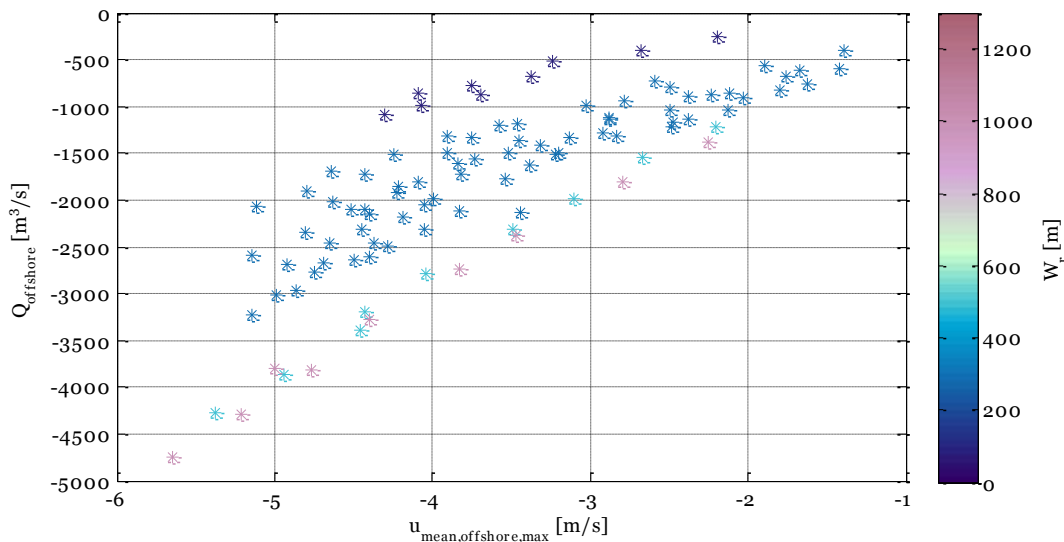


Figure 5.24, Channel discharge versus maximum time-averaged offshore flow velocity in the channel. The marker color indicates the reef width.

5.5 CONTRIBUTIONS OF FREQUENCY COMPONENTS TO RUNUP PATTERN

The different frequency components are shown to have different influence on the runup on the reef flat and in the channel in Section 5.2. To further assess the contribution to runup of the frequency components, this section compares the longshore patterns of the different frequency

parameters of runup for all simulations. Overview figures per geometry are made and presented in Appendix F. These overview figures were used to deduce conceptual figures per frequency component, presented in Figure 5.25 to Figure 5.28. In these figures, for every frequency component to runup (SS, IG, VLF and setup), the general pattern is shown, and how this pattern changes as an input parameter is varied. Furthermore, figures are made per input parameter: H_s , s , W_c , W_r and spacing, which shows the sensitivity to a parameter, but also the relative importance of a freq. component to runup and how this varies. As an example, Figure 5.29, shows the variations in longshore patterns due to varying H_s . The other input parameters are shown in Appendix G.

Overview of SS contribution to runup for variations in geometry and forcing

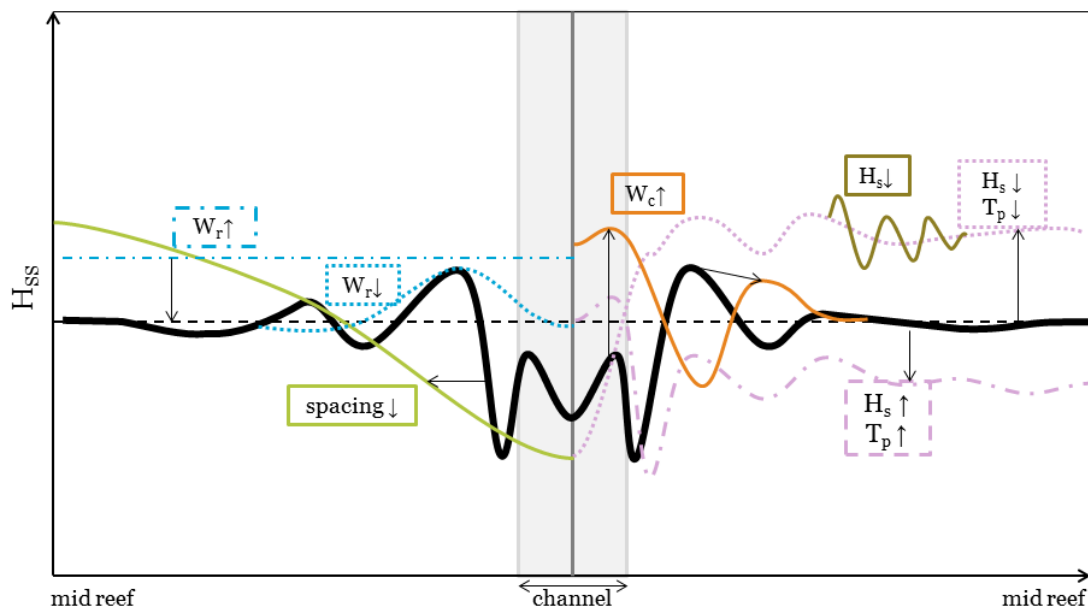


Figure 5.25, Overview of SS contribution to runup. The black line is the general pattern of the SS component of runup, and the colored graphs indicate how this pattern changes as input parameters are varied. The values on the y-axis are proportional to the reference runup line, so not absolute values.

SS component of runup:

- The magnitude of H_{ss} decreases for increasing H_s and decreasing steepness, but their relative importance to runup decreases. This indicates that less SS energy is transferred to LF waves or dissipated, and relatively more SS energy reaches the shoreline.
- For low wave heights, the pattern shows increasing small irregular wiggles.
- For long waves, there are multiple peaks on regular intervals, which might be a sign of interference of waves from different directions at the shoreline.
- The alongshore gradients in runup are strongest in the vicinity of the channel, and is around reference level at mid reef, indicating the influence of the channel on short waves is restricted to the zone nearby the channel
- For increasing H_s and decreasing s , both increasing the L_0 , and for wider channels the trough in the channel becomes less deep and transitions to a peak H_{ss} zone.
- When there is a subpeak in the channel, there are two peaks right at the edge of the channel and a small dip in the channel center. This might be a result of shoaling of refracted short waves along the channel slopes.
- The response to varying W_c , W_r and spacing is similar to the response of the runup pattern

Overview of IG contribution to runup for variations in geometry and forcing

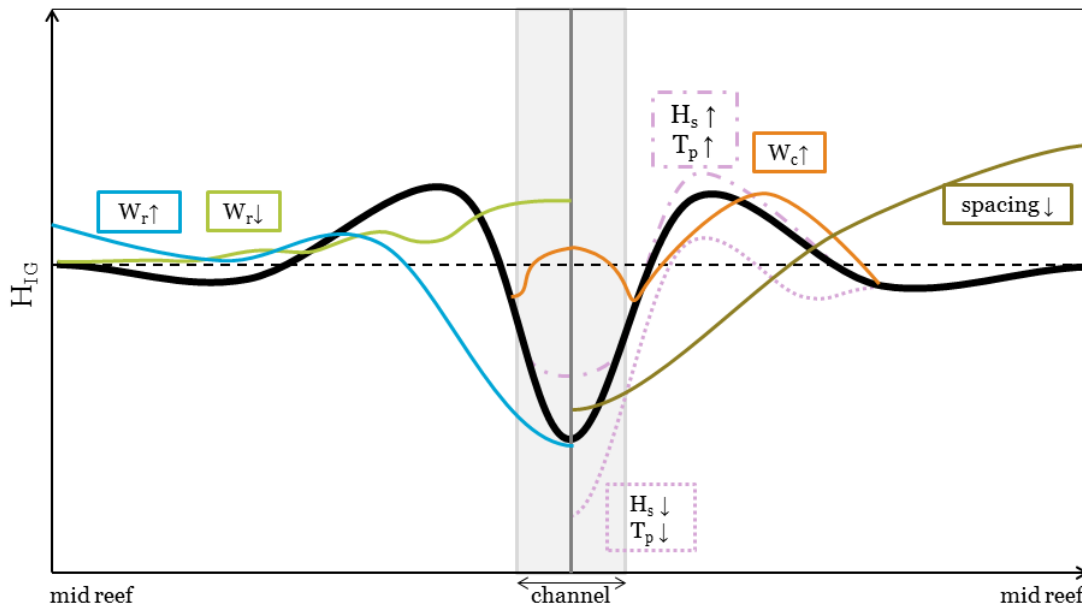


Figure 5.26, Overview of IG contribution to runup. The black graph is the general pattern of the IG component of runup, and the colored graphs indicate how this pattern changes as input parameters are varied.

IG component of runup:

- This frequency component is by far the most dominant to runup. The pattern shape largely resembles total runup pattern, except in channel, where the IG trough is generally deeper. There are distinct peaks next to the channel aligning with the runup peaks
- The trough in the channel becomes flatter with increasing H_s & decreasing steepness (so longer L_0). There is a secondary peak in the channel for wide channels or a very narrow reef, but less pronounced than other freq. components.
- Just like the runup pattern, the IG pattern is wiggly for $W_r=100m$.
- IG mid reef generally is around reference value, except for spacing =300m or $W_r=100m$
- For wider reefs, H_{IG} stays about the ref. level, while mean $Ru_{2\%}$ drops.

Overview of VLF contribution to runup for variations in geometry and forcing

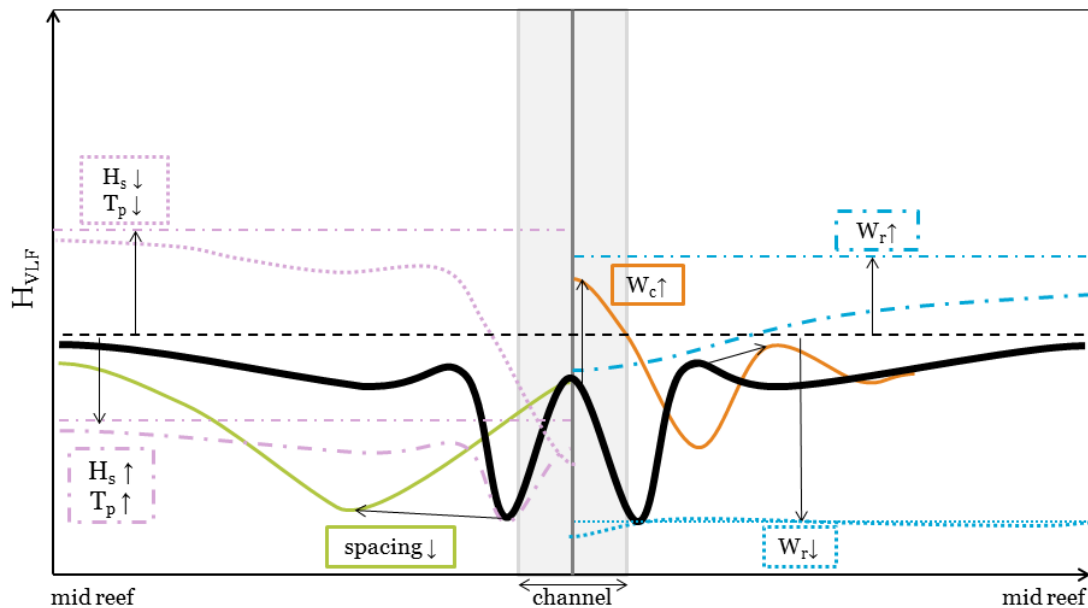


Figure 5.27, Overview of VLF contribution to runup. The black graph is the general pattern of the VLF component of runup, and the colored graphs indicate how this pattern changes as input parameters are varied. The horizontal lines show the reference line of the case without a channel, and how it shifts for variations in an input parameter

VLF component of runup:

- The VLF pattern is largely just a gradual trough without a peak. However, it shows a peak in the channel & peaks next to channel for 5 longest wave forcings. The peak in the channel becomes more pronounced for $s=0.01$.
- The longshore variations of VLF are more gradual than SS and IG
- The relative contribution to total runup decreases for increasing H_s
- Just like other frequency components, a channel peak occurs for wider channels,
- For $W_r=100m$ VLF wave heights are very low, and there is almost no visible influence from the channel
- For wide reefs, there is a global decrease from the reference level.

Overview of setup contribution to runup for variations in geometry and forcing

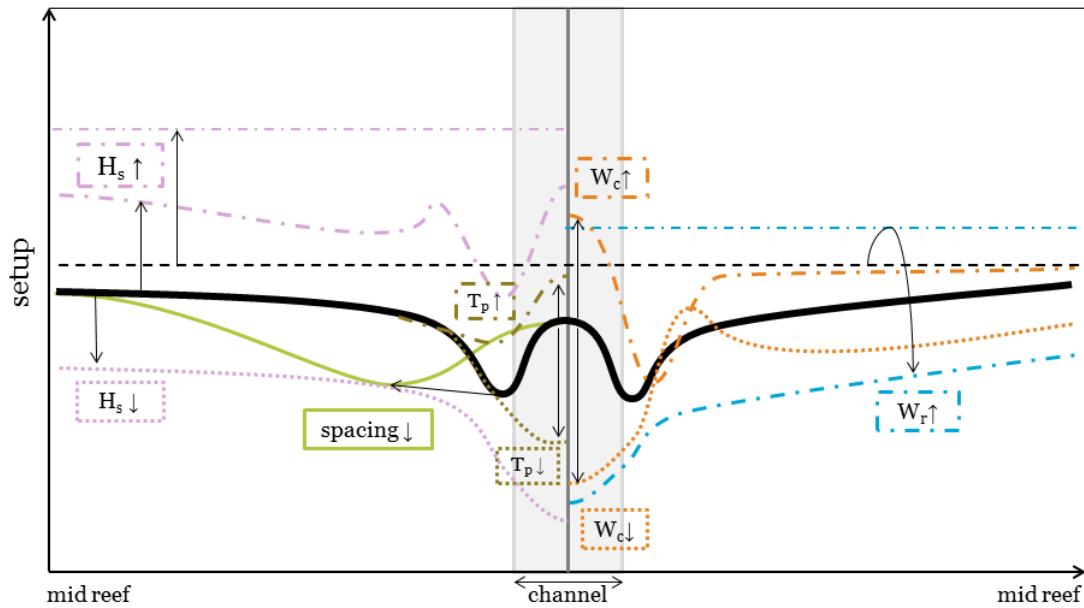


Figure 5.28, Overview of setup contribution to runup. The black graph is the general pattern of the setup component of runup, and the colored graphs indicate how this pattern changes as input parameters are varied.

Setup component of runup:

- The longshore variation of setup is very gradual, and there are no wiggles.
- Setup has low influence on runup for low and short waves, but becomes more important for higher and longer waves.
- The presence of a channel decreases setup along the entire reef flat especially for wide reefs, and setup decreases towards the channel which can be related to the increase of flow velocities towards the channel. There is a local peak of setup inside the channel.

The impact of variations of forcing and reef geometry on the different frequency components to runup is summarized in Table 5.4.

Parameter	Frequency components			
	SS [x-x Hz]	IG [x-x Hz]	VLF [x-x Hz]	Setup [x-x Hz]
$H_s \downarrow$	Trough gets deeper More small wiggles	Trough gets deeper	Higher relative contribution to runup	Lower relative contribution to runup Peaks next to channel decrease or disappear
$H_s \uparrow$	Absolute magnitude increases, but relative contribution to runup decreases, subpeaks in channel, right before the edge appear, Longshore “standing wave appears”	Absolute magnitude increases Channel Trough becomes flatter Smoothens	Lower relative contribution to runup. Peak in channel increases	Higher relative contribution to runup.
$s \uparrow$	Opposite from decrease	Magnitude decreases Trough gets deeper, peaks move slightly closer to channel and become sharper	Higher relative contribution to runup	Channel peak decreases
$s \downarrow$	Magnitude increases, but relative contribution to runup decreases, Subpeak increases in middle of channel Peak on reef shifts away from channel, especially for “interference” cases	Absolute Magnitude increases Channel Trough becomes flatter Peaks move away from channel and are rounder	Lower relative contribution to runup Peak in channel increases	Increasing peaks in center channel
$W_c \uparrow$	Dual set of peaks forms with peaks inside and next to channel, channel peak becomes more dominant, the peaks on the reef flat shift away from channel	Trough in channel becomes less deep, and rises further into a second peak, but peaks on reef remain larger. Mid reef runup becomes higher than ref.	A peak in channel appears, with a trough next to the channel	Peak is in the channel for large W_c , and next to channel for small W_c .
$W_r \downarrow$	Smaller range, Mostly higher than ref, peaks right next to channel	Maximum in channel, wiggly	Relative contribution to runup decreases, little longshore variation	Little longshore variation, peak in channel, becomes close to ref. line
$W_r \uparrow$	Absolute magnitude decreases Becomes lower than ref. Troughs get deeper mini peak in channel Wiggles decrease,	Absolute magnitude decreases, peaks next to channel disappear, just a wide trough, maximum near mid reef	Absolute magnitude decreases, but relative contribution to runup increases. Becomes lower than ref. Peaks disappear, just a trough	Relative contribution to runup increases, Becomes lower than ref. Peaks disappear, just a trough
Spacing \downarrow	Peak is around mid-reef	Peak increases and is around mid-reef	Peaks at mid reef and subpeak in channel	Globally lower than ref, gradual trough towards channel
Spacing \uparrow	Variations are restricted to zone nearby channel.	Variations are restricted to zone nearby channel.	Variations are restricted to zone nearby channel.	Variations are mostly restricted to zone nearby channel.

Table 5.4, influence of input parameters on different frequency components of runup pattern

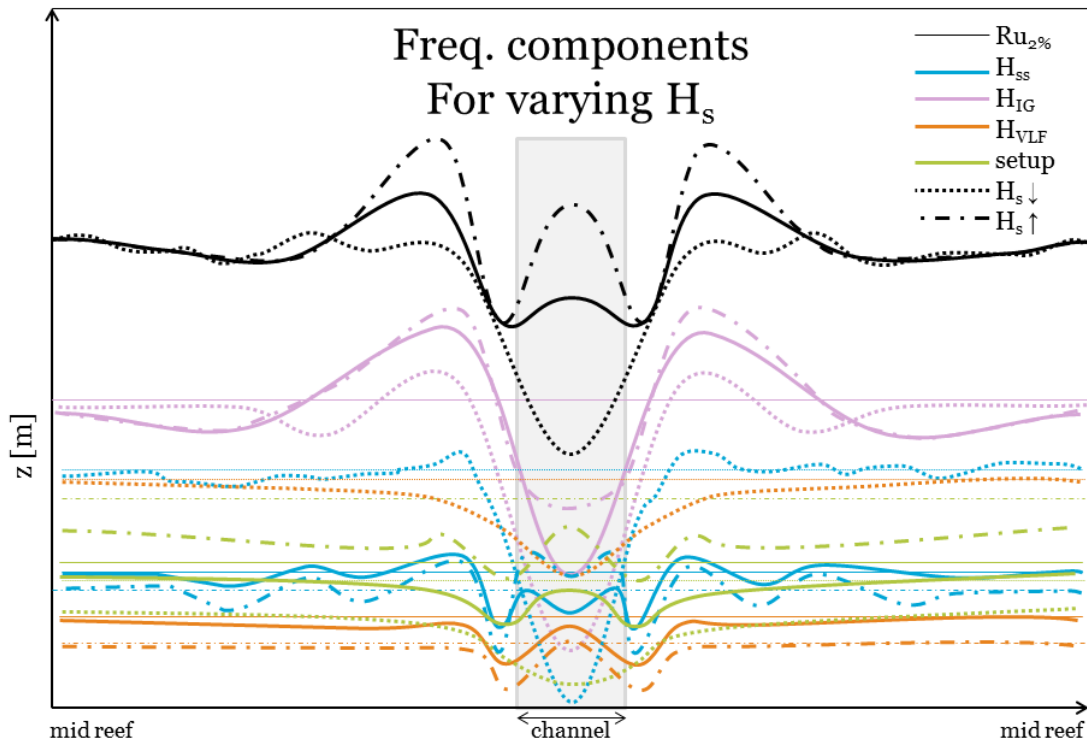


Figure 5.29, Overview impact of varying H_s on runup and its frequency components.

5.5.1 Conclusions and discussion: the contribution of frequencies components to runup for varying geometries and forcings

- IG waves are the dominant contribution to runup. The shape is similar to the runup pattern, except for the local peak inside the channel, and the wave height is larger than of SS, VLF and setup. This is in line with findings from 1D runup studies on reefs (Quataert et al. 2015; Cheriton, Storlazzi, and Rosenberger 2016; Pearson 2016)
- For short waves with low H_s and high steepness, SS has the second largest contribution to runup, while for long waves with high H_s and low steepness, setup becomes increasingly important. This is in line with expectations as setup is larger for increasing relative submergence and wave length, e.g. (Munk and Sargent 1948; Gourlay 1996a)
- For simulations where the runup is largely below the reference runup, setup and VLF are lower than their reference line as well, while longshore mean SS and IG are around their reference level. This indicates VLF and setup are responsible for the global decrease in runup
- Variations in VLF and setup are mostly gradual and reach towards mid reef, while SS gradients are clearly strongest in the vicinity of the channel and don't vary much towards mid reef. IG is in between. This might be an indicator that the wavelength of a frequency component is linked to the region of influence from the channel this component has. Further analysis of results may confirm this.

6

Discussion

6.1 INTRODUCTION

This chapter sets the present study into broader perspective. First, the implications of the necessary schematizations of the model are discussed in section 6.2. Second, the significance of this study, possible applications and implications for future studies are discussed in section 6.3. Discussion of the model setup and model results is covered in the previous chapters.

6.2 IMPLICATIONS OF MODEL SCHEMATIZATIONS

As always with the use of numerical models, reality is schematized and simplifications and assumptions are made. Therefore, results of numerical models need to be handled with care when translating them to real life situations. This section elaborates on how the results of this study should be interpreted.

The present study uses a conceptual model not with the goal to reproduce a reef perfectly, but to examine the influence of varying forcing and reef geometries on runup and to gain insight in the importance of different processes to runup in 2D reef-situations.

The applied forcings are common extreme wave conditions in the Western Pacific Ocean, where most fringing reefs with paleo-stream channels are located. Therefore, results of this study should be applicable to most reef-channel systems, but it should always be checked whether the expected extreme wave conditions are in the range applied here, as variations in forcing lead to more or less setup, LF wave generation, reef circulation et cetera and therefore affect the runup pattern.

The model uses a shore normal wave spectrum without directional spreading, while directional spreading is found to decrease runup on reefs (Veldt 2019). Regarding this, runup in the present study is expected to be a conservative overestimation.

The modeled shorelines are idealized, while natural coastlines generally show more variations. For instance, the modeled shoreline was straight while many channels are located in a bay, which makes refraction and diffraction even more important and where wave energy can be defocused along the entire bay, away from the channel. Wind setup can be important in bay area's as well, e.g. (Tajima, Gunasekara, et al. 2016). Another shoreline curvature occurs for very small islands, where flow doesn't have to go through the channel but flow along the sides of the island. This is expected to decrease setup and the return current and therefore also affect the runup pattern. It is hypothesized that the idealized straight shoreline leads to conservative runup values compared to natural situations, but further research is required to test this hypothesis.

The still water depth on the reef was kept constant at 1m in this study, while in reality this varies short term with tidal elevation on long term with sea level rise, which is higher than the global average in the Pacific and an order of magnitude larger than the grow speed of coral.

The actual water depth on the reef was varied implicitly by varying the wave forcing: as for different forcings the relative submergence $\gamma = H/h$ varies. Larger reef submergence decreases setup and longshore setup differences, and reduces the flow velocities, which might decrease the circulation over the reef flat, which is expected to affect runup. Runup was found to be highest for high submergence of the reef flat in 1D reef situations (Quataert et al. 2015), and therefore especially situations with high submergence of the reef flat are recommended to improve predictions of future vulnerability to flooding of reef lined coasts.

In the present study, the channel shape was chosen to be the extended beach profile, interpolated to the horizontal reef flat. With this profile, channel width had little influence on the magnitude of the return current, indicating that the flow carrying capacity of the channel is not a restricting factor for the magnitude of the return current, even for large return currents with discharges to large river discharges. This is in contrast with the reef-lagoon-channel study by Lowe, Hart, and Pattiaratchi (2010) which found the dimensions of the lagoon and channel were a restricting factor for the circulation over the channel. Possibly a channel with a more limited depth would have a restricting effect on the circulation. The downside of aiming to include actual measured channel topography in model simulations is that it is not possible to measure this from simple satellite images such as Google Earth. Either field measurements would have to be done which is complicated due to the remote locations of these reefs and the high flow velocities in channels, or more advanced remote sensing techniques have to be applied.

6.3 RESEARCH SIGNIFICANCE

This study's significance is that it provides general insight in the effect of a paleo-stream channel on the vulnerability to wave induced flooding of a coastline, while only requiring very few, and, more important, easily available input parameters: only two types of data are required:

- The dimensions of the reef flat and spacing: reef width, channel width and channel spacing, all available through satellite images, for instance from Google Earth.
- The offshore wave forcing, of which statistical data are available through for instance the website of NOAA ("National Oceanic and Atmospheric Administration | U.S. Department of Commerce" 2018).

This is very useful, as for remote islands in the Pacific, usually little to no hydrodynamic data is available and the present studies results can provide a lot of guidance, both for coastal zone management as in future studies.

6.3.1 Coastal zone management

For a given reef shoreline with a channel, predictions can be made to which parts of this shoreline are most likely to receive high runup levels of which offshore forcings. This knowledge can be used for a various range of coastal zone management policy decisions.

- Housing decisions, allocate construction projects to relatively safe locations, and know where housing at the shoreline should be omitted
- Coastal defense structures: if there already is housing and economic activity at the shoreline on a vulnerably location, which is likely the case as many settlements and villages are found next to channels, decide when and where to invest in coastal defense structures to prevent flooding.
- Evacuation plans and early warning systems, if it is known that for certain swell conditions high runup and coastal flooding can be expected at some locations, evacuation plans or

even an early warning system can be designed, to get people to the right safe locations in time.

It is recommended to use the insights from this study in coastal zone management policies. To further improve the range of applicability of these results, more simulations are recommended, especially in the range parameter variations where high runup values are expected. This can decrease scatter in results and eliminate the need to extrapolate results.

6.3.2 Implications for future studies

The present study provides insights to make educated decisions on the approach of future studies.

The results of the system analysis of Chapter 3 provide a good overview of the range of naturally occurring topographies of reef-channel systems and can be used as a basis for future studies on reef-channel systems.

The results of the numerical model study illustrate the importance of 2D effects to runup. Most previous modeling studies of coral reefs have been based on 1D schematizations, and it is expected that future studies will be so as well, due to the huge difference between computational demand and hence runtime of 1D versus 2D models. Whether or not it is justified to use a 1D transect rather than a 2D model depends on the distance from the channel. As runup maxima are found to decrease with distance from the channel expressed in number of offshore wave lengths (Figure 5.16), this is used to express the distance.

Far from a channel

Results show that even far from the channel, even at mid reef, the channel still has influence on runup levels, due to the decrease in setup. In the present study the channel increases the runup with maximum 5% of H_s for locations more than two offshore wavelenghts away from a channel. In this case a 1D schematization of a transect is expected to give a reasonable estimate of runup under extreme conditions.

Near a channel

Near a channel (within two offshore wave lengths of the channel), the channel increases runup locally, and a 1D schematization could underestimate extreme runup levels and flood risk. Furthermore, the strong gradients of wave height, water level and flow velocity near the channel indicate the importance of 2D processes in the region near the channel, which are not accounted for in 1D models. If one is interested in extreme runup levels in this region, a 2D model is recommended. If that is not possible due to for instance the high computational demand, and the only option is to use a 1D transect, a conservative correction factor should be applied to account for the expected increase in runup due to the presence of the channel. Based on the range of simulations in the present study, runup on the reef flat nearby the channel can be up to 20% of H_s higher than without a channel, but as scatter is large, more 2D simulations are recommended before determining such a correction factor.

Inside a channel

Inside a channel, runup is lower than without a channel for narrow channels and moderate to high waves, but runup can be up to 40% of H_s higher than without a channel for wide channels and high and long offshore waves. In those cases, runup is hypothesized to approach the runup of a case where there is no protective reef at all. Since in the present study no simulations were performed of beaches without a protective reef, it is unknown whether simulations using 1D transects would overestimate or underestimate runup inside the channel. If one is interested in the runup inside a channel, a 2D model is therefore recommended.

7

Conclusions

This study examined the influence of paleo-stream channels on runup along reef-fronted shorelines, specifically during extreme wave conditions. This is important to better understand and predict high runup and coastal flooding of vulnerable and densely populated coastal zones behind reef-lined coasts. To this extent, a system analysis and a parametrical study are performed, of which the conclusions are presented in this chapter.

Schematization of natural coastlines with fringing reefs and paleo-stream channels

A system analysis was performed using data from literature and satellite imagery. Most reefs with paleo-stream channels are found on volcanic islands in the Pacific Ocean. Swell events are more likely to lead to high runup and flooding than locally generated waves. As the interest of the research is to assess the vulnerability to flooding, extreme events are more of interest than average conditions. Therefore, wave forcing is schematized using extreme swell conditions in the Pacific with return intervals of 1 to 5 years.

A representative reef geometry was obtained by analyzing 70 reef sections with a channel. Most channels are approximately shore-normal. The shoreline curvature varies but is schematized as straight. Three key geometric parameters are selected to vary: reef width W_r is around 300m, channel width W_c is around 100m and channel spacing is around 1000m. Other parameters such as fore reef slope and channel orientation are kept constant at their most occurring value for simplicity.

The selected geometrical and forcing parameters have the great advantage that they are always known and do not require field measurements as offshore wave data are available through NOAA, and reef and channel dimensions are easily obtainable through satellite images from Google Earth.

Set-up of a conceptual model

A conceptual model was successfully setup using the 2D XBeach Non Hydrostatic model. The model performed satisfactorily, but was computationally expensive, which restricted the possible number of simulations performed within a reasonable time frame. This resulted in 135 simulated scenarios with varying wave forcing and reef geometries.

Impact of variations of wave forcing and reef geometry on longshore runup pattern.

The presence of a channel causes significant longshore variation in runup, with an average variation of 20% of H_s over the longshore. In general, the longshore runup pattern shows the following characteristics: (1) a minimum inside or right next to the channel, (2) a peak next to the channel, next to which $Ru_{2\%}^*$ drops again, (3) a gradual approach of the reference runup without a channel towards the mid reef, and (4) a local peak inside the channel. The last characteristic is present in only part of the simulations. Variations in both geometry and forcing change one or more of these characteristics:

- For small and short waves the runup pattern does not show a clear peak, just a decrease in runup towards the channel
- Long waves and wide channels both result in a dual peak system with a second peak inside the channel.
- Narrow reefs make the runup pattern more alternating and irregular, while wide reefs decrease runup compared to the reference runup without a channel
- Short channel spacings move the runup peak towards mid reef, while for long spacings the longshore runup variation stays restricted to the vicinity of the channel.

The presence of a channel is found to increase extreme runup values with 10-40% of incident wave height. The impact of the channel on runup peaks is larger for simulations with higher offshore wave height, lower wave steepness, very short channel spacing, a narrower reef, and wider channels. Of geometry, channel width W_c has the strongest influence on runup peaks. Furthermore, the channel has the most impact when large fractions of the shoreline consist of channel and when the period of the forcing is closer to the first order resonant period of the reef.

Contributions of frequency components to runup.

As in 1D cases, infra gravity waves have a dominant contribution to runup, but inside the channel the other frequency components (setup, short waves and very low frequency waves) are responsible for a local runup peak.

The frequency components show different responses to variations in forcing: the relative contribution to runup of setup increases for larger waves and lower steepness, while the contribution to runup of short waves is largest for low waves.

The presence of a channel decreases setup even far away from the channel, which is responsible for a general lowering of runup compared to without a channel.

Link between circulation on the reef and runup.

The presence of a channel results in a strong circulation on the reef, with onshore flow over the reef flat and an offshore directed return current in the channel. Mean flow velocities in the return current are -3.6m/s on average and the discharge of the return current is comparable to large rivers, ranging -250 to 4750 m³/s.

Both runup as the reef circulation increase for increasing H_s and decreasing steepness (larger T_p), but circulation increases for wider reefs, while runup decreases for wider reefs.

Drivers for longshore differences in runup.

Differences between the runup pattern, short wave height and setup near the shoreline indicate more factors than solely wave height and setup play a role in generating extreme runup values. Results suggest the presence of a channel acts as a drain and on average lowers runup, while processes such as wave-current interaction, refraction and diffraction lead to a focusing of wave energy next to the channel causing a local increase in runup compared to a situation without a channel.

Concluding, the findings of this exploratory study show that paleo-stream channels in fringing reefs have a large influence on extreme runup levels and locally increase the risk of extreme water levels and coastal flooding. This is relevant for the prediction of coastal hazards and to guide coastal management policies. Furthermore, it illustrates the importance of accounting for channels in flooding studies of reef-lined coasts with channels.

8

Recommendations

This study has contributed to insights on wave runup on longshore non-uniform coral reefs. As this study is part of a broader study on the understanding and prediction of runup and flooding of reef-lined coasts, recommendations are made with this broader study in mind.

Compare model results with field data

The present study is a conceptual model based on numerical simulations. Realistic forcings and reef and channel dimensions are applied, but no actual field data are used to calibrate this model. For the present study this was acceptable as the interest was in the qualitative effects and relative importance of variations in reef geometry and forcing, but for a future study it is relevant to quantify these found effects and see in the range of variations in runup corresponds with observations on real reefs.

Further analyze the results regarding wave direction and energy and momentum balances.

It is concluded that there is longshore variation in runup due to the presence of the channel, but the actual physical processes responsible for this variation remain uncertain. It is hypothesized that the return current carries away mass from the reef flat and decreases setup and runup, while focusing of wave energy locally increases runup. Refraction, diffraction and wave-current interaction are expected to be important processes in this. Further analysis of wave direction and the energy and momentum balance can improve insights on this. The model results of the present study can be used for this.

Further investigate the role of resonance

In 1D schematizations, resonance is found to be a relevant process regarding runup (Gawehn et al. 2016). Results show that the difference between runs with and without a channel are largest for higher values of T_p/T_{res} , when the period of incoming waves is closer to the first order resonant period of the reef. The value of T_p/T_{res} remains below 0.25, so still far from 1, when resonance is expected. However, as infra gravity waves have a lower frequency than the incoming waves, the infra gravity waves may very well be around the resonant timescale of the reef. Further analysis can clarify whether resonance occurs and if this is the cause for the highest runup values. The model results of the present study can be used for this.

Perform additional simulations

Additional simulations can increase the density of results and improve the understanding of various processes and the influence of parameters which are excluded from the present study. More runup results for various reef-channel systems reduce the need to extrapolate the current results to real life situations where the flood risk is assessed. A large database of results can be very useful in coastal zone management policies and provide guidance for future modeling studies.

Three categories of extra simulations are suggested, as they are hypothesized to be the most promising to improve insights on runup on reef-channel systems:

1. Perform simulations without a reef. Results show that for wider channels runup in the center of the channel becomes very high compared to situations without a channel. It is hypothesized that in this case the situation in the channel approaches a situation where there is no protective reef at all, and runup approaches the runup without a reef. Simulations where the beach slope is extended under water for all forcings can be used to test this hypothesis, or that wave-current interaction is an important driver for the extreme runup values in the centers of wide channels.
2. Perform simulations with varying parameters that are affected by climate change: still water depth of the reef flat and friction coefficient c_f . Due to the limited number of simulations, these two parameters were not varied between simulations, while in reality, they will change due to climate change: sea level rise will increase the reef submergence and coral bleaching will decrease the roughness of the reef (Hoegh-Guldberg 1999). Between simulations the actual water depth on the reef did vary, as for different forcings the relative submergence $\gamma = H/h$ varied and therefore changed setup. Still, the submergence of reefs will change in the future as sea level rise exceeds the growing speed of coral and reefs. Larger reef submergence decreases setup and longshore setup differences and reduces the flow velocities, which decreases the circulation over the reef flat, which is expected to affect runup. While bottom friction has less impact on runup than for instance reef width, reduced bottom friction does increase runup (Quataert et al. 2015), and especially the infra gravity component to runup, which has a dominant contribution to the runup peaks, is expected to increase for lower bottom friction (Cheriton, Storlazzi, and Rosenberger 2016; Pearson et al. 2017). Therefore, simulations with varying reef submergence and bottom friction can provide insight in future extreme runup.
3. Perform more simulations in the range of parameters where the influence of the channel is largest: wide channels, and high and long waves. Situations with a large difference with and without a channel are of interest, but only 10% of performed simulations show a maximum runup which is more than 15% of H_s of the reference runup. Furthermore, in the present study geometric variables were not varied simultaneously, while in reality, wide channels often occur at locations with wide reefs or longer channel spacings, for instance at Fiji. By performing more simulations with high and long waves and wide channels, combined with variations of reef width and channel spacing more insight can be gained in the observed trends in runup patterns.

References

- Baldock, T. E. 2012. "Dissipation of Incident Forced Long Waves in the Surf Zone-Implications for the Concept of 'Bound' Wave Release at Short Wave Breaking." *Coastal Engineering* 60 (1): 276–85. <https://doi.org/10.1016/j.coastaleng.2011.11.002>.
- Baldock, T. E., and D. A. Huntley. 2002. "Long-Wave Forcing by the Breaking of Random Gravity Waves on a Beach." *Proceedings of the Royal Society A: Mathematical, Physical and Engineering Sciences* 458 (2025): 2177–2201. <https://doi.org/10.1098/rspa.2002.0962>.
- Battjes, J. A., H. J. Bakkenes, T. Janssen, and Ap R. van Dongeren. 2004. "Shoaling of Subharmonic Gravity Waves." *Journal of Geophysical Research* 109 (C2): C02009. <https://doi.org/10.1029/2003JC001863>.
- Battjes, J A. 1974. "Surf Similarity." *Proceedings of of the 14th International Conference on Coastal Engineering, ASCE*, no. 1: 466–80. <https://doi.org/10.1007/978-1-61779-361-5>.
- Becker, Janet M., Mark A. Merrifield, and M. Ford. 2014. "Water Level Effects on Breaking Wave Setup for Pacific Island Fringing Reefs." *Journal of Geophysical Research: Oceans* 119 (2): 914–32. <https://doi.org/10.1002/2013JC009373>.
- Beetham, Edward, Paul S. Kench, Joanne O'Callaghan, and Stéphane Popinet. 2016. "Wave Transformation and Shoreline Water Level on Funafuti Atoll, Tuvalu." *Journal of Geophysical Research: Oceans* 121 (1): 311–26. <https://doi.org/10.1002/2015JC011246>.
- Bellotti, Giorgio. 2004. "A Simplified Model of Rip Currents Systems around Discontinuous Submerged Barriers." *Coastal Engineering* 51 (4): 323–35. <https://doi.org/10.1016/j.coastaleng.2004.04.001>.
- Birkeland, Charles. 1997. *Life and Death of Coral Reefs*. Chapman & Hall. <https://doi.org/10.1007/978-1-4615-5995-5>.
- Blacka, Matt J, Francois Flocard, Kristen D Splinter, and Ron J Cox. 2015. "Estimating Wave Heights and Water Levels inside Fringing Reefs during Extreme Conditions." *Coast and Ports 2015*, no. September: 1–7.
- Bonneton, P, Jean Pierre Lefebvre, P Bretel, S Oiuillon, and Pascal Douillet. 2007. "Tidal Modulation of Wave-Setup and Wave-Induced Currents on the Aboré Coral Reef, New Caledonia." *Journal of Coastal Research* 50 (April): 762–66. http://www.epoc.u-bordeaux1.fr/indiv/bonneton/publications/Talks/Expose_Bonneton_et_al_ICS2007.pdf.
- Bosserelle, Cyprien, Jens Kruger, Make Movono, and Sandeep Reddy. 2015. "Wave Inundation on the Coral Coast of Fiji." *Australasian Coasts & Ports Conference 2015*, no. September: 96–101.
- Buckley, Mark L, Ryan J Lowe, Jeff E Hansen, and Ap R Van Dongeren. 2015. "Dynamics of Wave Setup over a Steeply-Sloping Fringing Reef." *Journal of Physical Oceanography*, no. SEPTEMBER 2015: 150923131654000. <https://doi.org/10.1175/JPO-D-15-0067.1>.
- Cheriton, Olivia M., Curt D. Storlazzi, and Kurt J. Rosenberger. 2016. "Observations of Wave Transformation over a Fringing Coral Reef and the Importance of Low-Frequency Waves and Offshore Water Levels to Runup, Overwash, and Coastal Flooding." *Journal of Geophysical Research: Oceans* 121 (5): 3121–40. <https://doi.org/10.1002/2015JC011231>.
- Costa, Mirella B.S.F., Moacyr Araújo, Tereza C.M. Araújo, and Eduardo Siegle. 2016. "Influence of Reef Geometry on Wave Attenuation on a Brazilian Coral Reef." *Geomorphology* 253 (January): 318–27. <https://doi.org/10.1016/j.geomorph.2015.11.001>.

- Damlamian, Hervé, Cyprien Bosserelle, Jens Kruger, Amrit Raj, Zulfikar Begg, Salesh Kumar, Ryan J Lowe, Mark L Buckley, and Aseri Baleilevuka. 2015. "Bonriki Inundation Vulnerability Assessment: Inundation Modelling of Bonriki Islet, Tarawa, Kiribati," 61. http://biva.gsd.spc.int/files/BIVA_InundationModelling_Report.pdf.
- Darwin, Charles R. 1842. *The Structure and Distribution of Coral Reefs*.
- Demirbilek, Zeki, Okey Nwogu, and Donald Ward. 2007. "Laboratory Study of Wind Effect on Runup over Fringing Reefs-Report 1: Data Report." *Surge and Wave Island Modeling Studies (SWIMS) Program & Coastal Inlets Research Program (CIRP)*, no. July 2007: ERDC/CHL TR-07-4.
- Dongeren, Ap R. Van, Ryan Lowe, Andrew Pomeroy, Duong Minh Trang, Dano Roelvink, Graham Symonds, and Roshanka Ranasinghe. 2013. "Numerical Modeling of Low-Frequency Wave Dynamics over a Fringing Coral Reef." *Coastal Engineering* 73 (March): 178–90. <https://doi.org/10.1016/j.coastaleng.2012.11.004>.
- Eldeberky, Y. 1996. "Nonlinear Transformations of Wave Spectra in the Nearshore Zone." *Doctoral Theses*. <https://repository.tudelft.nl/islandora/object/uuid:707ca57d-81c3-4103-bc6e-aae1c90fce63>.
- Fairbridge, Rhodes W. 1975. "Biology and Geology of Coral Reefs." *Environmental Research* 9 (2): 208–9. [https://doi.org/10.1016/0013-9351\(75\)90066-3](https://doi.org/10.1016/0013-9351(75)90066-3).
- Falter, James L., Marlin J. Atkinson, Mark A. Merrifield, Jim Fleming, Kimball Millikan, Eric Hochberg, Jérôme P. Aucan, Serge Andrefouet, and Kim Anthony. 2004. "Falter, James L., Marlin J. Atkinson, and Mark A. Merrifield. Mass-Transfer Limitation of Nutrient Uptake by a Wave-Dominated Reef Flat Community. *Limnol. Oceanogr.*, 49(5), 2004, 1820–1831." *Limnol. Oceanogr* 49 (5): 1820–31. http://m.aslo.net/lo/toc/vol_49/issue_5/1820.pdf.
- Ferrario, Filippo, Michael W. Beck, Curt D. Storlazzi, Fiorenza Micheli, Christine C. Shepard, and Laura Airoidi. 2014. "The Effectiveness of Coral Reefs for Coastal Hazard Risk Reduction and Adaptation." *Nature Communications* 5 (1): 3794. <https://doi.org/10.1038/ncomms4794>.
- Foda, Mostafa A., and Chiang C. Mei. 1981. "Nonlinear Excitation of Long-Trapped Waves by a Group of Short Swells." *Journal of Fluid Mechanics* 111 (1): 319. <https://doi.org/10.1017/S0022112081002401>.
- Gattuso, J.-P, M Pichon, B Delesalle, and M Frankignoulle. 1993. "Community Metabolism and Air-Sea CO₂ Fluxes in a Coral-Reef Ecosystem (Moorea, French-Polynesia)." *Marine Ecology-Progress Series* 96 (3): 259–67. <https://doi.org/10.3354/meps096259>.
- Gawehn, Matthijs. 2015. "Incident, Infragravity and Very Low Frequency Wave Motions on an Atoll Reef Platform."
- Gawehn, Matthijs, Ap R. van Dongeren, Arnold van Rooijen, Curt D. Storlazzi, Olivia M. Cheriton, and Ad J.H.M. Reniers. 2016. "Identification and Classification of Very Low Frequency Waves on a Coral Reef Flat." *Journal of Geophysical Research: Oceans* 121 (10): 7560–74. <https://doi.org/10.1002/2016JC011834>.
- Gelfenbaum, Guy, Alex Apotsos, Andrew W Stevens, and Bruce Jaffe. 2011. "Effects of Fringing Reefs on Tsunami Inundation: American Samoa." *Earth-Science Reviews* 107 (1–2): 12–22. <https://doi.org/10.1016/j.earscirev.2010.12.005>.
- Gent, Marcel R A Van. 2001. "Wave Run-Up on Dikes with Shallow Foreshores WAVE RUNUP ON DIKES WITH SHALLOW FORESHORES." *Article in Journal of Waterway Port Coastal and Ocean Engineering*. [https://doi.org/10.1061/\(ASCE\)0733-950X\(2001\)127:5\(254\)](https://doi.org/10.1061/(ASCE)0733-950X(2001)127:5(254)).
- Gourlay, Michael Richard. 1996a. "Wave Set-up on Coral Reefs. 1. Set-up and Wave-Generated Flow on an Idealised Two Dimensional Horizontal Reef." *El-SEVIER Coastal Engineering* 27: 161–93.

- . 1996b. “Wave Set-up on Coral Reefs. 2. Set-up on Reefs with Various Profiles.” *Coastal Engineering* 28 (1–4): 17–55. [https://doi.org/10.1016/0378-3839\(96\)00009-9](https://doi.org/10.1016/0378-3839(96)00009-9).
- Gourlay, Michael Richard, and Gildas Colleter. 2005. “Wave-Generated Flow on Coral Reefs - An Analysis for Two-Dimensional Horizontal Reef-Tops with Steep Faces.” *Coastal Engineering*. <https://doi.org/10.1016/j.coastaleng.2004.11.007>.
- Guza, R. T., and Falk Feddersen. 2012. “Effect of Wave Frequency and Directional Spread on Shoreline Runup.” *Geophysical Research Letters* 39 (11): n/a-n/a. <https://doi.org/10.1029/2012GL051959>.
- Haberkorn, Gerald. 2008. “Pacific Islands Population and Development: Facts, Fictions and Follies.” *New Zealand Population Review* 33/34: 95–127.
- Haller, Merrick C., Robert A. Dalrymple, and Ib A. Svendsen. 2002. “Experimental Study of Nearshore Dynamics on a Barred Beach with Rip Channels.” *Journal of Geophysical Research* 107 (C6): 3061. <https://doi.org/10.1029/2001JC000955>.
- Haller, Merrick C, and R. A. Dalrymple. 2001. “Rip Current Instabilities.” *Journal of Fluid Mechanics* 433: 161–92. <https://doi.org/10.1017/S0022112000003414>.
- Hardy, Thomas A., and Ian R. Young. 1996. “Field Study of Wave Attenuation on an Offshore Coral Reef.” *Journal of Geophysical Research: Oceans* 101 (C6): 14311–26. <https://doi.org/10.1029/96JC00202>.
- Harris, D. L., A. Vila-Concejo, J. M. Webster, and H. E. Power. 2015. “Spatial Variations in Wave Transformation and Sediment Entrainment on a Coral Reef Sand Apron.” *Marine Geology* 363: 220–29. <https://doi.org/10.1016/j.margeo.2015.02.010>.
- “Hawaii Population. (2018-01-24).” n.d. Accessed August 1, 2018. <http://worldpopulationreview.com/states/hawaii/>.
- Hearn, Clifford J. 1999. “Wave-Breaking Hydrodynamics within Coral Reef Systems and the Effect of Changing Relative Sea Level.” *Journal of Geophysical Research* 104: 30,007–30,019. <https://doi.org/10.1029/1999JC900262>.
- Hench, James L, James J. Leichter, and Stephen G. Monismith. 2008. “Episodic Circulation and Exchange in a Wave-Driven Coral Reef and Lagoon System.” *Limnology and Oceanography* 53 (6): 2681–94. <https://doi.org/10.4319/lo.2008.53.6.2681>.
- Hench, James L, and Johanna H. Rosman. 2013. “Observations of Spatial Flow Patterns at the Coral Colony Scale on a Shallow Reef Flat.” *Journal of Geophysical Research: Oceans* 118 (3): 1142–56. <https://doi.org/10.1002/jgrc.20105>.
- Hoegh-Guldberg, Ove. 1999. “Climate Change, Coral Bleaching and the Future of the World’s Coral Reefs.” *Marine and Freshwater Research*. CSIRO. <https://doi.org/10.1071/MF99078>.
- Hoeke, Ron K., Kathleen L. McInnes, Jens C. Kruger, Rebecca J. McNaught, John R. Hunter, and Scott G. Smithers. 2013. “Widespread Inundation of Pacific Islands Triggered by Distant-Source Wind-Waves.” *Global and Planetary Change* 108: 1–11. <https://doi.org/10.1016/j.gloplacha.2013.06.006>.
- Hoeke, Ron K., Curt D. Storlazzi, and Peter. Ridd. 2011. “Hydrodynamics of a Bathymetrically Complex Fringing Coral Reef Embayment: Wave Climate, in Situ Observations, and Wave Prediction.” *Journal of Geophysical Research: Oceans* 116 (4): 1–19. <https://doi.org/10.1029/2010JC006170>.
- Hoeke, Ron K., Curt D. Storlazzi, and Peter V. Ridd. 2013. “Drivers of Circulation in a Fringing Coral Reef Embayment: A Wave-Flow Coupled Numerical Modeling Study of Hanalei Bay, Hawaii.” *Continental Shelf Research* 58: 79–95. <https://doi.org/10.1016/j.csr.2013.03.007>.
- Holman, R. A. 1986. “Extreme Value Statistics for Wave Run-up on a Natural Beach.” *Coastal*

- Engineering* 9 (6): 527–44. [https://doi.org/10.1016/0378-3839\(86\)90002-5](https://doi.org/10.1016/0378-3839(86)90002-5).
- Holthuijsen, L. H. 2011. “Waves in Oceanic and Coastal Waters.” *Contemporary Physics* 52 (1): 75. <https://doi.org/10.1080/00107514.2010.529511>.
- Hopley, D. 2011. *Encyclopedia of Modern Coral Reef: Structure, Form and Process. Encyclopedia of Modern Coral Reefs*. <https://doi.org/10.1007/978-90-481-2639-2>.
- Hunt, I. A. 1959. “Design of Seawalls and Breakwaters.” *Journal of the Waterways and Harbors Division* 85: 123– 152.
- Jago, O. K., P. S. Kench, and R. W. Brander. 2007. “Field Observations of Wave-Driven Water-Level Gradients across a Coral Reef Flat.” *Journal of Geophysical Research: Oceans* 112 (6): 1–14. <https://doi.org/10.1029/2006JC003740>.
- Kennedy, A B, and Y Zhang. 2008. “The Stability of Wave-Driven Rip Current Circulation.” *Journal of Geophysical Research: Oceans* 113 (3). <https://doi.org/10.1029/2006JC003814>.
- Klaver, Sebastiaan. 2018. “Modelling the Effects of Excavation Pits on Fringing Reefs.” <https://repository.tudelft.nl/islandora/object/uuid%3A17620c42-8c1b-491c-b862-f4c1f6c92a48?collection=education>.
- Leal Campos Fonseca da Silva, Renan. 2017. “Three-Dimensional Flow Over Spur-and-Groove Morphology.” <https://repository.tudelft.nl/islandora/object/uuid%3Ac647278b-6774-4c09-893b-1638812e7c59?collection=education>.
- Lentz, S. J., J. H. Churchill, K. A. Davis, J. T. Farrar, J. Pineda, and V. Starczak. 2016. “The Characteristics and Dynamics of Wave-Driven Flow across a Platform Coral Reef in the Red Sea.” *Journal of Geophysical Research: Oceans* 121 (2): 1360–76. <https://doi.org/10.1002/2015JC011141>.
- Longuet-Higgins, M. S. 1974. “On the Mass, Momentum, Energy and Circulation of a Solitary Wave.” *Proc. R. Soc. Lond. A* 337 (1608): 1–13. <http://rspa.royalsocietypublishing.org/content/337/1608/1>.
- Longuet-Higgins, M. S., and R. W. Stewart. 1962. “Radiation Stress and Mass Transport in Gravity Waves, with Application to ‘Surf Beats.’” *Journal of Fluid Mechanics* 13 (04): 481. <https://doi.org/10.1017/S0022112062000877>.
- Lowe, Ryan J., James L. Falter, Stephen G. Monismith, and Marlin J. Atkinson. 2008. “Wave-Driven Circulation of a Coastal Reef–Lagoon System.” *Journal of Physical Oceanography* 39 (4): 873–93. <https://doi.org/10.1175/2008jpo3958.1>.
- . 2009. “A Numerical Study of Circulation in a Coastal Reef-Lagoon System.” *Journal of Geophysical Research: Oceans* 114 (6): 1–18. <https://doi.org/10.1029/2008JC005081>.
- Lowe, Ryan J., Colin Hart, and Charitha B. Pattiaratchi. 2010. “Morphological Constraints to Wave-Driven Circulation in Coastal Reef-Lagoon Systems: A Numerical Study.” *Journal of Geophysical Research: Oceans* 115 (9): C09021. <https://doi.org/10.1029/2009JC005753>.
- McCall, R.T., G. Masselink, T.G. Poate, J.A. Roelvink, and L.P. Almeida. 2015. “Modelling the Morphodynamics of Gravel Beaches during Storms with XBeach-G.” *Coastal Engineering* 103 (September): 52–66. <https://doi.org/10.1016/J.COASTALENG.2015.06.002>.
- Merrifield, M. A., J M Becker, M Ford, and Y Yao. 2014. “Observations and Estimates of Wave-Driven Water Level Extremes at the Marshall Islands.” *Geophysical Research Letters* 41 (20): 7245–53. <https://doi.org/10.1002/2014GL061005>.
- Mimura, N.L., R.F. Nurse, J. McLean, L. Agard, P. Briguglio, R. Lefale, and Payet G. 2007. *Small Islands. Climate Change 2007: Impacts, Adaptation and Vulnerability. Contribution of Working Group II to the Fourth Assessment Report of the Intergovernmental Panel on Climate Change*. Cambridge, UK: Cambridge University Press.

- https://www.ipcc.ch/pdf/assessment-report/ar4/wg2/ar4_wg2_full_report.pdf.
- Moulton, Melissa, Steve Elgar, Britt Raubenheimer, John C Warner, and Nirnimesh Kumar. 2017. "Rip Currents and Alongshore Flows in Single Channels Dredged in the Surf Zone." *Journal of Geophysical Research: Oceans* 122 (5): 3799–3816. <https://doi.org/10.1002/2016JC012222>.
- Munk, Walter H., and Martson C. Sargent. 1948. "Adjustment of Bikini Atoll to Ocean Waves." *Eos, Transactions American Geophysical Union* 29 (6): 855–60. <https://doi.org/10.1029/TR029i006p00855>.
- "National Oceanic and Atmospheric Administration | U.S. Department of Commerce." 2018. NOAA. 2018. <https://www.noaa.gov/>.
- Nielsen, Peter, Rob W. Brander, and Michael G. Hughes. 2001. "Rip Currents: Observations of Hydraulic Gradients, Friction Factors and Wave Pump Efficiency." In *Coastal Dynamics '01*, 483–92. Reston, VA: American Society of Civil Engineers. [https://doi.org/10.1061/40566\(260\)49](https://doi.org/10.1061/40566(260)49).
- Nwogu, Okey, and Zeki Demirebilek. 2010. "Infragravity Wave Motions and Runup over Shallow Fringing Reefs." *Journal of Waterway, Port, Coastal, and Ocean Engineering* 136 (6): 295–305. [https://doi.org/10.1061/\(ASCE\)WW.1943-5460.0000050](https://doi.org/10.1061/(ASCE)WW.1943-5460.0000050).
- Pearson, S. G., Curt D. Storlazzi, A. R. van Dongeren, M. F.S. Tissier, and A. J.H.M. Reniers. 2017. "A Bayesian-Based System to Assess Wave-Driven Flooding Hazards on Coral Reef-Lined Coasts." *Journal of Geophysical Research: Oceans* 122 (12): 10099–117. <https://doi.org/10.1002/2017JC013204>.
- Pearson, S.G. 2016. "Predicting Wave-Induced Flooding on Low-Lying Tropical Islands Using a Bayesian Network." <http://repository.tudelft.nl/islandora/object/uuid%3Ac3988f4b-99f8-4936-9504-261b32bb0cd1?collection=education>.
- Péquignet, Anne Christine N., Janet M. Becker, M. A. Merrifield, and S. J. Boc. 2011. "The Dissipation of Wind Wave Energy across a Fringing Reef at Ipan, Guam." *Coral Reefs* 30 (SUPPL. 1): 71–82. <https://doi.org/10.1007/s00338-011-0719-5>.
- Péquignet, Anne Christine N., Janet M. Becker, and Mark A. Merrifield. 2014. "Energy Transfer between Wind Waves and Low-Frequency Oscillations on a Fringing Reef, Ipan, Guam." *Journal of Geophysical Research: Oceans* 119 (10): 6709–24. <https://doi.org/10.1002/2014JC010179>.
- Péquignet, Anne Christine N., Janet M. Becker, Mark A. Merrifield, and Jérôme P. Aucan. 2009. "Forcing of Resonant Modes on a Fringing Reef during Tropical Storm Man-Yi." *Geophysical Research Letters* 36 (3): n/a-n/a. <https://doi.org/10.1029/2008GL036259>.
- Pomeroy, Andrew, Ap R. van Dongeren, Ryan J Lowe, Jaap S. M. van Thiel de Vries, and J. A. Roelvink. 2012. "Low-Frequency Wave Resonance in Fringing Reef Environments." *Coastal Engineering* 2012, 1–10. <https://doi.org/doi:http://dx.doi.org/10.9753/icce.v33.currents.25>.
- Pomeroy, Andrew, Ryan Lowe, Graham Symonds, Ap R. Van Dongeren, and Christine Moore. 2012. "The Dynamics of Infragravity Wave Transformation over a Fringing Reef." *Journal of Geophysical Research: Oceans* 117 (11). <https://doi.org/10.1029/2012JC008310>.
- Quataert, Ellen. 2015. "Wave Runup on Atoll Reefs," no. January: 89. <https://repository.tudelft.nl/islandora/object/uuid%3Af9ba5835-66bf-4907-9823-4ff56edf5909?collection=education>.
- Quataert, Ellen, Curt D. Storlazzi, Arnold van Rooijen, Olivia M. Cheriton, and Ap R. van Dongeren. 2015. "The Influence of Coral Reefs and Climate Change on Wave-Driven Flooding of Tropical Coastlines." *Geophysical Research Letters* 42 (15): 6407–15. <https://doi.org/10.1002/2015GL064861>.

- Reniers, Ad J.H.M., J. H. MacMahan, E. B. Thornton, and T. P. Stanton. 2007. "Modeling of Very Low Frequency Motions during RIPEX." *Journal of Geophysical Research: Oceans* 112 (7): 1–14. <https://doi.org/10.1029/2005JC003122>.
- Ridder, Menno P. De. 2018. "Non-Hydrostatic Wave Modelling of Coral Reefs with the Addition of a Porous in-Canopy Model." <http://resolver.tudelft.nl/uuid:4f738968-be52-4484-af1d-60a0e74fdbab>.
- Roelvink, Dano, Ap van Dongeren, Robert McCall, Bas Hoonhout, Arnold van Rooijen, Pieter van Geer, Lodewijk de Vet, Kees Nederhoff, and Ellen Quataert. n.d. "XBeach User Manual." Accessed May 7, 2018. https://xbeach.readthedocs.io/en/latest/user_manual.html.
- Roelvink, Dano, Robert McCall, Seyedabdolhossein Mehvar, Kees Nederhoff, and Ali Dastgheib. 2018. "Improving Predictions of Swash Dynamics in XBeach: The Role of Groupiness and Incident-Band Runup." *Coastal Engineering* 134 (April): 103–23. <https://doi.org/10.1016/j.coastaleng.2017.07.004>.
- Roelvink, Dano, Ad J.H.M. Reniers, Ap R Van Dongeren, Jaap Van Thiel De Vries, Robert Mccall, and Jamie Lescinski. 2009. "Modelling Storm Impacts on Beaches, Dunes and Barrier Islands." <https://doi.org/10.1016/j.coastaleng.2009.08.006>.
- Rogers, Justin S., Stephen G. Monismith, Robert B Dunbar, and David A Kowcek. 2015. "Field Observations of Wave-Driven Circulation over Spur and Groove Formations on a Coral Reef." *Journal of Geophysical Research* 120 (January): 145–60. <https://doi.org/doi:10.1002/2014JC010464>.
- Rogers, Justin S, Stephen G. Monismith, David A Kowcek, and Robert B Dunbar. 2016. "Wave Dynamics of a Pacific Atoll with High Frictional Effects." *Journal of Geophysical Research: Oceans* 121 (1): 350–67. <https://doi.org/10.1002/2015JC011170>.
- Rooijen, A.A. Van, J.S.M. Van Thiel de Vries, R.T. McCall, A.R. Van Dongeren, J.A. Roelvink, and A.J.H.M. Reniers. 2015. "Modeling of Wave Attenuation by Vegetation with XBeach." *E-Proceedings of the 36th IAHR World Congress, The Hague, the Netherlands, 28 June-3 July 2015*. <https://repository.tudelft.nl/islandora/object/uuid:98a66b95-8fed-421a-9bfe-4ae978375dbe?collection=research>.
- Sand, Stig E. 1982. "Long Waves in Directional Seas." *Coastal Engineering* 6 (3): 195–208. [https://doi.org/10.1016/0378-3839\(82\)90018-7](https://doi.org/10.1016/0378-3839(82)90018-7).
- Schaffer, Hemming A., and Ib A. Svendsen. 1988. "Surf Beat Generation on a Mild-Slope Beach." *Proceedings of Coastal Engineering* 19716 (21): 1058–72. <https://doi.org/10.9753/ICCE.V21.%P>.
- Seelig, William N. 1983. "Laboratory Study of Reef-Lagoon System Hydraulics." *Journal of Waterway, Port, Coastal, and Ocean Engineering* 109 (4): 380–91. [https://doi.org/10.1061/\(ASCE\)0733-950X\(1983\)109:4\(380\)](https://doi.org/10.1061/(ASCE)0733-950X(1983)109:4(380)).
- Seelig, William N., and A. M. Asce. 1983. "Laboratory Study or Reef-Lagoon System Hydraulics." *Journal of Waterway, Port, Coastal and Ocean Engineering* 109 (4): 380–91. [https://doi.org/10.1061/\(ASCE\)0733-950X\(1983\)109:4\(380\)](https://doi.org/10.1061/(ASCE)0733-950X(1983)109:4(380)).
- Senechal, Nadia. 2017. "Alongshore Variability in Observed Runup under Dissipative Conditions." *Coastal Dynamics*, no. 208. http://coastaldynamics2017.dk/onewebmedia/208_senechal.pdf.
- Shimozono, Takenori, Yoshimitsu Tajima, Andrew B. Kennedy, Hisamichi Nobuoka, Jun Sasaki, and Shinji Sato. 2015. "Combined Infragravity Wave and Sea-Swell Runup over Fringing Reefs by Super Typhoon Haiyan." *Journal of Geophysical Research: Oceans* 120 (6): 4463–86. <https://doi.org/10.1002/2015JC010760>.
- Smit, P.B., G.S. Stelling, Dano Roelvink, Jaap S. M. van Thiel de Vries, Robert McCall, Ap R. Van Dongeren, Cilia Zwinkels, and R. Jacobs. 2010. "XBeach : Non-Hydrostatic Model." Delft.

- Smith, Ernest R, Tyler J Hesser, and Jane Mckee Smith. 2012. "Studies of Wave Breaking , Dissipation , Setup , and Runup on Reefs Coastal and Hydraulics Laboratory Two- and Three-Dimensional Laboratory Studies of Wave Breaking , Dissipation , Setup , and Runup on Reefs," no. September. http://www.frf.usace.army.mil/pilot/swims/SWIMS_lab_report_DRAFT.pdf.
- Smithers, S. G., and Ron K. Hoeke. 2014. "Geomorphological Impacts of High-Latitude Storm Waves on Low-Latitude Reef Islands - Observations of the December 2008 Event on Nukutoa, Takuu, Papua New Guinea." *Geomorphology* 222 (October): 106–21. <https://doi.org/10.1016/j.geomorph.2014.03.042>.
- Stockdon, Hilary F., Rob A. Holman, Peter A. Howd, and Asbury H. Sallenger. 2006. "Empirical Parameterization of Setup, Swash, and Runup." *Coastal Engineering* 53 (7): 573–88. <https://doi.org/10.1016/j.coastaleng.2005.12.005>.
- Storlazzi, Curt D., Edwin P.L. Elias, and Paul Berkowitz. 2015. "Many Atolls May Be Uninhabitable Within Decades Due to Climate Change." *Scientific Reports* 5 (1): 14546. <https://doi.org/10.1038/srep14546>.
- Storlazzi, Curt D., Stephen B. Gingerich, A. R. van Dongeren, Olivia M. Cheriton, Peter W. Swarzenski, Ellen Quataert, Clifford I. Voss, et al. 2018. "Most Atolls Will Be Uninhabitable by the Mid-21st Century Because of Sea-Level Rise Exacerbating Wave-Driven Flooding." *Science Advances* v. 4 (eaap9741): eaap9741. <https://doi.org/10.1126/sciadv.aap9741>.
- Storlazzi, Curt D., J B Logan, and M E Field. 2003. "Quantitative Morphology of a Fringing Reef Tract from High-Resolution Laser Bathymetry: Southern Molokai, Hawaii." *GSA Bulletin* 115 (11): 1344–55. <http://dx.doi.org/10.1130/B25200.1>.
- Storlazzi, Curt D., M. K. Presto, and Joshua B Logan. 2009. "Coastal Circulation and Sediment Dynamics in War-in-the-Pacific National Historical Park, Guam. Measurements of Waves, Currents, Temperature, Salinity, and Turbidity: July 2007–January 2008," no. January 2008: 84. <https://pubs.usgs.gov/of/2009/1195/of2009-1195.pdf>.
- Storlazzi, Curt D., James B. Shope, Li H. Erikson, Christine A. Hegermiller, and Patrick L. Barnard. 2015. "Future Wave and Wind Projections for United States and United States-Affiliated Pacific Islands." *U.S. Geological Survey Open-File Report 2015–1001*, 426 p. <https://doi.org/http://dx.doi.org/10.3133/ofr20151001>.
- Svendsen, Ib A., Kevin A. Haas, and Qun Zhao. 2001. "Analysis of Rip Current Systems." In *Coastal Engineering 2000*, 1127–40. Reston, VA: American Society of Civil Engineers. [https://doi.org/10.1061/40549\(276\)87](https://doi.org/10.1061/40549(276)87).
- Symonds, Graham, Kerry P. Black, and Ian R. Young. 1995. "Wave-Driven Flow over Shallow Reefs." *Journal of Geophysical Research* 100 (C2): 2639–48. <https://doi.org/10.1029/94JC02736>.
- Symonds, Graham, David A. Huntley, and Anthony J. Bowen. 1982. "Two-Dimensional Surf Beat: Long Wave Generation by a Time-Varying Breakpoint." *Journal of Geophysical Research* 87 (C1): 492. <https://doi.org/10.1029/JC087iC01p00492>.
- Taebi, Soheila, Ryan J. Lowe, Charitha B. Pattiaratchi, Greg N. Ivey, Graham Symonds, and Richard Brinkman. 2011. "Nearshore Circulation in a Tropical Fringing Reef System." *Journal of Geophysical Research: Oceans* 116 (2): 1–15. <https://doi.org/10.1029/2010JC006439>.
- Tait, Robert J. 1972. "Wave Set-up on Coral Reefs." *Journal of Geophysical Research* 77 (12): 2207–11. <https://doi.org/10.1029/JC077i012p02207>.
- Tajima, Yoshimitsu, Kavinda H Gunasekara, Takenori Shimozone, and Eric C Cruz. 2016. "Study on Locally Varying Inundation Characteristics Induced by Super Typhoon Haiyan. Part 1: Dynamic Behavior of Storm Surge and Waves around San Pedro Bay." *Coastal Engineering Journal* 58 (1): 1–24. <https://doi.org/10.1142/S0578563416400039>.

- Tajima, Yoshimitsu, Takenori Shimoazono, Kavinda H Gunasekara, and Eric C Cruz. 2016. "Study on Locally Varying Inundation Characteristics Induced by Super Typhoon Haiyan. Part 2: Deformation of Storm Waves on the Beach with Fringing Reef Along the East Coast of Eastern Samar." *Coastal Engineering Journal* 58 (1). <https://doi.org/10.1142/S0578563416400039>.
- United Nation Population Fund, Pacific sub-regional Office. 2014. "Population and Development Profiles : Pacific Island Countries." Pacific Sub Regional Office.
- Veldt, Timo. 2019. "The Effect of Wave Directional Spread on Coastal Hazards at Coastlines Fronted by a Coral Reef." <https://repository.tudelft.nl/islandora/object/uuid%3A0fd0b73b-fdf3-4d18-a932-c4fc226684cb?collection=education>.
- Vetter, O., Janet M. Becker, Mark A. Merrifield, Anne Christine N. Péquignet, Jérôme P. Aucan, S. J. Boc, and C. E. Pollock. 2010. "Wave Setup over a Pacific Island Fringing Reef." *Journal of Geophysical Research* 115 (C12): C12066. <https://doi.org/10.1029/2010JC006455>.
- Young, Ian R. 1989. "Wave Transformation over Coral Reefs." *J. Geophys. Res.* 94 (C7): 9779–89. <https://doi.org/10.1029/JC094iC07p09779>.
- Yu, Jie, and Donald N. Slinn. 2003. "Effects of Wave-Current Interaction on Rip Currents." *Journal of Geophysical Research* 108 (C3): 3088. <https://doi.org/10.1029/2001JC001105>.
- Zhang, Zhenlin, James L. Falter, Ryan Lowe, and Greg Ivey. 2012. "The Combined Influence of Hydrodynamic Forcing and Calcification on the Spatial Distribution of Alkalinity in a Coral Reef System." *Journal of Geophysical Research: Oceans* 117 (4): n/a-n/a. <https://doi.org/10.1029/2011JC007603>.
- Zhang, Zhenlin, Ryan Lowe, James L. Falter, and Greg Ivey. 2011. "A Numerical Model of Wave- and Current-Driven Nutrient Uptake by Coral Reef Communities." *Ecological Modelling* 222 (8): 1456–70. <https://doi.org/10.1016/j.ecolmodel.2011.01.014>.
- Zijlema, M, and G S Stelling. 2008. "Efficient Computation of Surf Zone Waves Using the Nonlinear Shallow Water Equations with Non-Hydrostatic Pressure." <https://doi.org/10.1016/j.coastaleng.2008.02.020>.

Appendix A. DIMENSIONS OF STUDIED FRINGING REEF SECTIONS WITH A CHANNEL

Location	Channel number	Reef width [m]	Channel width [m]	Spacing left [m]	Spacing right [m]	Channel angle [deg.]
Fiji	South 1	700	130	300	600	15
Fiji	South 2	800	200	1500	3000	0
Fiji	South 3	500	100	800	1500	0
Fiji	South 4	500	90	700	800	15
Fiji	South 5	530	600	1300	2700	0
Fiji	South 6	520	580	1200	2700	0
Fiji	South 7	650	70	1800	2900	0
Fiji	South 8	350	75	2900	1250	0
Fiji	South 9	700	450	1250	3200	5
Guam	south 1	750	85	-	1150	0
Guam	south 2	480	40	1150	870	15
Guam	south 3	400	45	870	1100	15
Guam	south 4	400	95	1100	-	20
Guam	West 1	50	30	900	-	0
Guam	West 2	500	50	3000	2700	0
Guam	West 3	300	200	2800	3000	30
Ile Emao		200	90	-	-	0
Ile Futuna	West 1	220	40	370	370	0
Ile Futuna	West 2	200	50	800	370	0
Ile Moso Shefa	North	340	70	550	390	0
Kandavu, Fiji	1	980	120	2200	1900	5
Lanai, Hawaii	1	350	40	-	-	0
Molokai, Hawaii	South 1	1400	160	-	6600	15
Molokai, Hawaii	South 2	800	230	6600	-	10
Molokai, Hawaii	West 1	800	170	5500	2100	0
Molokai, Hawaii	West 2	800	160	2100	880	0
Molokai, Hawaii	West 3	700	170	880	350	0
Molokai, Hawaii	West 4	600	350	350	1200	0
Molokai, Hawaii	West 5	400	50	1200	730	50
Nggamea, Fiji	1	350	150	1400	1000	15
Oahu, Hawaii	East 1	400	150	1500	1500	15
Oahu, Hawaii	East 2	600	250	2000	2000	8
Palau	West 1	1400	260	-	800	0
Palau	West 2	600	125	800	4700	20
Palau	West 3	900	120	4700	-	0

APPENDIX A
DIMENSIONS OF STUDIED FRINGING REEF SECTIONS WITH A CHANNEL

Location	Channel number	Reef width [m]	Channel width [m]	Spacing left [m]	Spacing right [m]	Channel angle [deg.]
Pulau Liki	1	240	70	600	720	0
Pulau Liki	2	200	100	370	600	0
Pulau Liki	3	270	100	700	850	0
Rambutyo Islands	1	400	130	2000	1300	5
Rambutyo Islands	2	300	100	1300	1100	25
Rambutyo Islands	3	530	130	360	1100	15
Rarotonga, Cook Islands	North1	150	130	-	800	0
Rarotonga, Cook Islands	South 1	500	80	2000	-	15
Samoa	North 1	500	75	750	1700	10
Samoa	West 1	750	180	-	3000	0
San Cristobal, Solomon Islands	South 1	550	80	850	2000	8
San Cristobal, Solomon Islands	South 2	360	100	500	500	10
San Cristobal, Solomon Islands	South 3	400	120	800	500	0
San Cristobal, Solomon Islands	South 4	220	80	650	550	0
Sangafa	North	420	120	-	709	10
Sangafa	South	230	70	1200	-	0
Talikud, Indonesia	1	600	165	900	1500	0
Talikud, Indonesia	2	240	70	1800	1500	5
Tutuila, Samoa	South 1	150	50	-	500	0
Tutuila, Samoa	South 2	230	40	500	-	0
Tutuila, Samoa	West 1	480	80	-	-	0
Tutuila, Samoa	West 2	160	160	-	-	0
Upolu, Samoa	North 1	800	300	100	2500	5
Upolu, Samoa	North 2	280	130	500	350	0
Upolu, Samoa	North 3	160	35	500	1200	20
Upolu, Samoa	North 4	180	80	1200	-	25
Upolu, Samoa	South 1	800	80	-	-	8
Upolu, Samoa	South 2	280	50	800	260	5
Upolu, Samoa	South 3	260	50	260	280	10
Upolu, Samoa	South 4	140	65	100	240	0
Upolu, Samoa	South 5	250	40	240	750	0
Upolu, Samoa	South 6	700	350	750	1200	0
Upolu, Samoa	South 7	600	70	1700	750	15
Upolu, Samoa	South 8	800	260	500	500	0
Yap Island	1	1200	320	6000	6000	15

Table A.1, Dimensions of fringing reefs with a channel, measured in Google Earth

Appendix B. EXAMPLE XBEACH INPUT FILE

An example XBeach input file (params.txt file) is presented below. This file is used to define the input for the XBeach model, dictates model settings and what output should be generated. The file below is for the baseline scenario, test221.

```

%%
%%
%%
%% XBeach parameter
settings input
file
%%
%%
%%
%% date:      11-Nov-2017
00:37:33
%%
%%
%% function:
xb_write_params
%%
%%
%%
%% Flow boundary
condition
parameters
%%
%%
front          = nonh_1D
%% Flow
parameters
%%
%%
bedfriction    = cf
bedfricfile    = fric.txt
%%
General
%%
%%
cyclic         = 1
%% Grid
parameters
%%
%%
depfile        = bed.dep
posdwn        = 0
nx             = 714
ny            = 563
alfa          = 0
vardx         = 1
xfile         = x.grd
yfile         = y.grd
xori          = 0
yori          = 0
thetamin      = -10
thetamax      = 10
dtheta        = 20
%% MPI
parameters
%%
mpiboundary    = x
%% Model
time
%%
tstop         = 16560
%% Physical
processes
%%
swave         = 0
sedtrans      = 0
morphology    = 0
nonh          = 1
%% Tide boundary
conditions
%%
zs0file       = tidel.txt
tideloc       = 1
%% Wave boundary
condition
parameters
%%
instat        = jons_table
%% Wave-current
interaction
parameters
%%
wci           = 1
%% Wave-spectrum
boundary condition
parameters
%%
bcfile        = waves1.txt
random        = 0
%% Output
variables
%%
outputformat  = netcdf
tintm         = 500
tintp         = 0.500000
tintg         = 500
tstart        = 1
nmeanvar     = 5
zs
u
v
qx
qy
nglobal      = 5
u
v
zs
qx
qy
npointvar    = 3
zs
u
v
npoints      = 88
0. 0. point_A1_320_0
0. 250. point_A2_320_250
0. 400. point_A3_320_400
0. 490. point_A4_320_490
0. 500. point_A5_320_500
0. 550. point_A6_320_550
0. 600. point_A7_320_600
0. 610. point_A8_320_610
0. 700. point_A9_320_700
0. 850. point_A10_320_850
0. 1100.
point_A11_320_1100
29. 0. point_B1_-292_0
29. 250. point_B2_-
292_250
29. 400. point_B3_-
292_400
29. 490. point_B4_-
292_490
29. 500. point_B5_-
292_500
29. 550. point_B6_-
292_550
29. 600. point_B7_-
292_600
29. 610. point_B8_-
292_610

```

APPENDIX B
EXAMPLE XBEACH INPUT FILE

29. 700. point_B9_-	343. 250.	0. 128. transect128
292_700	point_G2_153_250	0. 132. transect132
29. 850. point_B10_-	343. 400.	0. 136. transect136
292_850	point_G3_153_400	0. 140. transect140
29. 1100. point_B11_-	343. 490.	0. 144. transect144
292_1100	point_G4_153_490	0. 148. transect148
180. 0. point_C1_-140_0	343. 500.	0. 152. transect152
180. 250. point_C2_-	point_G5_153_500	0. 156. transect156
140_250	343. 550.	0. 160. transect160
180. 400. point_C3_-	point_G6_153_550	0. 164. transect164
140_400	343. 600.	0. 168. transect168
180. 490. point_C4_-	point_G7_153_600	0. 172. transect172
140_490	343. 610.	0. 176. transect176
180. 500. point_C5_-	point_G8_153_610	0. 180. transect180
140_500	343. 700.	0. 184. transect184
180. 550. point_C6_-	point_G9_153_700	0. 188. transect188
140_550	343. 850.	0. 192. transect192
180. 600. point_C7_-	point_G10_153_850	0. 196. transect196
140_600	343. 1100.	0. 200. transect200
180. 610. point_C8_-	point_G11_153_1100	0. 204. transect204
140_610	620. 0. point_H1_300_0	0. 208. transect208
180. 700. point_C9_-	620. 250.	0. 212. transect212
140_700	point_H2_300_250	0. 216. transect216
180. 850. point_C10_-	620. 400.	0. 220. transect220
140_850	point_H3_300_400	0. 224. transect224
180. 1100. point_C11_-	620. 490.	0. 228. transect228
140_1100	point_H4_300_490	0. 232. transect232
303. 0. point_D1_-18_0	620. 500.	0. 236. transect236
303. 250. point_D2_-	point_H5_300_500	0. 240. transect240
18_250	620. 550.	0. 244. transect244
303. 400. point_D3_-	point_H6_300_550	0. 248. transect248
18_400	620. 600.	0. 252. transect252
303. 490. point_D4_-	point_H7_300_600	0. 256. transect256
18_490	620. 610.	0. 260. transect260
303. 500. point_D5_-	point_H8_300_610	0. 264. transect264
18_500	620. 700.	0. 268. transect268
303. 550. point_D6_-	point_H9_300_700	0. 272. transect272
18_550	620. 850.	0. 276. transect276
303. 600. point_D7_-	point_H10_300_850	0. 280. transect280
18_600	620. 1100.	0. 284. transect284
303. 610. point_D8_-	point_H11_300_1100	0. 288. transect288
18_610		0. 292. transect292
303. 700. point_D9_-	nrugauge = 361	0. 296. transect296
18_700	0. 0. transect0	0. 300. transect300
303. 850. point_D10_-	0. 4. transect4	0. 304. transect304
18_850	0. 8. transect8	0. 308. transect308
303. 1100. point_D11_-	0. 12. transect12	0. 312. transect312
18_1100	0. 16. transect16	0. 316. transect316
323. 0. point_E1_3_0	0. 20. transect20	0. 320. transect320
323. 250. point_E2_3_250	0. 24. transect24	0. 324. transect324
323. 400. point_E3_3_400	0. 28. transect28	0. 328. transect328
323. 490. point_E4_3_490	0. 32. transect32	0. 332. transect332
323. 500. point_E5_3_500	0. 36. transect36	0. 336. transect336
323. 550. point_E6_3_550	0. 40. transect40	0. 340. transect340
323. 600. point_E7_3_600	0. 44. transect44	0. 344. transect344
323. 610. point_E8_3_610	0. 48. transect48	0. 348. transect348
323. 700. point_E9_3_700	0. 52. transect52	0. 352. transect352
323. 850. point_E10_3_850	0. 56. transect56	0. 356. transect356
323. 1100.	0. 60. transect60	0. 360. transect360
point_E11_3_1100	0. 64. transect64	0. 364. transect364
343. 0. point_F1_23_0	0. 68. transect68	0. 368. transect368
343. 250. point_F2_23_250	0. 72. transect72	0. 372. transect372
343. 400. point_F3_23_400	0. 76. transect76	0. 376. transect376
343. 490. point_F4_23_490	0. 80. transect80	0. 380. transect380
343. 500. point_F5_23_500	0. 84. transect84	0. 382. transect382
343. 550. point_F6_23_550	0. 88. transect88	0. 384. transect384
343. 600. point_F7_23_600	0. 92. transect92	0. 386. transect386
343. 610. point_F8_23_610	0. 96. transect96	0. 388. transect388
343. 700. point_F9_23_700	0. 100. transect100	0. 390. transect390
343. 850.	0. 104. transect104	0. 392. transect392
point_F10_23_850	0. 108. transect108	0. 394. transect394
343. 1100.	0. 112. transect112	0. 396. transect396
point_F11_23_1100	0. 116. transect116	0. 398. transect398
343. 0. point_G1_153_0	0. 120. transect120	0. 400. transect400
	0. 124. transect124	0. 402. transect402

0. 404. transect404	0. 558. transect558	0. 712. transect712
0. 406. transect406	0. 560. transect560	0. 714. transect714
0. 408. transect408	0. 562. transect562	0. 716. transect716
0. 410. transect410	0. 564. transect564	0. 718. transect718
0. 412. transect412	0. 566. transect566	0. 720. transect720
0. 414. transect414	0. 568. transect568	0. 724. transect724
0. 416. transect416	0. 570. transect570	0. 728. transect728
0. 418. transect418	0. 572. transect572	0. 732. transect732
0. 420. transect420	0. 574. transect574	0. 736. transect736
0. 422. transect422	0. 576. transect576	0. 740. transect740
0. 424. transect424	0. 578. transect578	0. 744. transect744
0. 426. transect426	0. 580. transect580	0. 748. transect748
0. 428. transect428	0. 582. transect582	0. 752. transect752
0. 430. transect430	0. 584. transect584	0. 756. transect756
0. 432. transect432	0. 586. transect586	0. 760. transect760
0. 434. transect434	0. 588. transect588	0. 764. transect764
0. 436. transect436	0. 590. transect590	0. 768. transect768
0. 438. transect438	0. 592. transect592	0. 772. transect772
0. 440. transect440	0. 594. transect594	0. 776. transect776
0. 442. transect442	0. 596. transect596	0. 780. transect780
0. 444. transect444	0. 598. transect598	0. 784. transect784
0. 446. transect446	0. 600. transect600	0. 788. transect788
0. 448. transect448	0. 602. transect602	0. 792. transect792
0. 450. transect450	0. 604. transect604	0. 796. transect796
0. 452. transect452	0. 606. transect606	0. 800. transect800
0. 454. transect454	0. 608. transect608	0. 804. transect804
0. 456. transect456	0. 610. transect610	0. 808. transect808
0. 458. transect458	0. 612. transect612	0. 812. transect812
0. 460. transect460	0. 614. transect614	0. 816. transect816
0. 462. transect462	0. 616. transect616	0. 820. transect820
0. 464. transect464	0. 618. transect618	0. 824. transect824
0. 466. transect466	0. 620. transect620	0. 828. transect828
0. 468. transect468	0. 622. transect622	0. 832. transect832
0. 470. transect470	0. 624. transect624	0. 836. transect836
0. 472. transect472	0. 626. transect626	0. 840. transect840
0. 474. transect474	0. 628. transect628	0. 844. transect844
0. 476. transect476	0. 630. transect630	0. 848. transect848
0. 478. transect478	0. 632. transect632	0. 852. transect852
0. 480. transect480	0. 634. transect634	0. 856. transect856
0. 482. transect482	0. 636. transect636	0. 860. transect860
0. 484. transect484	0. 638. transect638	0. 864. transect864
0. 486. transect486	0. 640. transect640	0. 868. transect868
0. 488. transect488	0. 642. transect642	0. 872. transect872
0. 490. transect490	0. 644. transect644	0. 876. transect876
0. 492. transect492	0. 646. transect646	0. 880. transect880
0. 494. transect494	0. 648. transect648	0. 884. transect884
0. 496. transect496	0. 650. transect650	0. 888. transect888
0. 498. transect498	0. 652. transect652	0. 892. transect892
0. 500. transect500	0. 654. transect654	0. 896. transect896
0. 502. transect502	0. 656. transect656	0. 900. transect900
0. 504. transect504	0. 658. transect658	0. 904. transect904
0. 506. transect506	0. 660. transect660	0. 908. transect908
0. 508. transect508	0. 662. transect662	0. 912. transect912
0. 510. transect510	0. 664. transect664	0. 916. transect916
0. 512. transect512	0. 666. transect666	0. 920. transect920
0. 514. transect514	0. 668. transect668	0. 924. transect924
0. 516. transect516	0. 670. transect670	0. 928. transect928
0. 518. transect518	0. 672. transect672	0. 932. transect932
0. 520. transect520	0. 674. transect674	0. 936. transect936
0. 522. transect522	0. 676. transect676	0. 940. transect940
0. 524. transect524	0. 678. transect678	0. 944. transect944
0. 526. transect526	0. 680. transect680	0. 948. transect948
0. 528. transect528	0. 682. transect682	0. 952. transect952
0. 530. transect530	0. 684. transect684	0. 956. transect956
0. 532. transect532	0. 686. transect686	0. 960. transect960
0. 534. transect534	0. 688. transect688	0. 964. transect964
0. 536. transect536	0. 690. transect690	0. 968. transect968
0. 538. transect538	0. 692. transect692	0. 972. transect972
0. 540. transect540	0. 694. transect694	0. 976. transect976
0. 542. transect542	0. 696. transect696	0. 980. transect980
0. 544. transect544	0. 698. transect698	0. 984. transect984
0. 546. transect546	0. 700. transect700	0. 988. transect988
0. 548. transect548	0. 702. transect702	0. 992. transect992
0. 550. transect550	0. 704. transect704	0. 996. transect996
0. 552. transect552	0. 706. transect706	0. 1000. transect1000
0. 554. transect554	0. 708. transect708	0. 1004. transect1004
0. 556. transect556	0. 710. transect710	0. 1008. transect1008

APPENDIX B
EXAMPLE XBEACH INPUT FILE

0. 1012. transect1012
0. 1016. transect1016
0. 1020. transect1020
0. 1024. transect1024
0. 1028. transect1028
0. 1032. transect1032
0. 1036. transect1036
0. 1040. transect1040

0. 1044. transect1044
0. 1048. transect1048
0. 1052. transect1052
0. 1056. transect1056
0. 1060. transect1060
0. 1064. transect1064
0. 1068. transect1068
0. 1072. transect1072

0. 1076. transect1076
0. 1080. transect1080
0. 1084. transect1084
0. 1088. transect1088
0. 1092. transect1092
0. 1096. transect1096
0. 1100. transect1100

Appendix C.

STATISTICAL RUNUP VALUES COMPLEMENTARY TO $Ru_{2\%}$

In addition $Ru_{2\%}$, the statistical values $Ru_{5\%}$, and $Ru_{10\%}$ are determined, as well as the maximum runup level and the minimum rundown level, defined as in Table C.1.

Statistical value	Definition
Ru_{\max}	The maximum occurring water level at the shoreline during the entire simulation
$Ru_{n\%}$, in which $n = 2, 5, 10$	Runup level which is exceeded by the highest $n\%$ of the waves.
Rd_{\min}	Minimum rundown, the lowest occurring water level at the shoreline during the entire simulation

Table C.1, definitions of statistical runup values

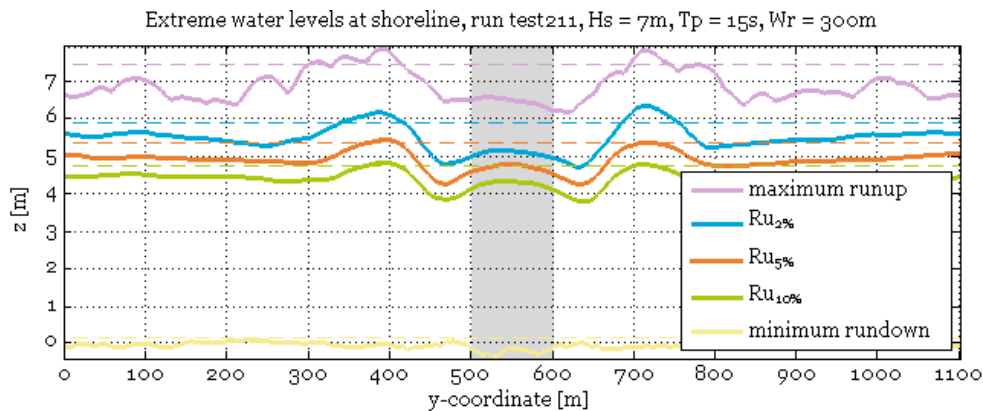


Figure C.1, longshore runup statistics: $Ru_{2\%}$, $Ru_{5\%}$, $Ru_{10\%}$ the maximum runup level and the minimum rundown level (solid lines), compared to their reference run (dashed lines), with the same forcing and a similar reef geometry but without a channel.

Regarding the statistical runup values, presented in Figure C.1, the following things can be noted:

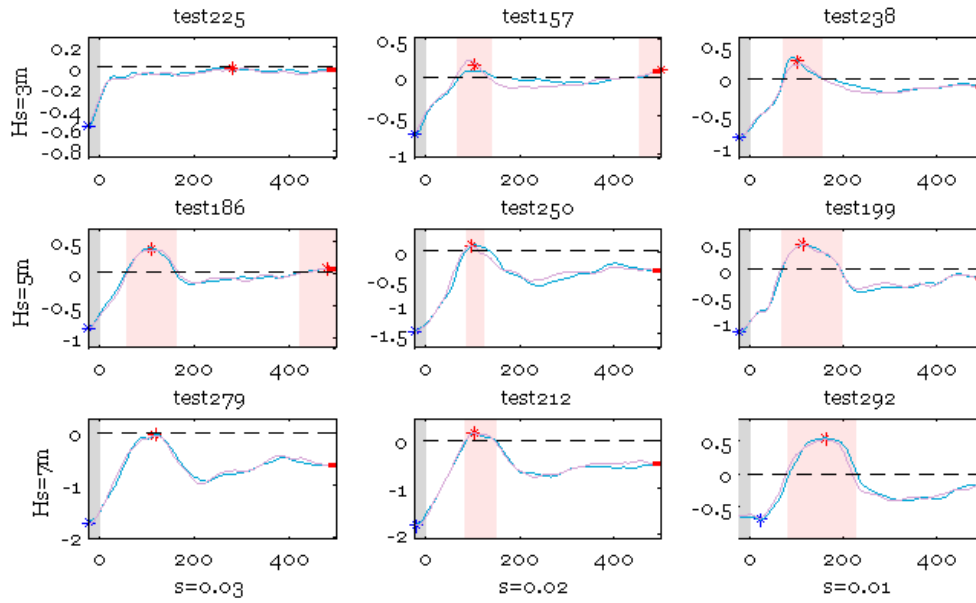
- Maximum runup to minimum rundown is descending order, which is in line with the definitions of these terms.
- The shape of the three $Ru_{n\%}$ values is comparable, and the peaks and troughs are on the same longshore locations.
- Ru_{\max} and Rd_{\min} are more irregular than $Ru_{n\%}$, which is to be expected as they are determined by a single occurrence during the entire simulation, while $Ru_{n\%}$ values are determined by a large number of waves.
- $Ru_{5\%}$ and $Ru_{10\%}$ differ from $Ru_{2\%}$, on three points:
 - First they are lower, which is to be expected as the levels of 5 and 10% are exceeded by more waves.
 - Second, their vertical range is smaller.
 - Third, $Ru_{5\%}$ and $Ru_{10\%}$ barely exceed the reference level, while the peaks of $Ru_{2\%}$ do so significantly.
- Rd_{\min} shows a smaller vertical range, being around the offshore SWL along the entire reef, with two troughs in the channel up to -0.30m . This is lower than the reference run, in which Rd_{\min} is $\text{SWL}+0.18\text{m}$.

Summarizing: $Ru_{n\%}^*$ follows a similar pattern for different values of n , but the vertical range and difference with the reference level may vary.

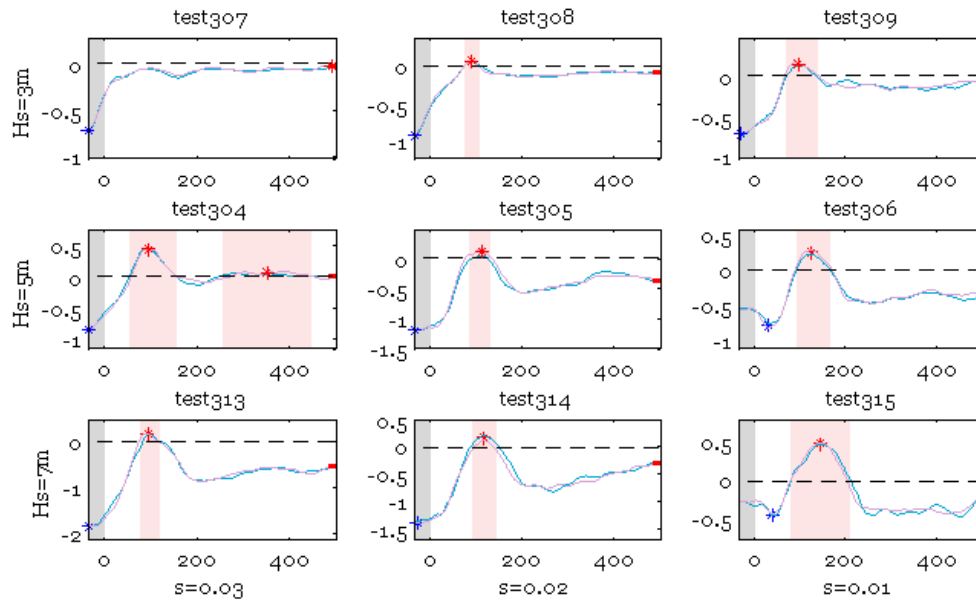
In the present study, $Ru_{2\%}$ is used, as it is the most commonly used value to describe runup.

Appendix D. RUNUP PATTERNS, ORGANIZED BY GEOMETRY

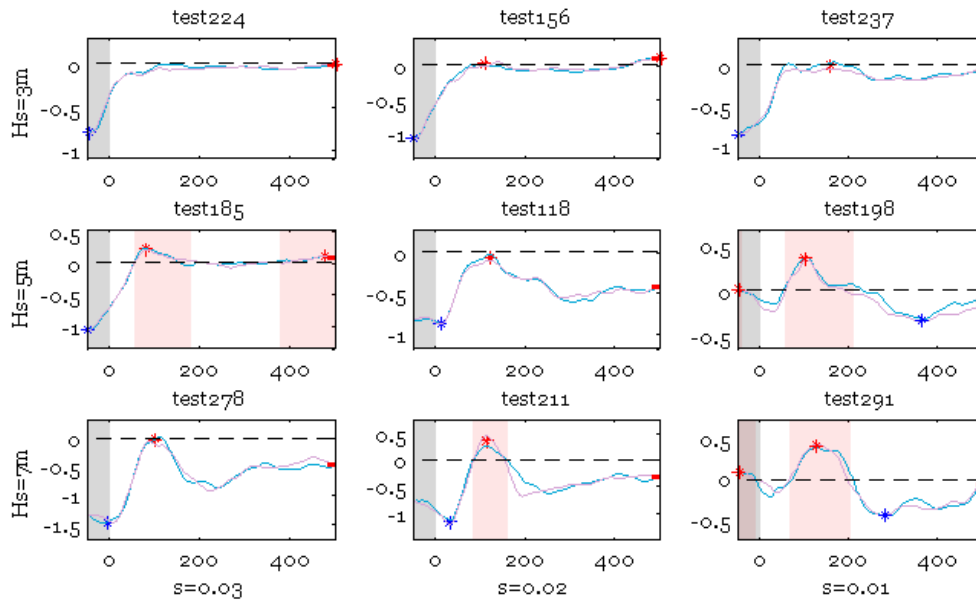
Runup patternsRu2%, Geometry1:
 $W_r=300m, W_c=50m, \text{spacing}=1000m$



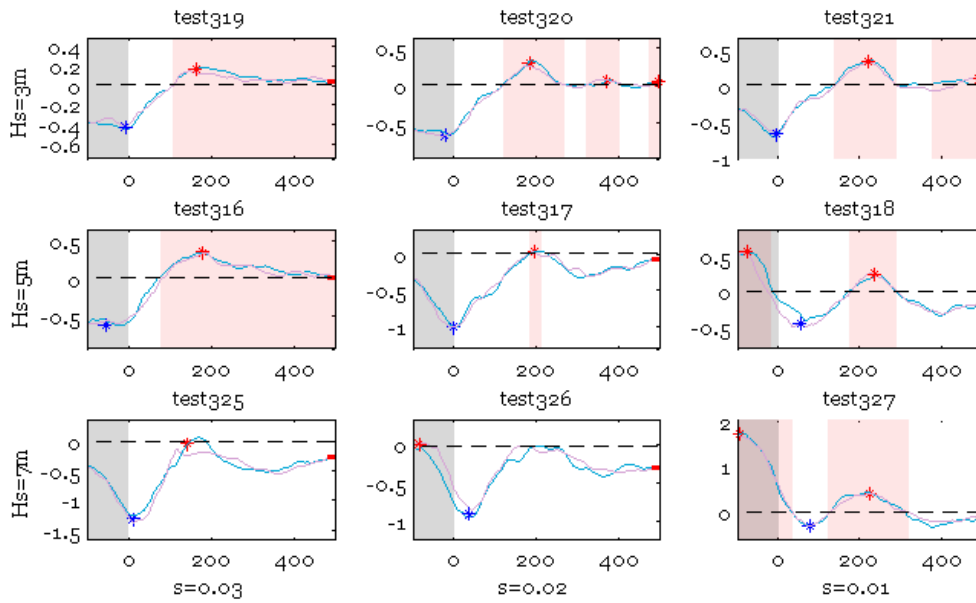
Runup patternsRu2%, Geometry2:
 $W_r=300m, W_c=70m, \text{spacing}=1000m$



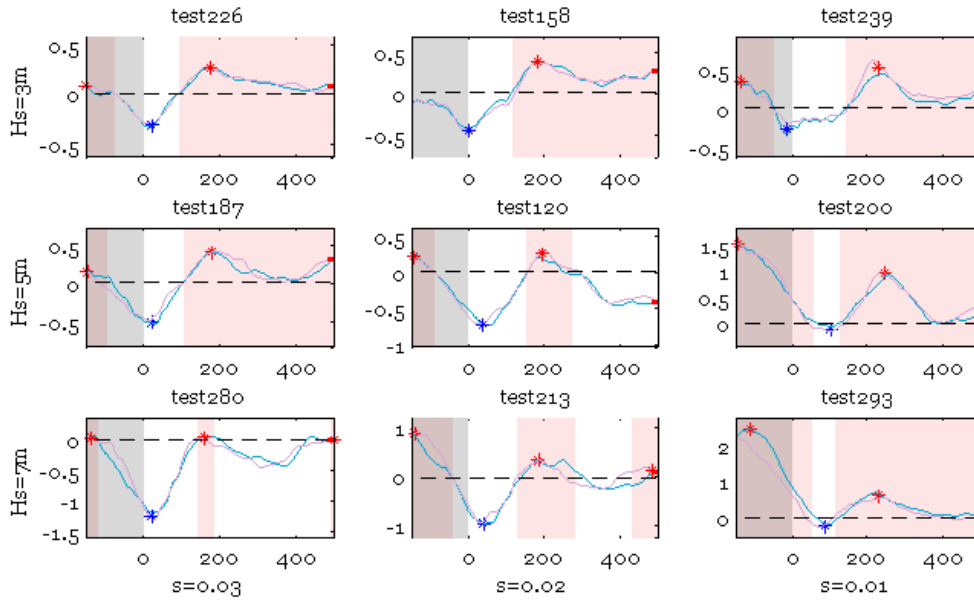
Runup patternsRu2%, Geometry3:
 $W_r=300m, W_c=100m, \text{spacing}=1000m$



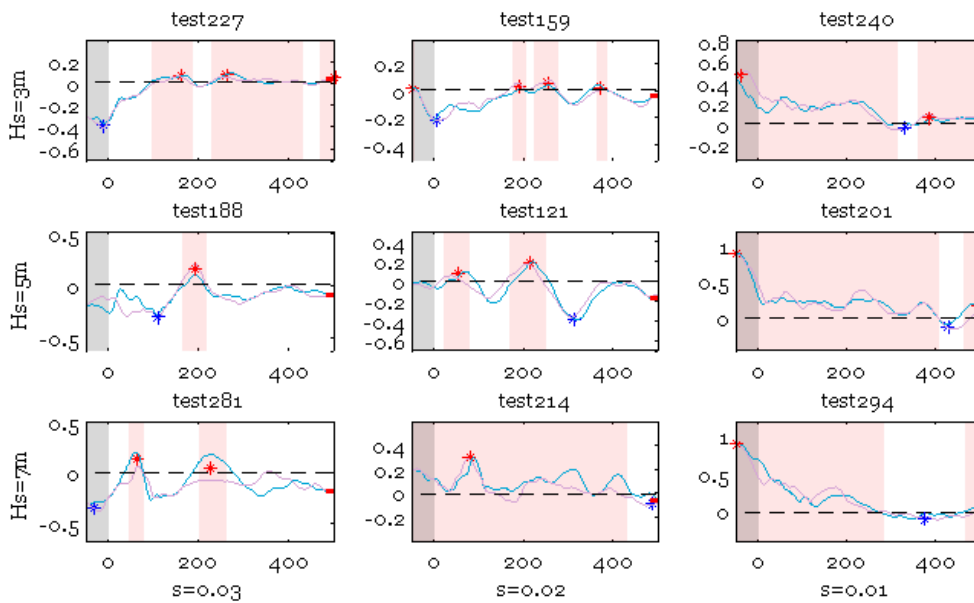
Runup patternsRu2%, Geometry4:
 $W_r=300m, W_c=200m, \text{spacing}=1000m$



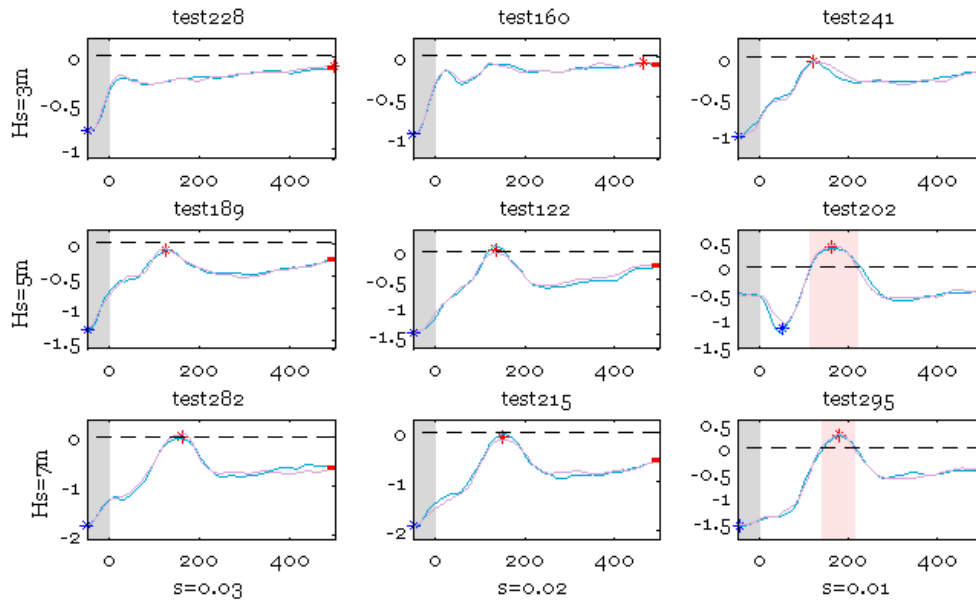
Runup patternsRu2%, Geometry5:
 $W_r=300m, W_c=300m, \text{spacing}=1000m$



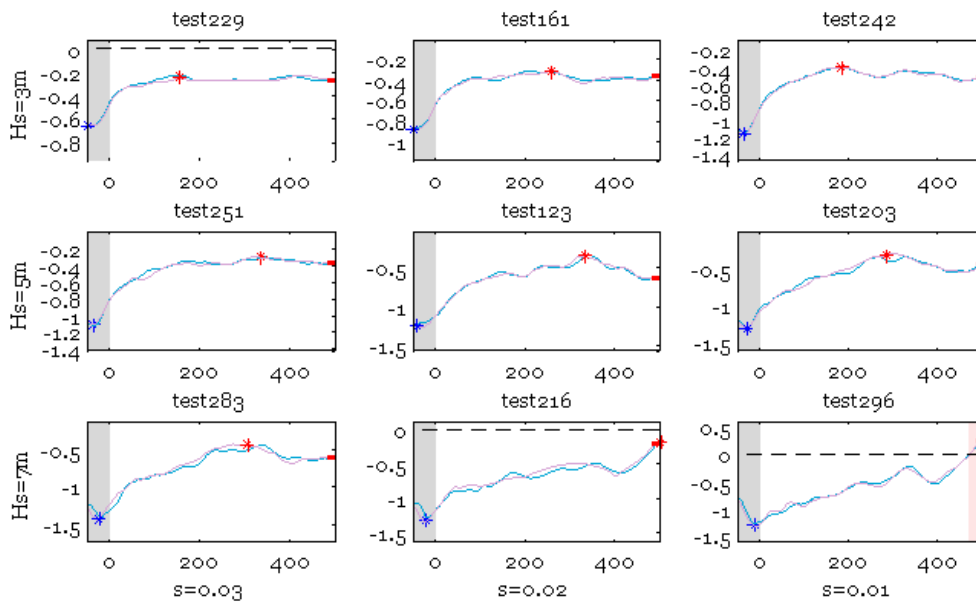
Runup patternsRu2%, Geometry6:
 $W_r=100m, W_c=100m, \text{spacing}=1000m$



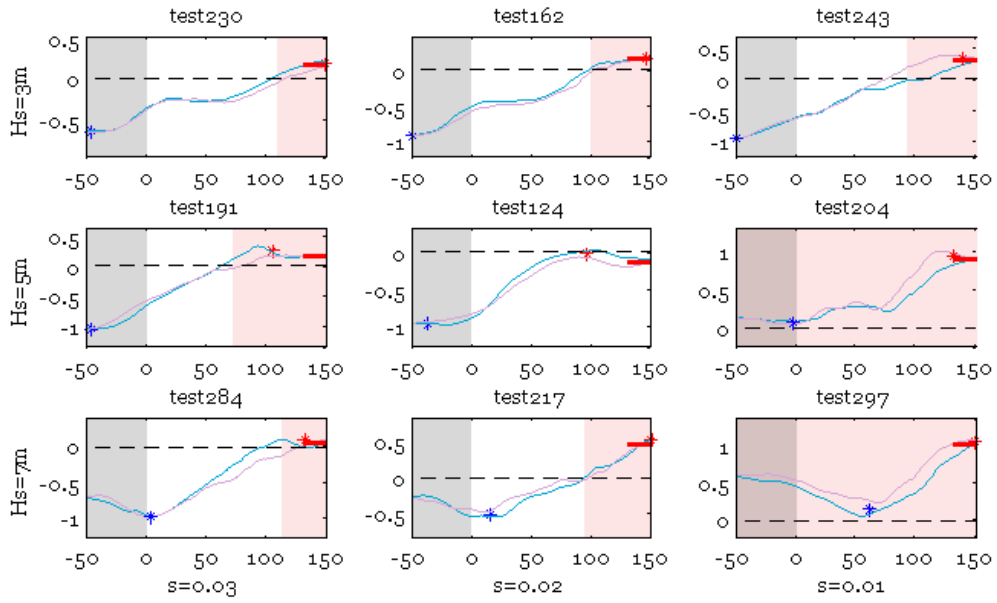
Runup patterns $Ru_2\%$, Geometry 7:
 $W_r=500m, W_c=100m, spacing=1000m$



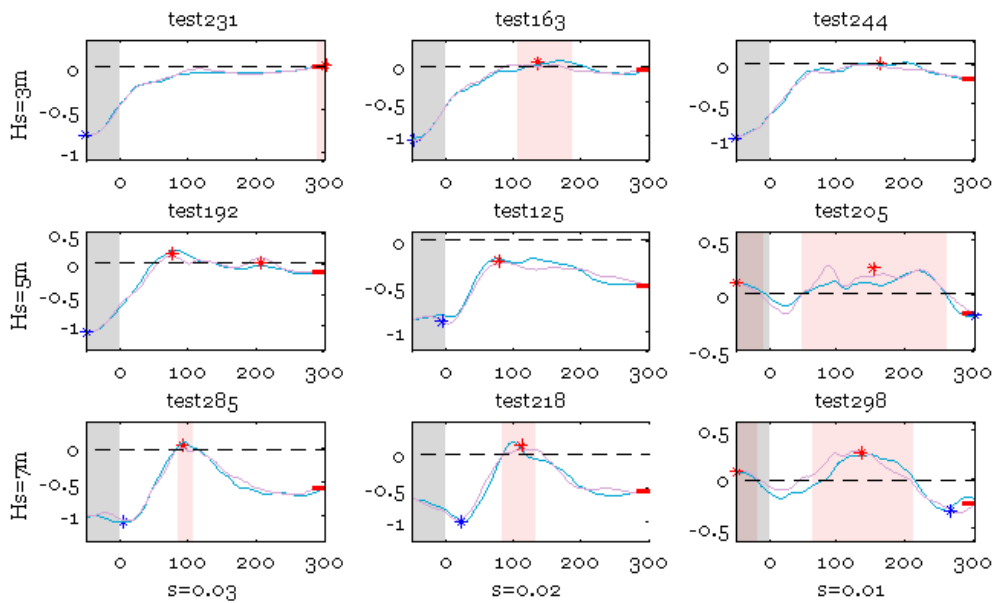
Runup patterns $Ru_2\%$, Geometry 8:
 $W_r=1000m, W_c=100m, spacing=1000m$



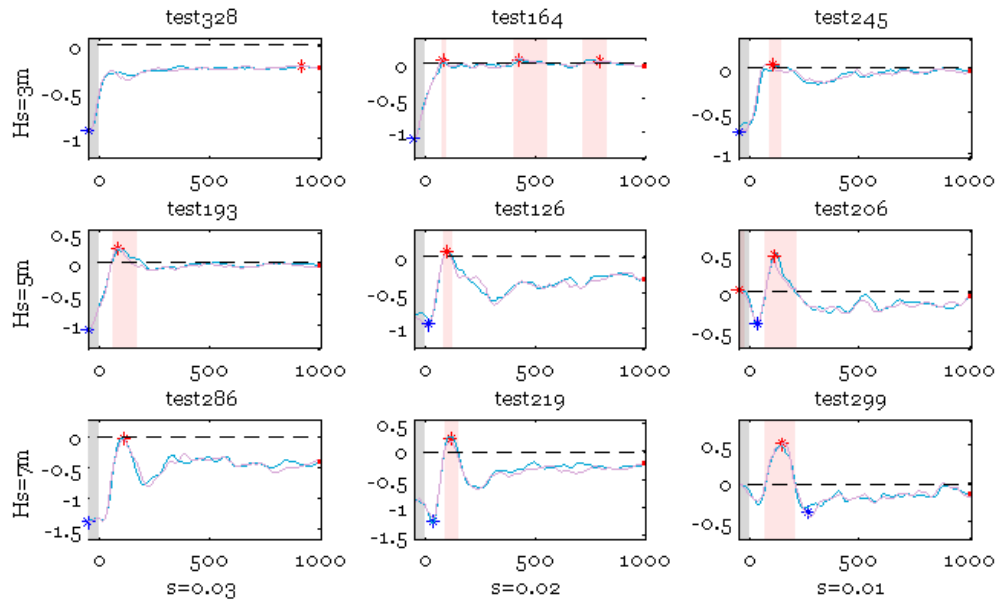
Runup patternsRu2%, Geometry9:
 Wr=300m, Wc=100m, spacing =300m



Runup patternsRu2%, Geometry10:
 Wr=300m, Wc=100m, spacing =600m

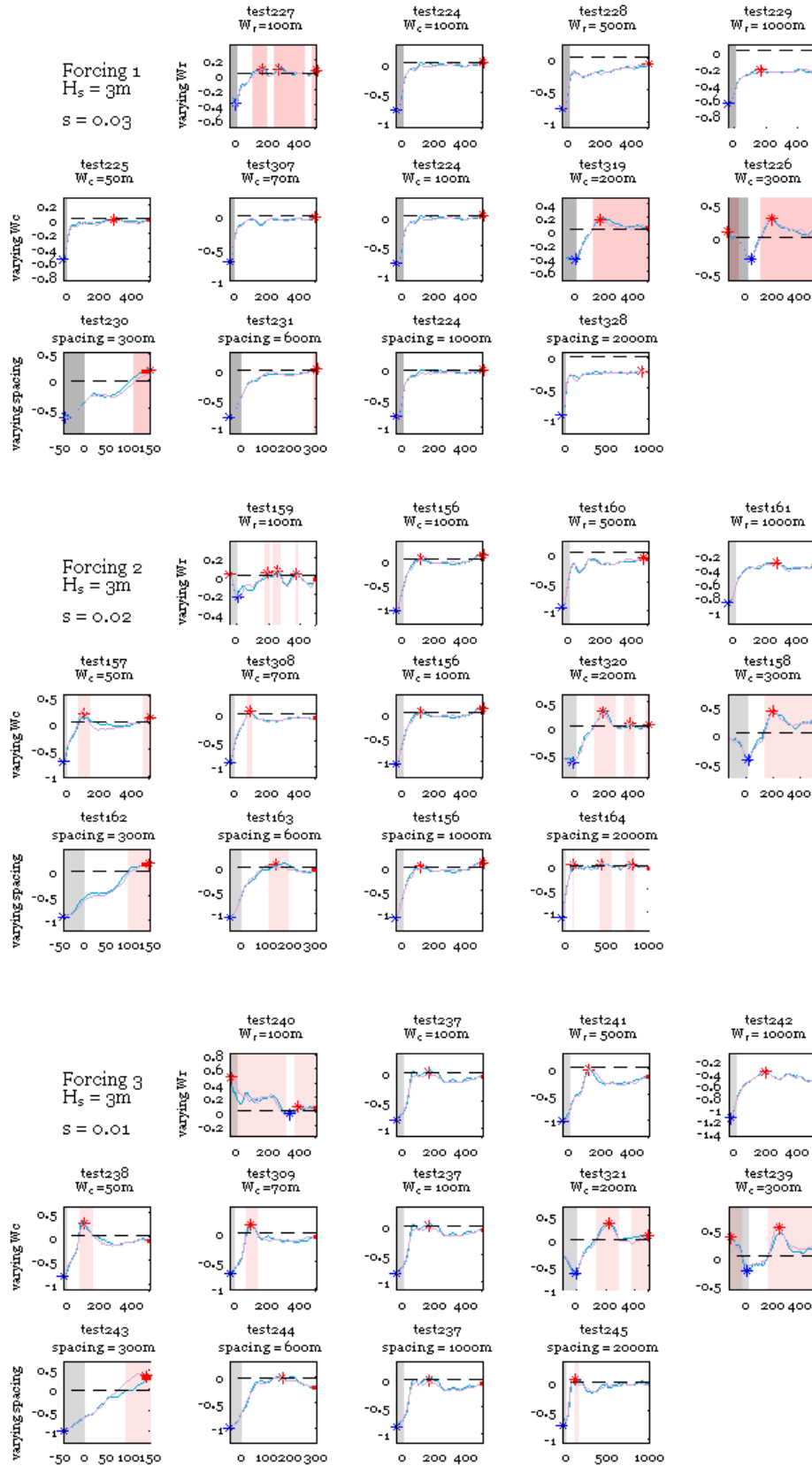


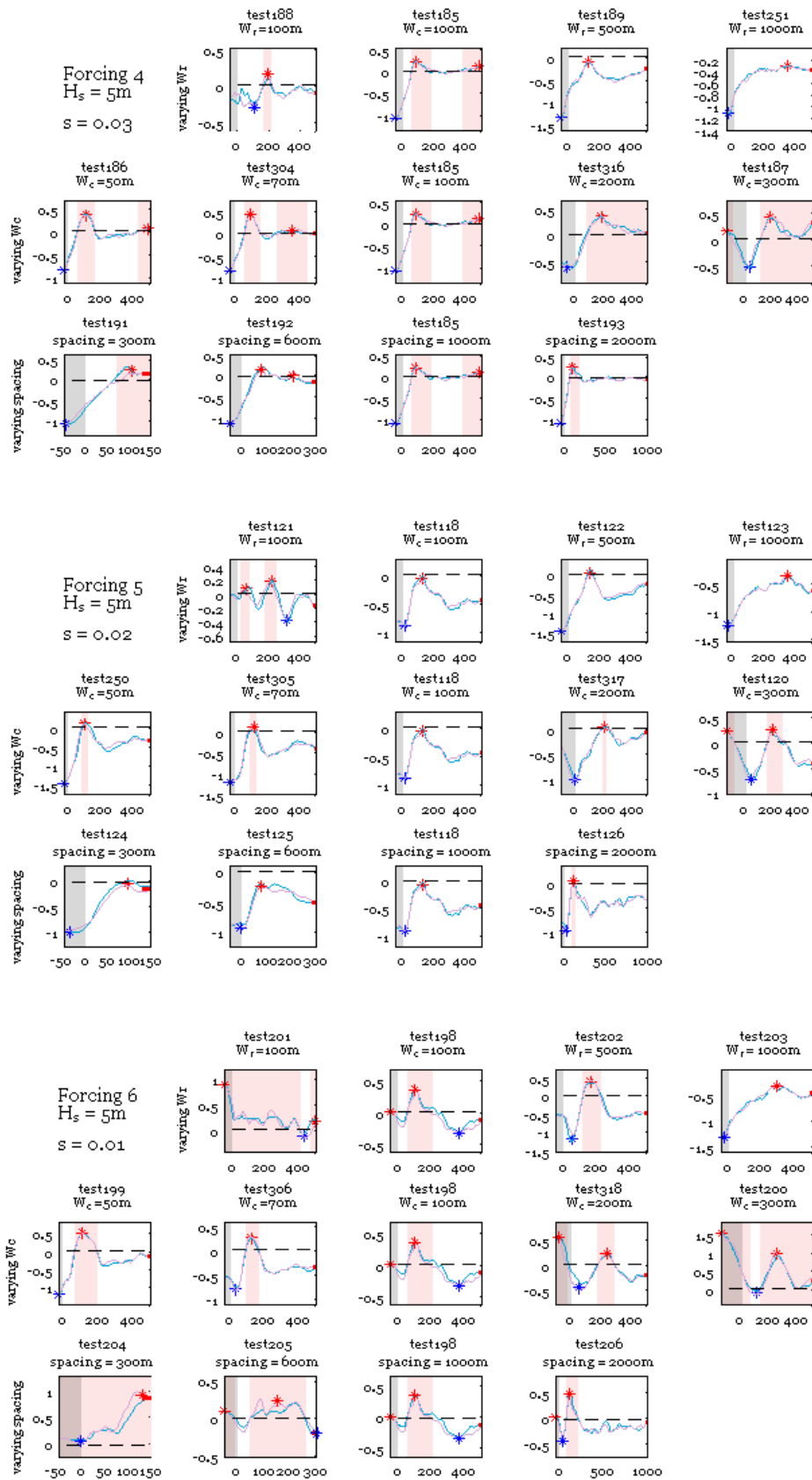
Runup patterns $R_{u2\%}$, Geometry 11:
 $W_r=300m$, $W_c=100m$, spacing = 2000m

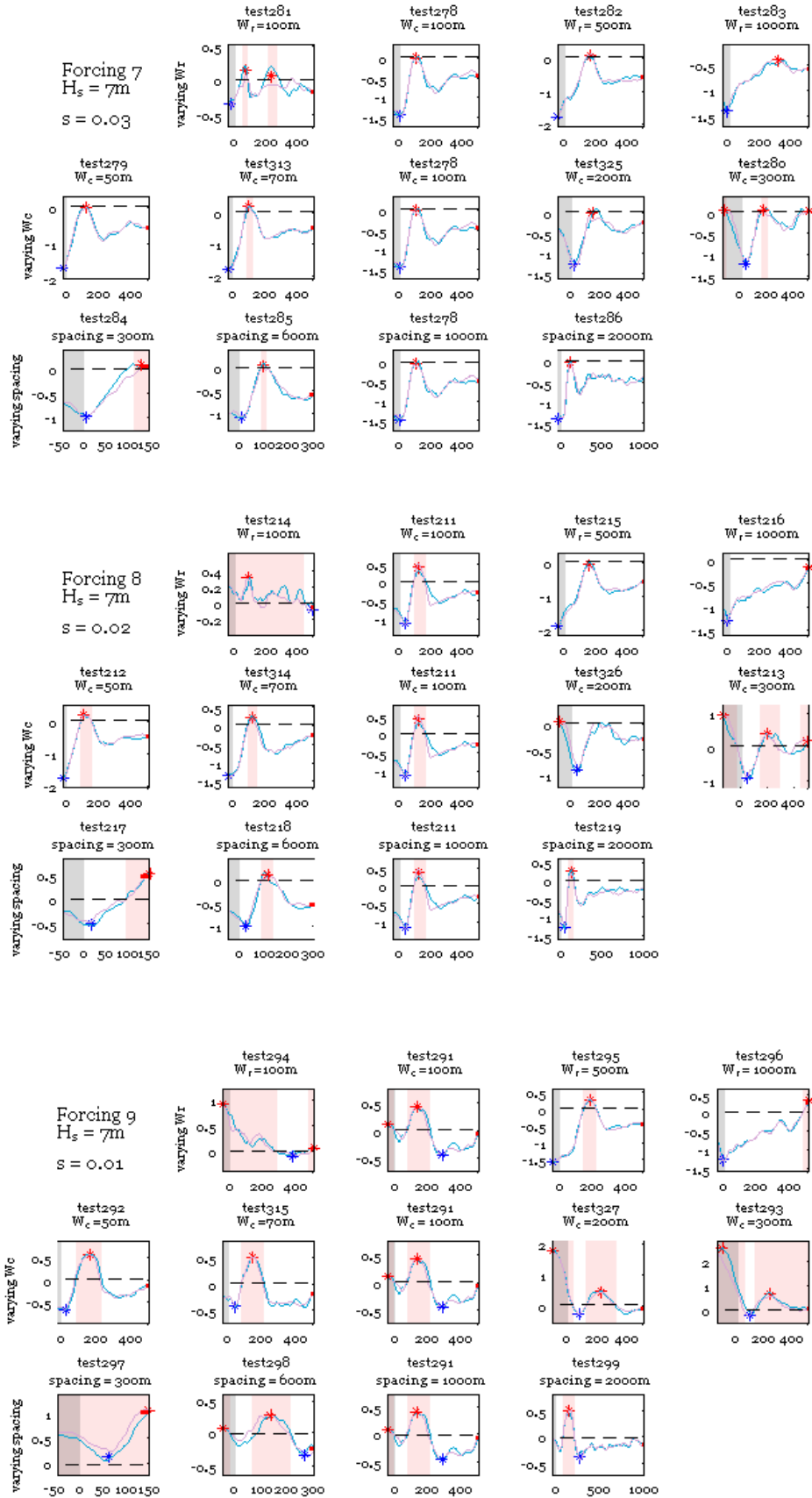


Appendix E.

RUNUP PATTERNS, ORGANIZED BY FORCING



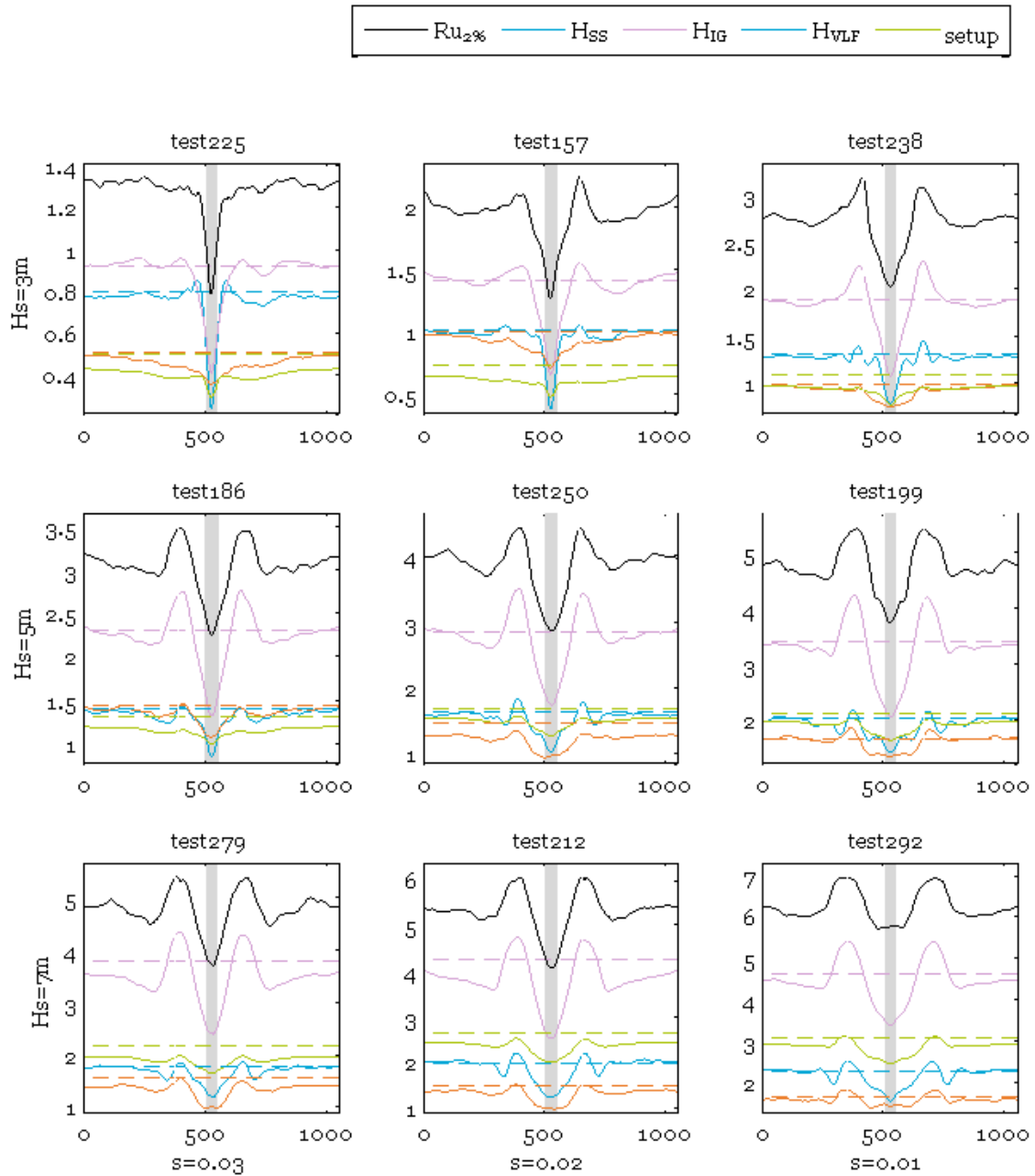




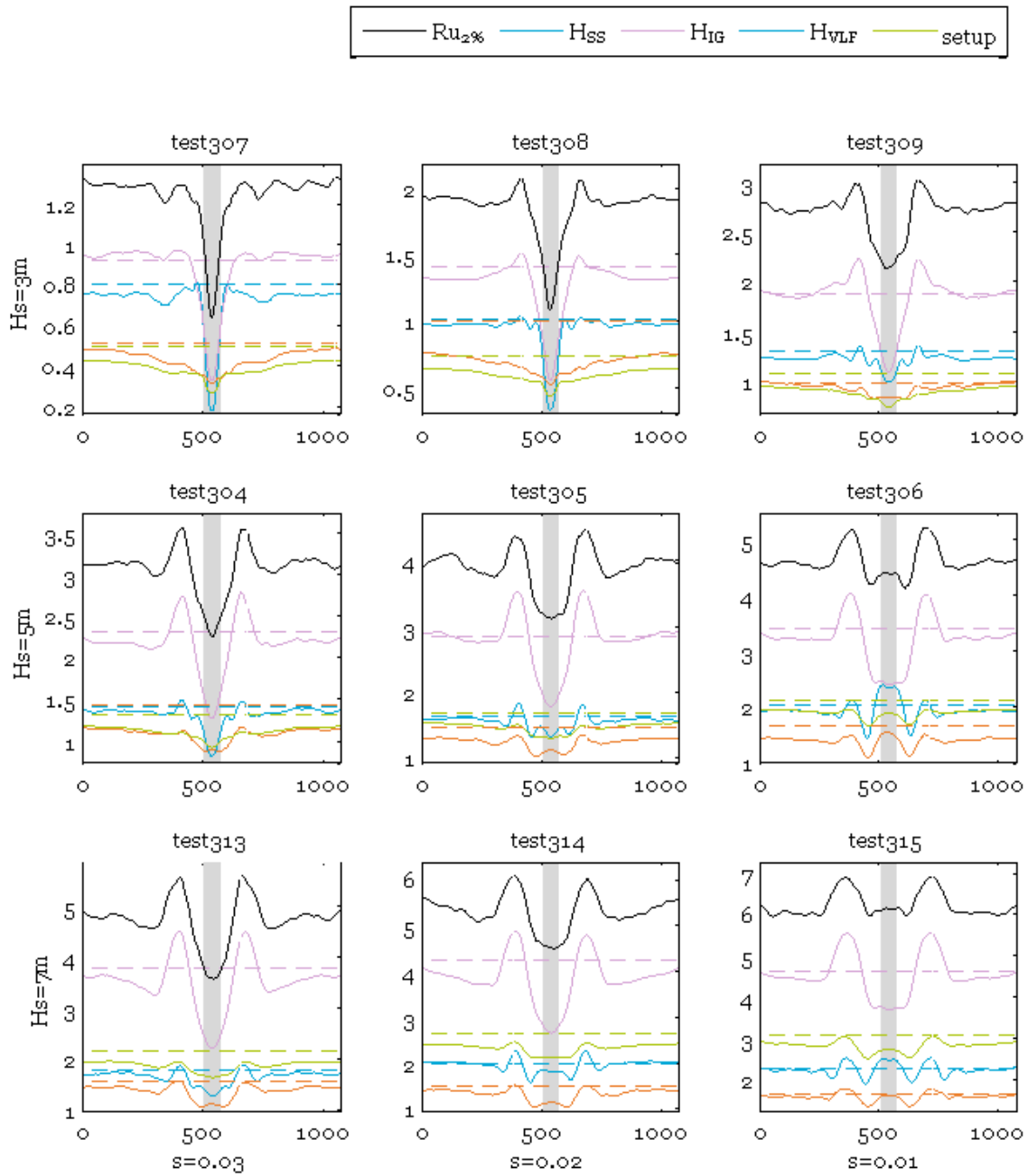
Appendix F.

CONTRIBUTIONS OF FREQUENCY COMPONENTS TO RUNUP, OVERVIEW PER GEOMETRY

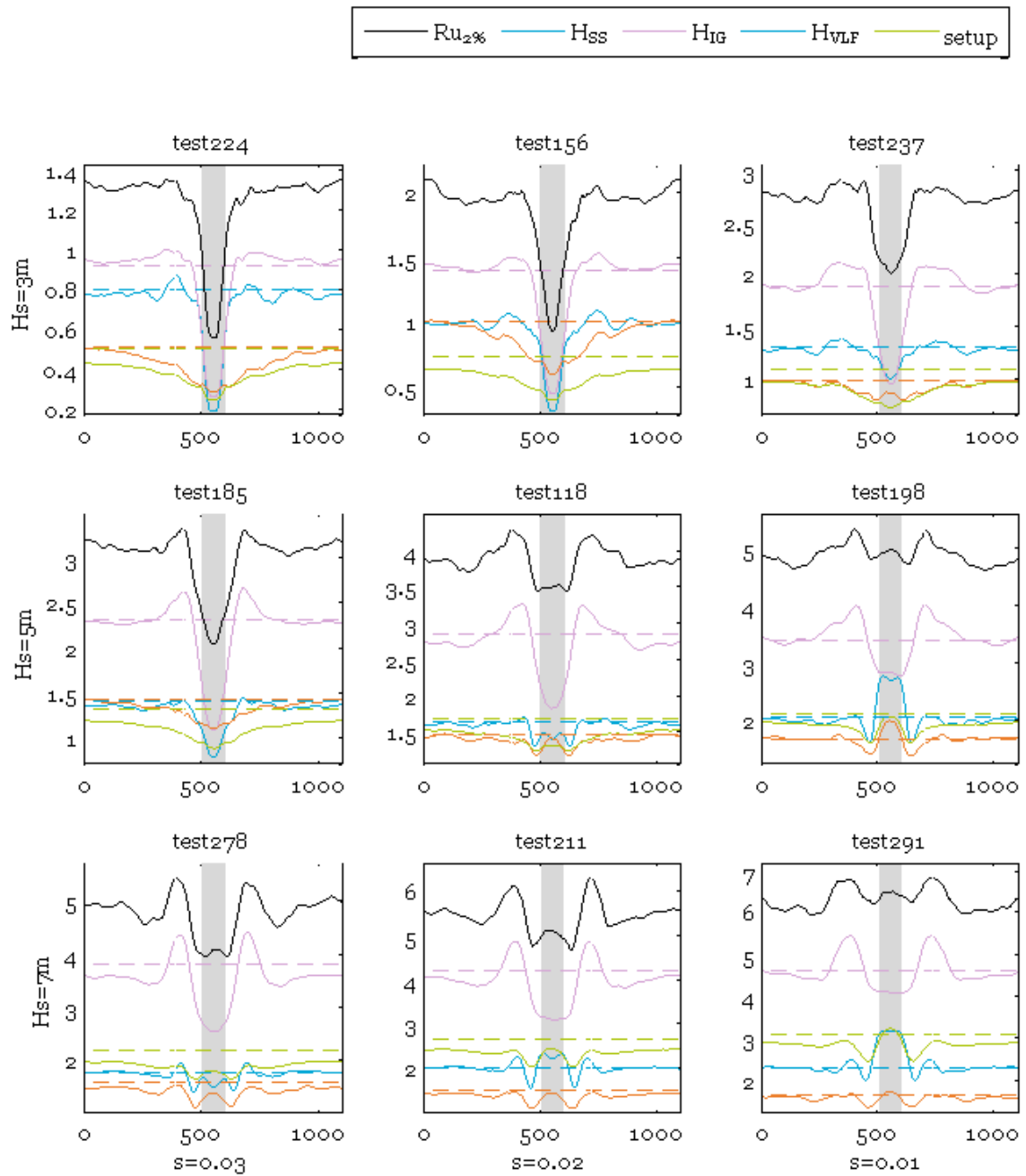
Runup by frequency components, Geometry1:
 $W_r=300m$, $W_c=50m$, $spacing=1000m$



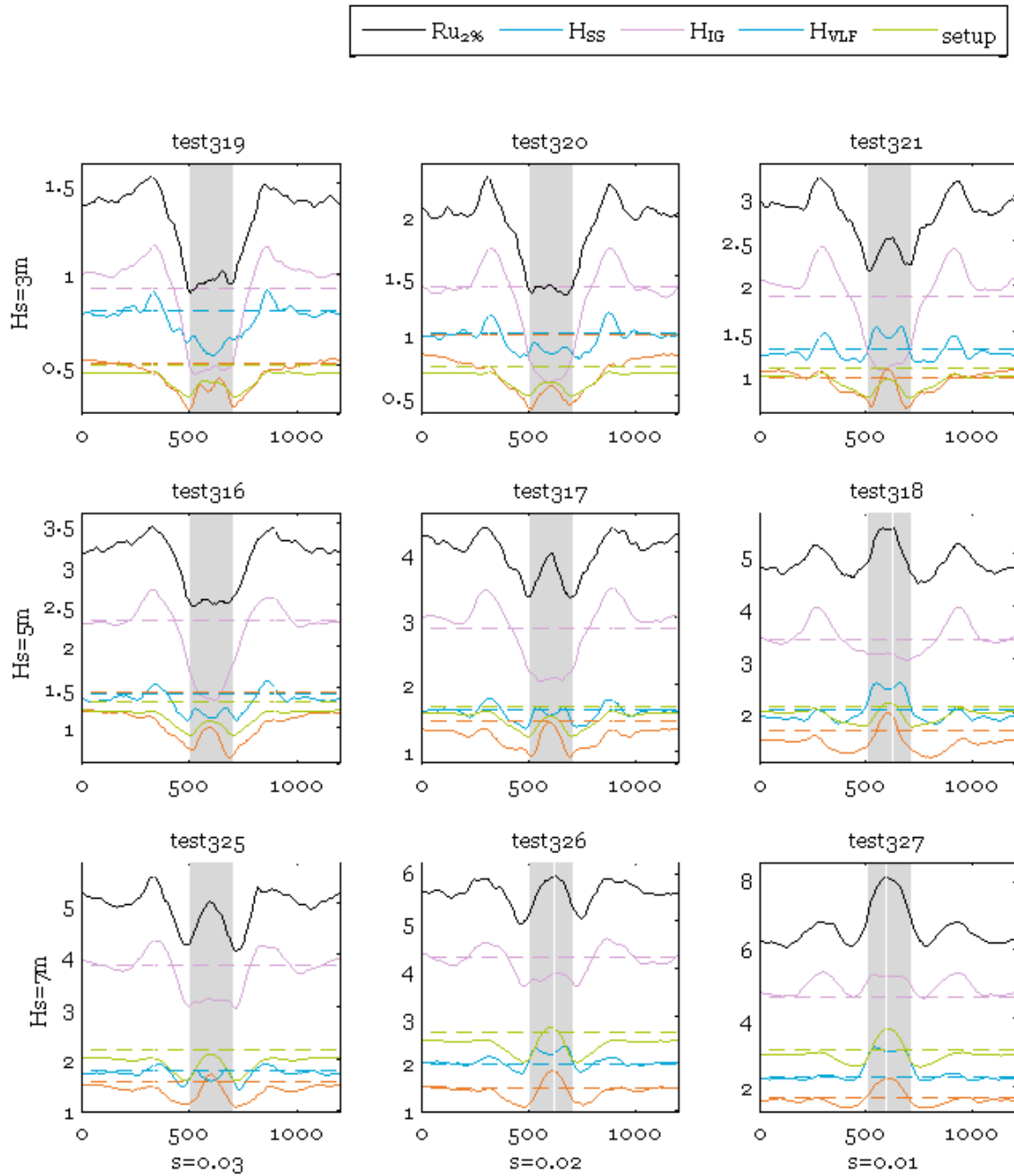
Runup by frequency components, Geometry2:
 $W_r=300m$, $W_c=70m$, spacing = $1000m$



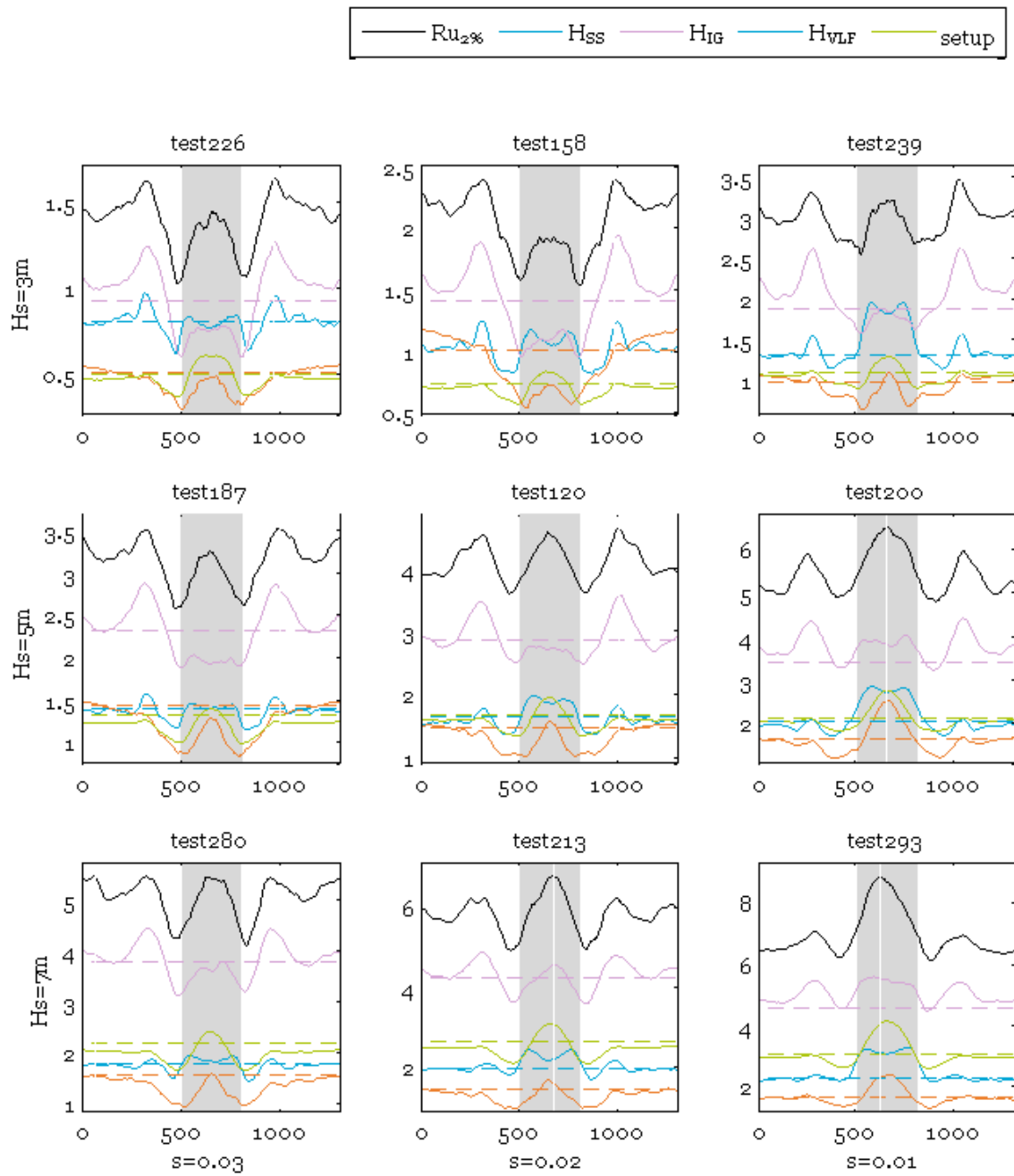
Runup by frequency components, Geometry 3:
 $W_r=300m$, $W_c=100m$, spacing = $1000m$



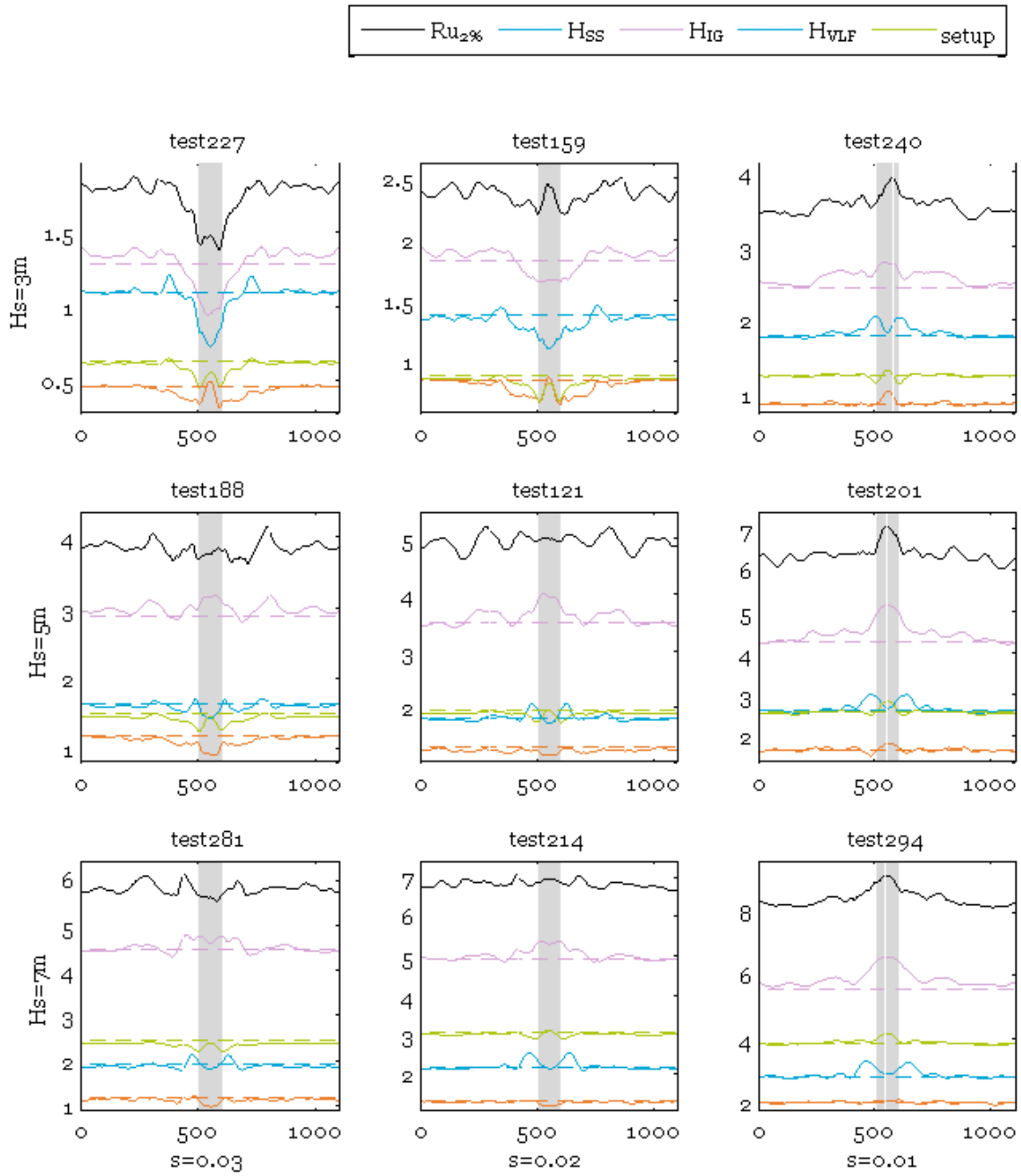
Runup by frequency components, Geometry 4:
 $W_r=300m$, $W_c=200m$, $spacing=1000m$



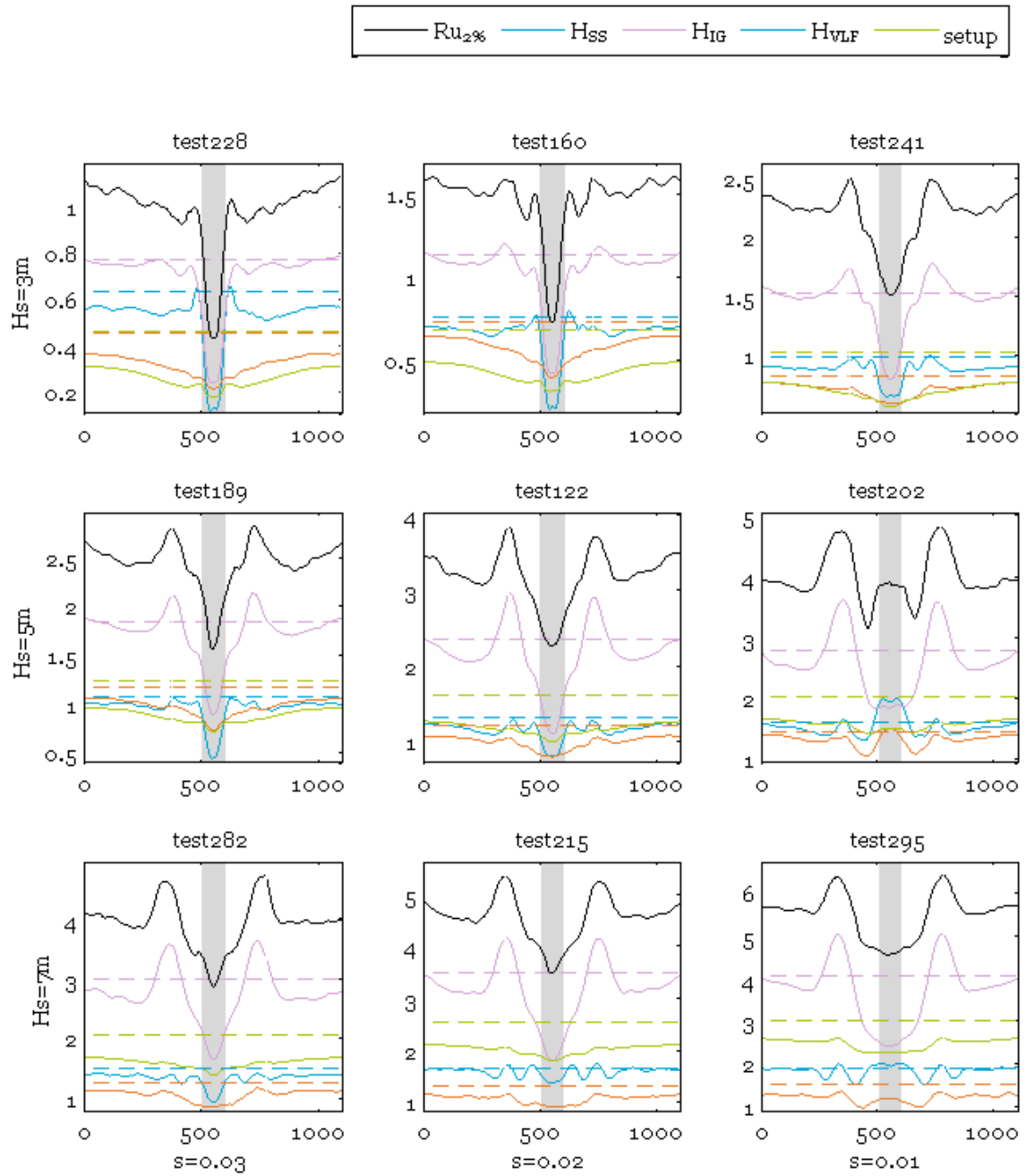
Runup by frequency components, Geometry 5:
 $W_r=300m$, $W_c=300m$, spacing = $1000m$



Runup by frequency components, Geometry6:
 $W_r=100m$, $W_c=100m$, $spacing=1000m$

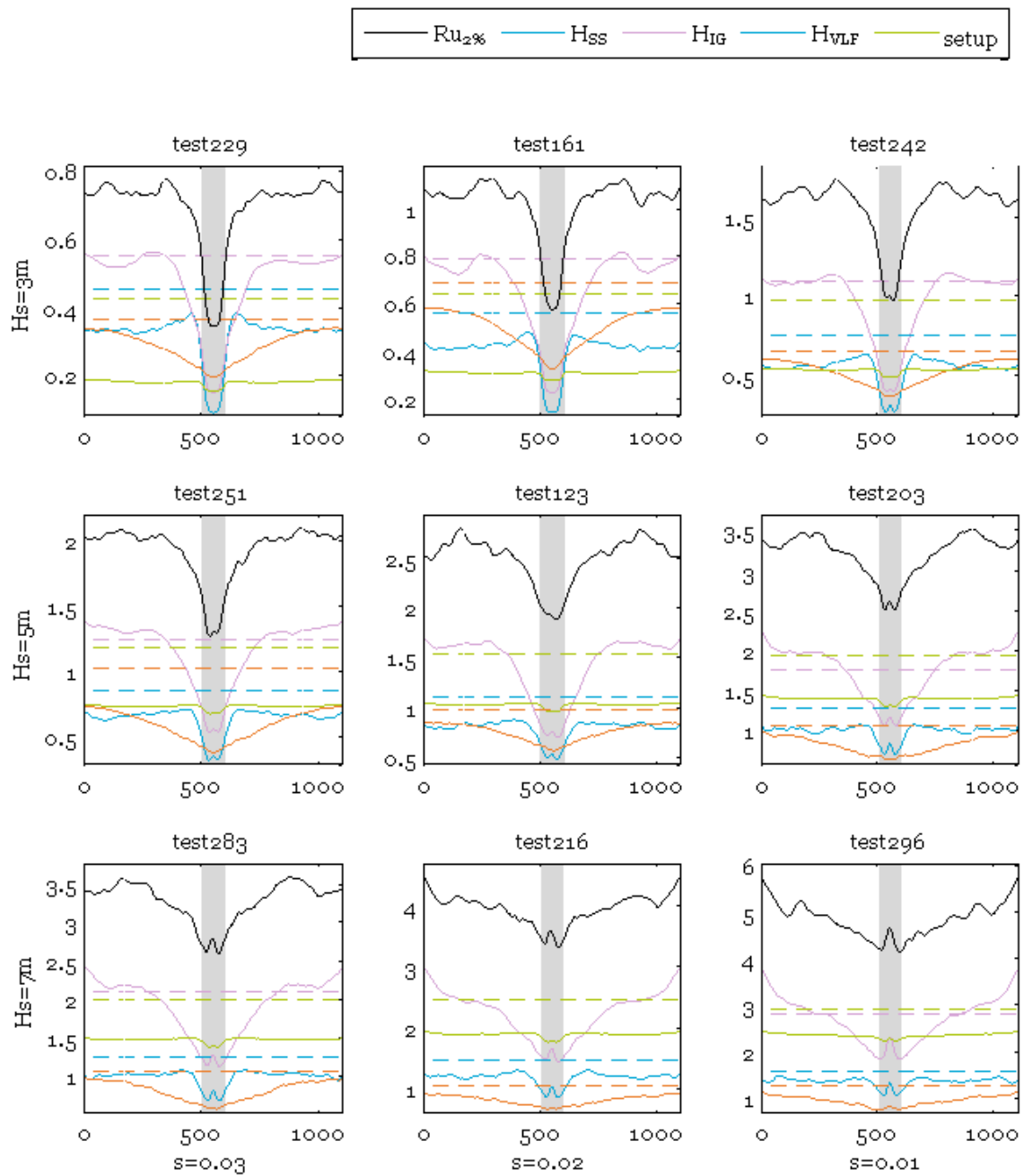


Runup by frequency components, Geometry 7:
 $W_r=500m$, $W_c=100m$, spacing = $1000m$

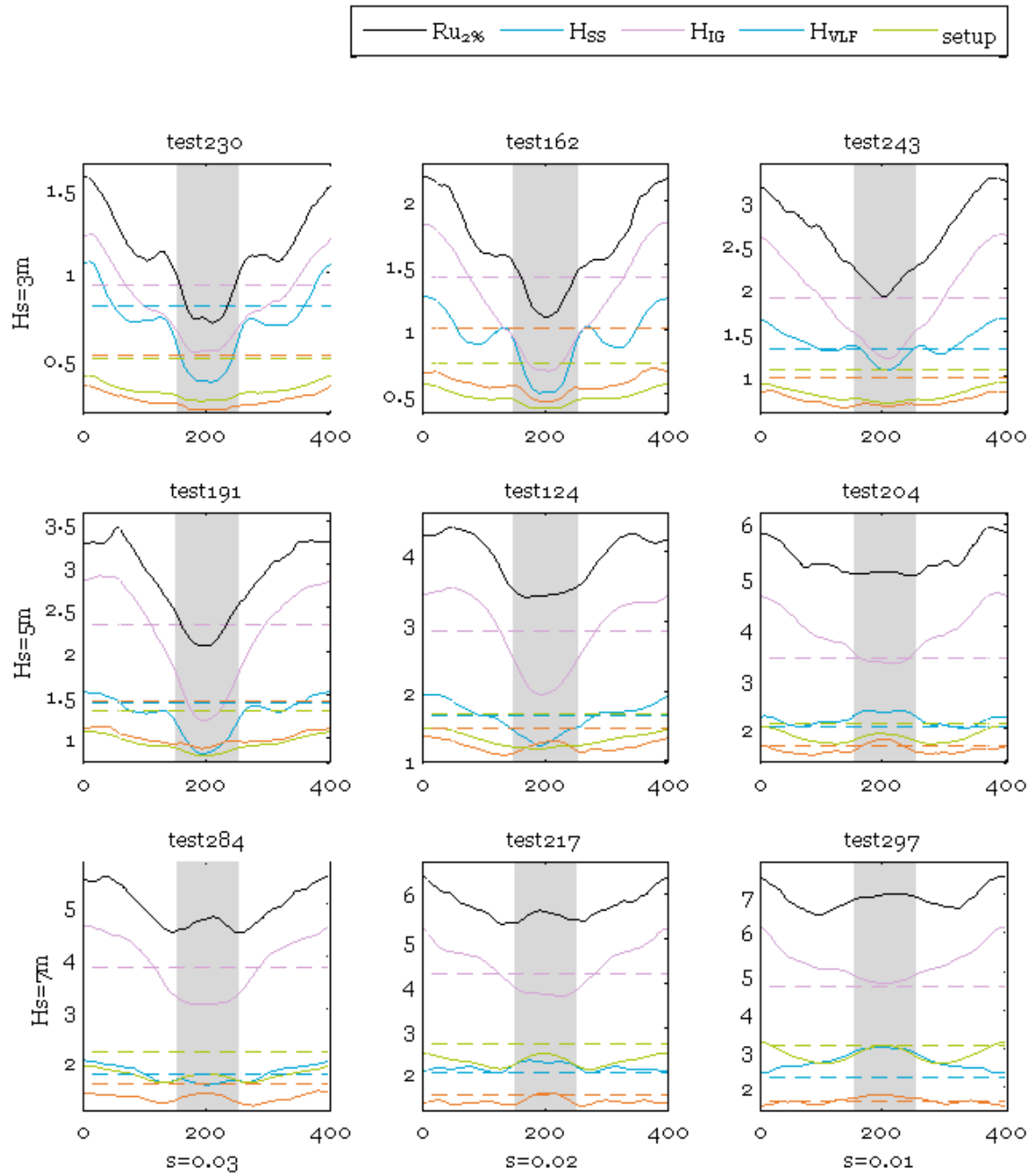


Runup by frequency components, Geometry8:

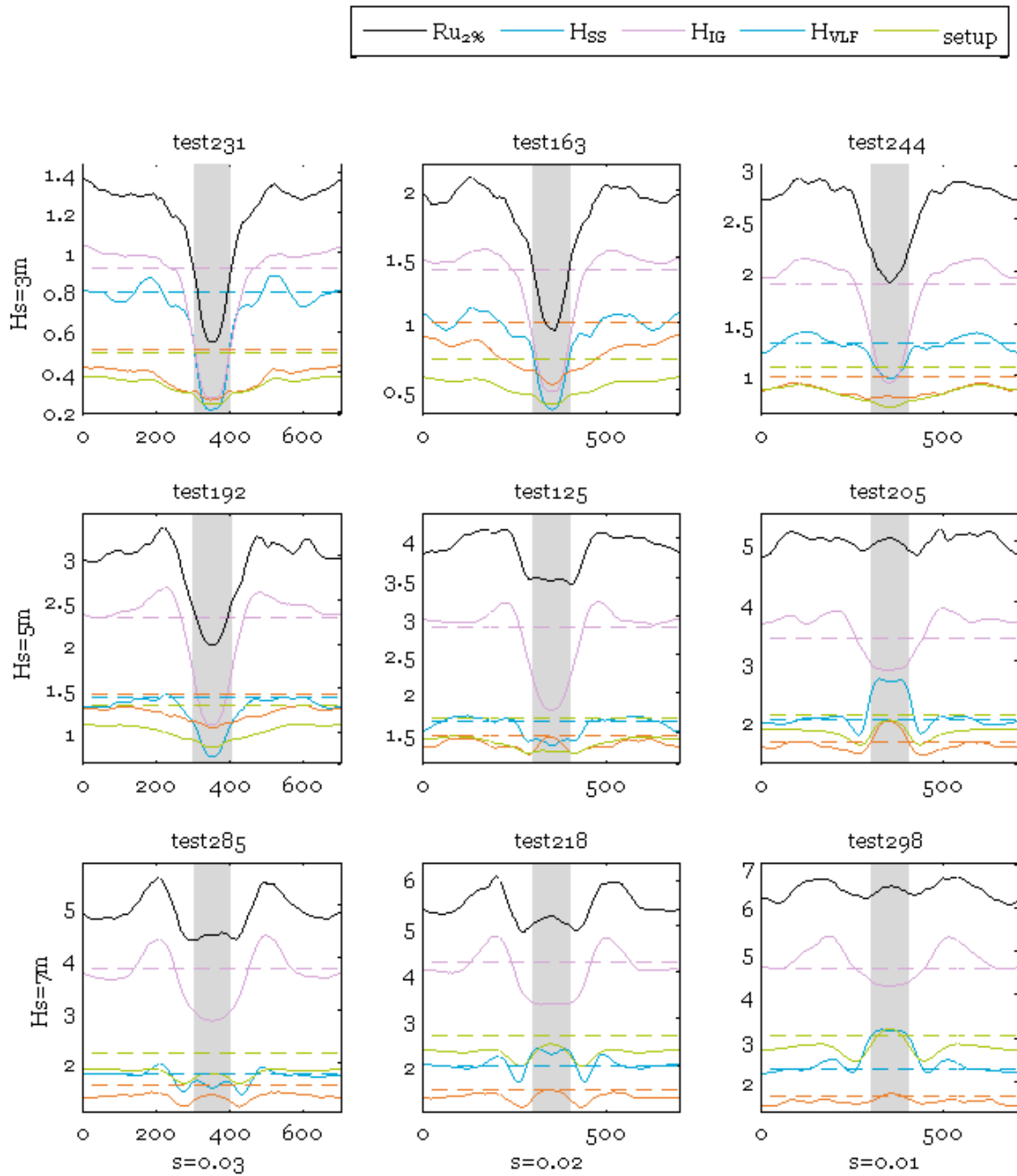
Wr=1000m, Wc=100m, spacing =1000m



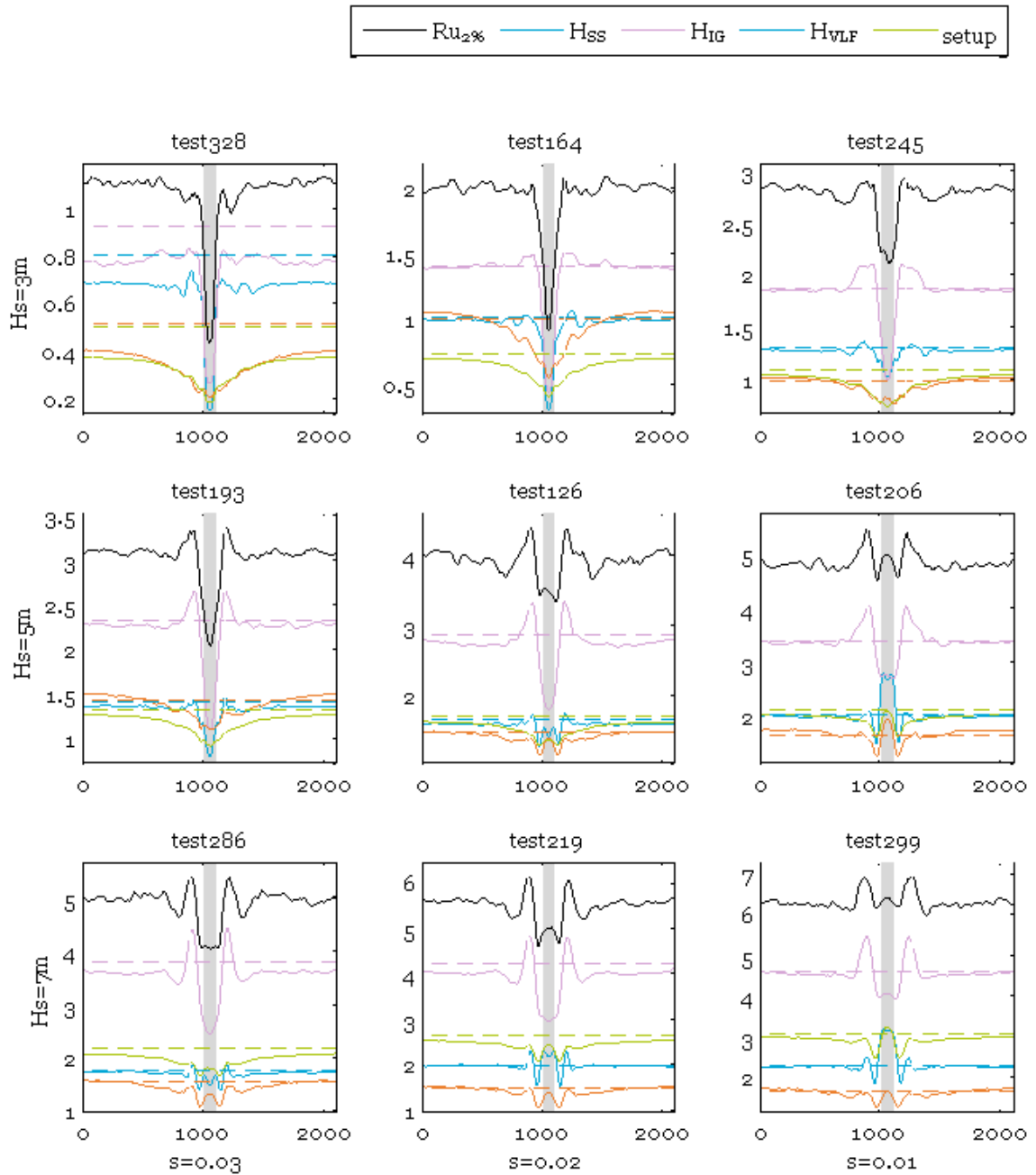
Runup by frequency components, Geometry9:
 $W_r=300m$, $W_c=100m$, $spacing=300m$



Runup by frequency components, Geometry10:
 $W_r=300m$, $W_c=100m$, $spacing=600m$

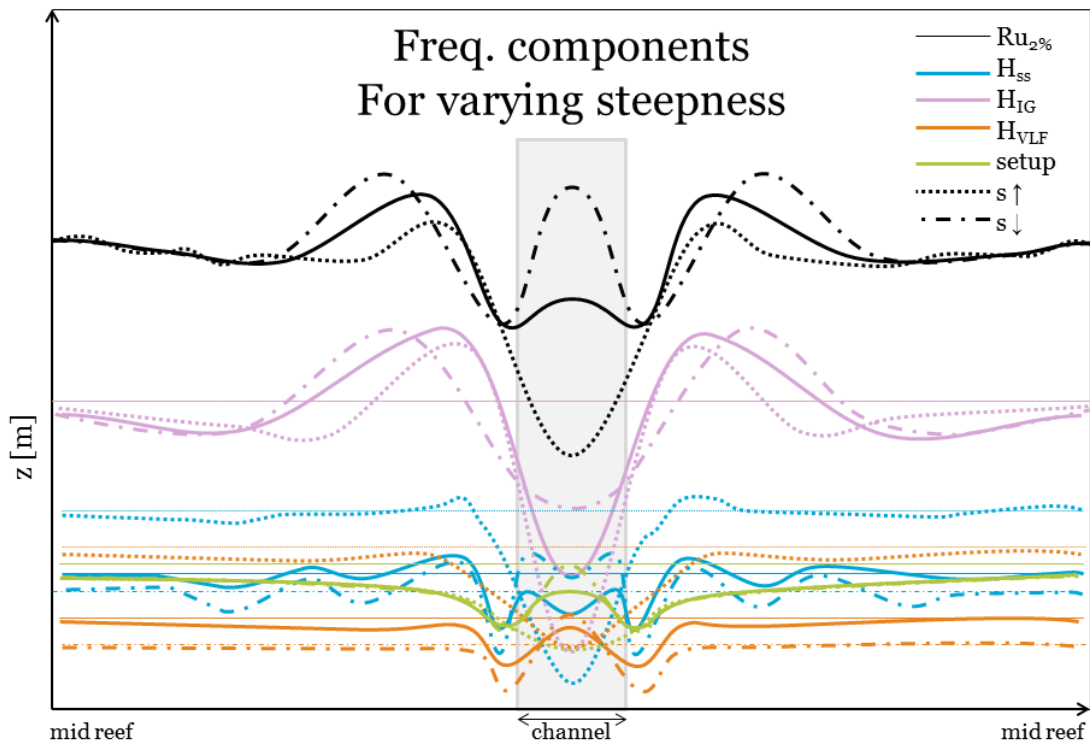
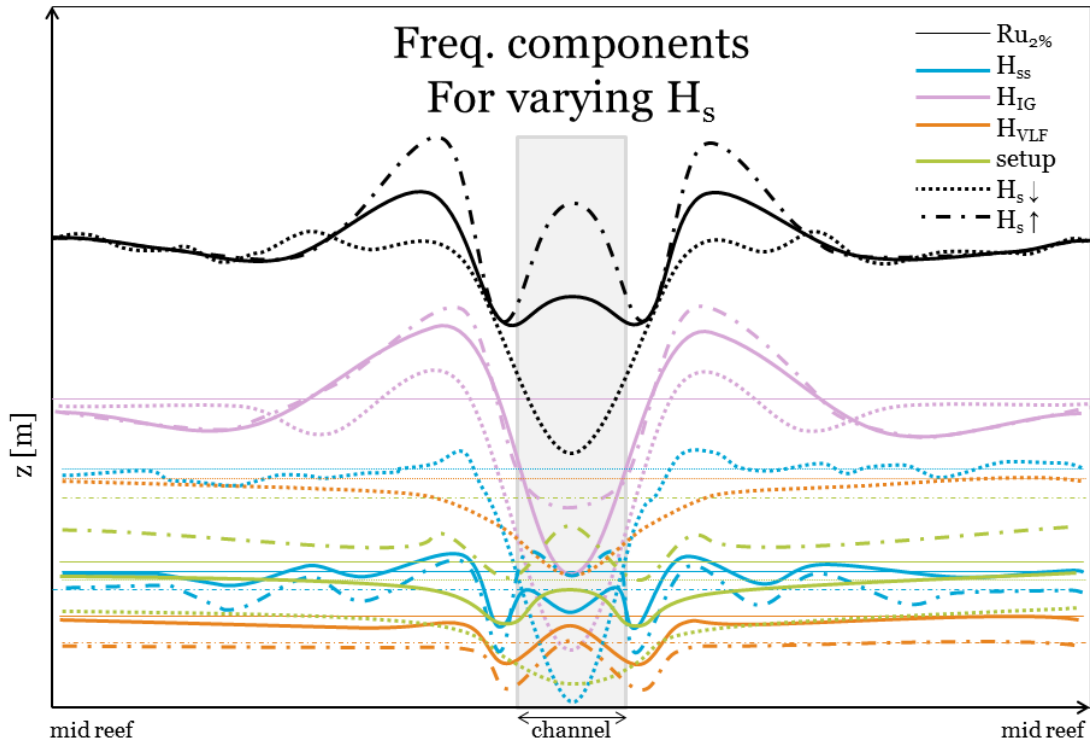


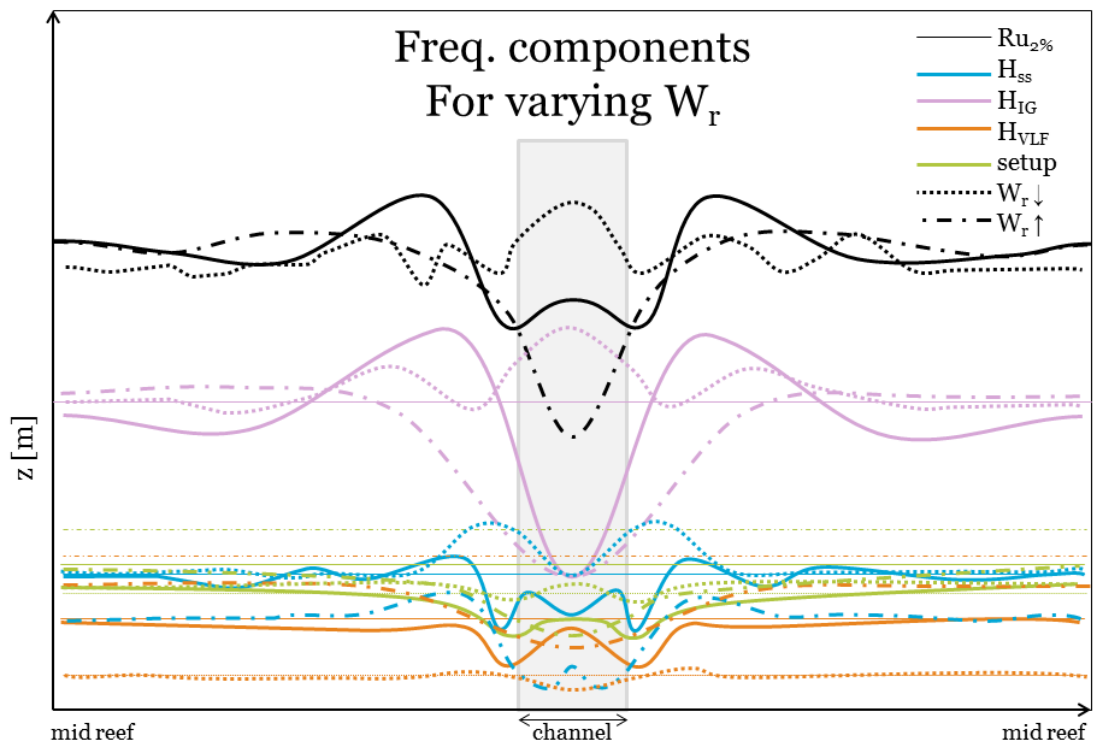
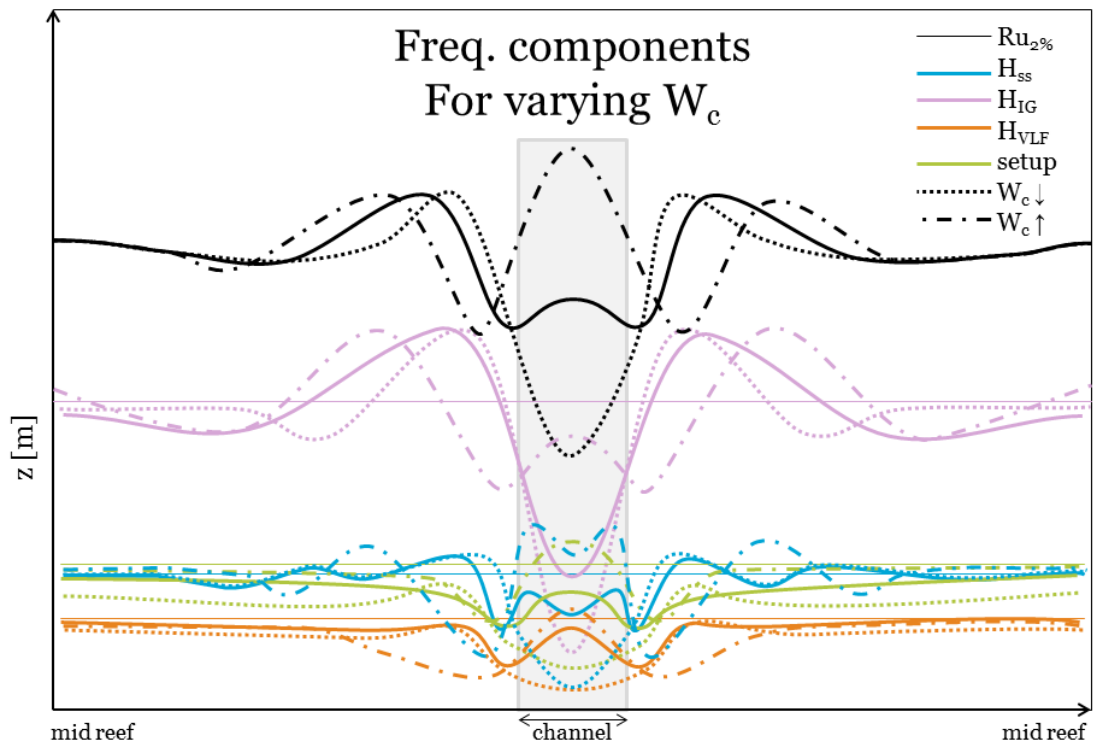
Runup by frequency components, Geometry11:
 $W_r=300m$, $W_c=100m$, $spacing=2000m$

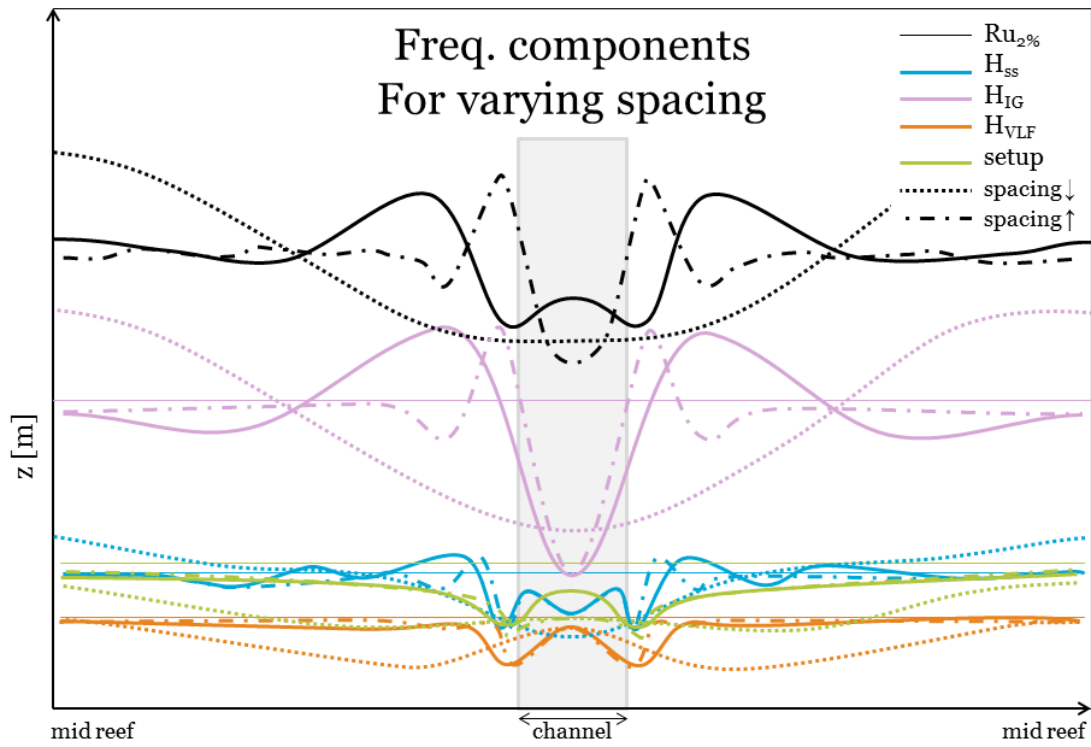


Appendix G. CONCEPTUAL FIGURES OF THE IMPACT OF INPUT PARAMETERS TO FREQUENCY COMPONENTS OF RUNUP

Impact of single input parameter on all freq. components

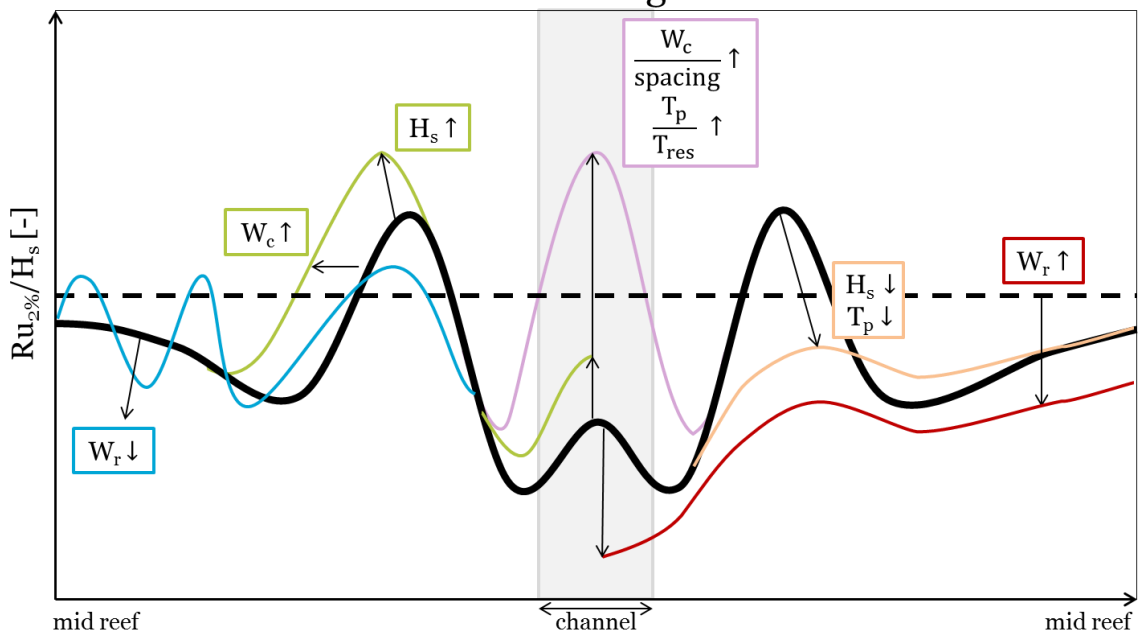




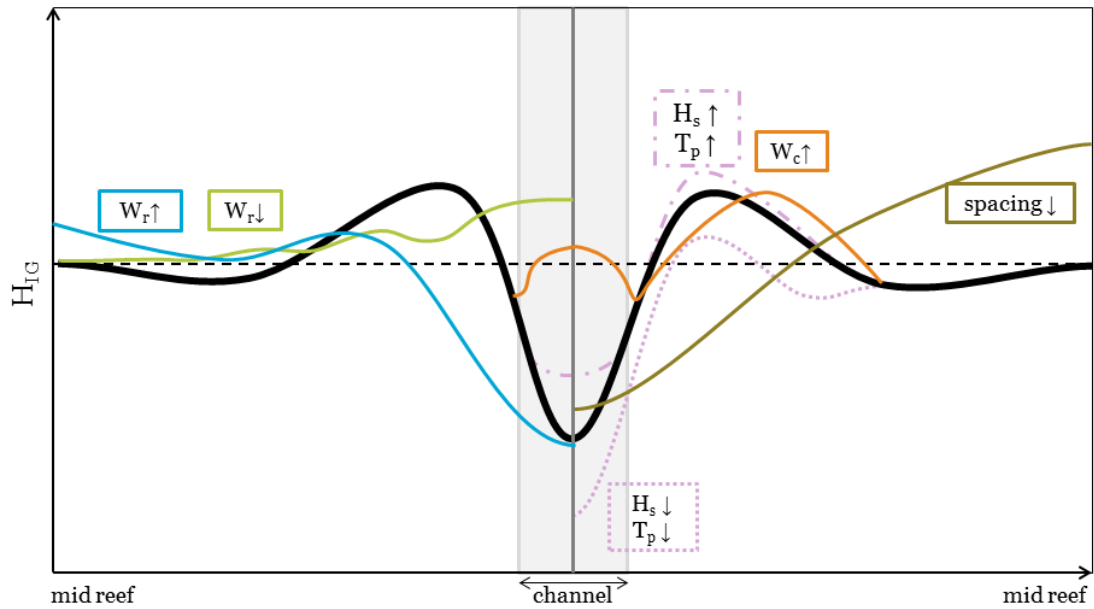


Impact of all input parameters on single frequency component

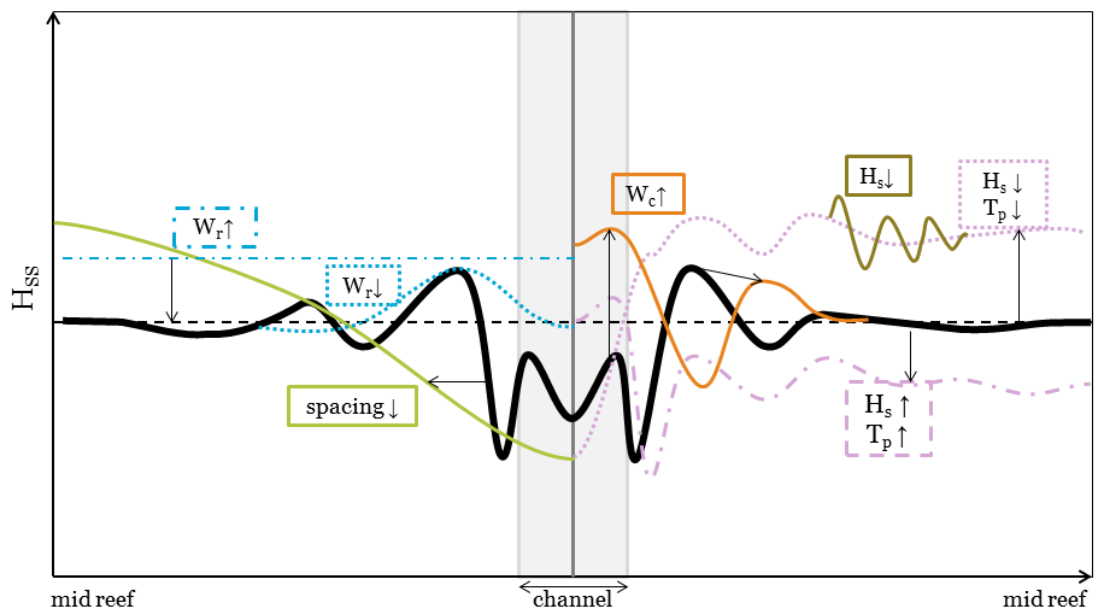
Overview of runup pattern for variations in geometry and forcing



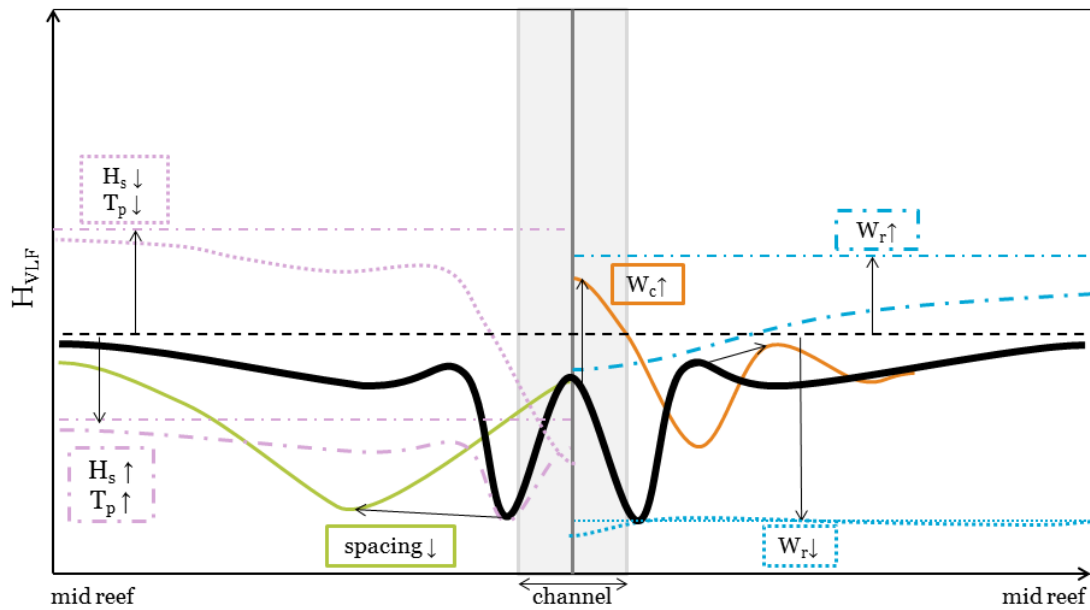
Overview of IG contribution to runup for variations in geometry and forcing



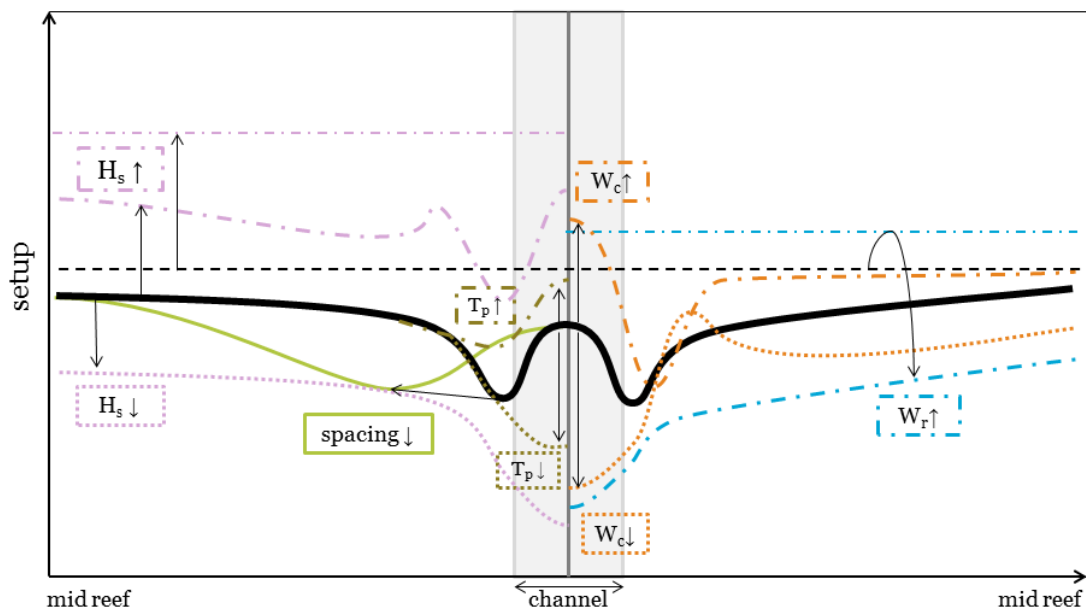
Overview of SS contribution to runup for variations in geometry and forcing



Overview of VLF contribution to runup for variations in geometry and forcing

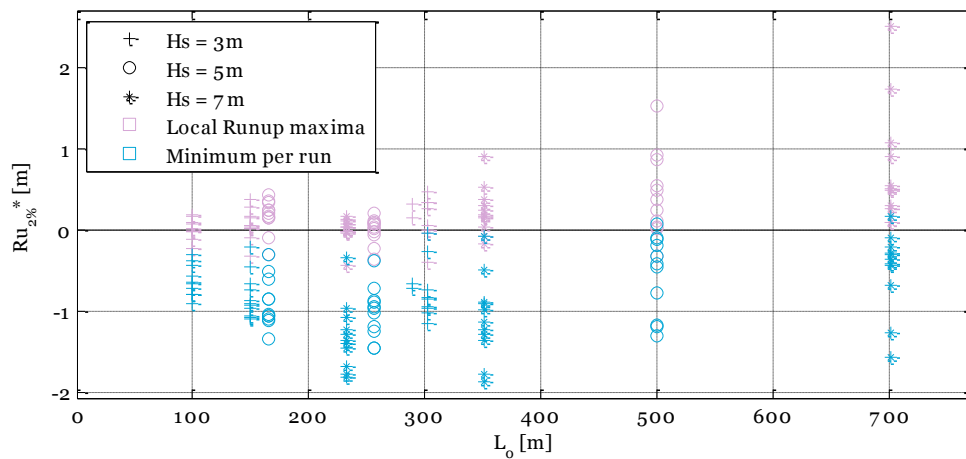
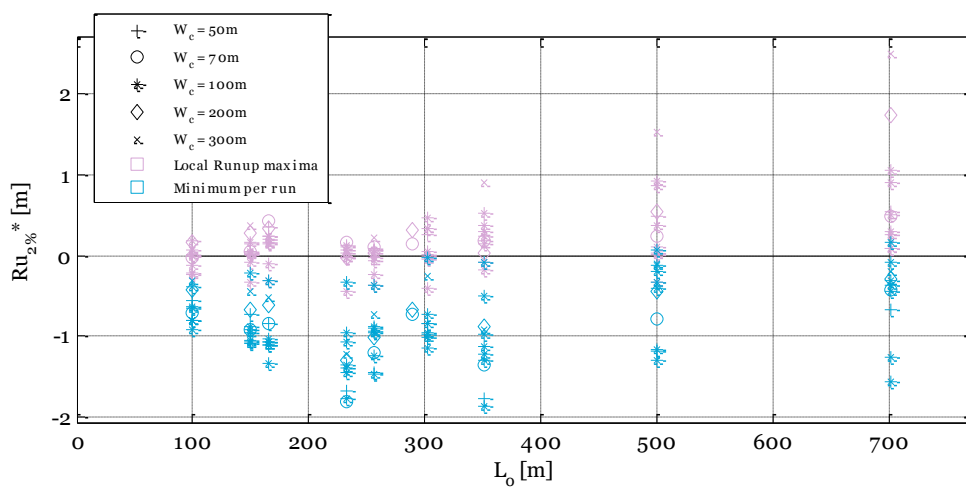
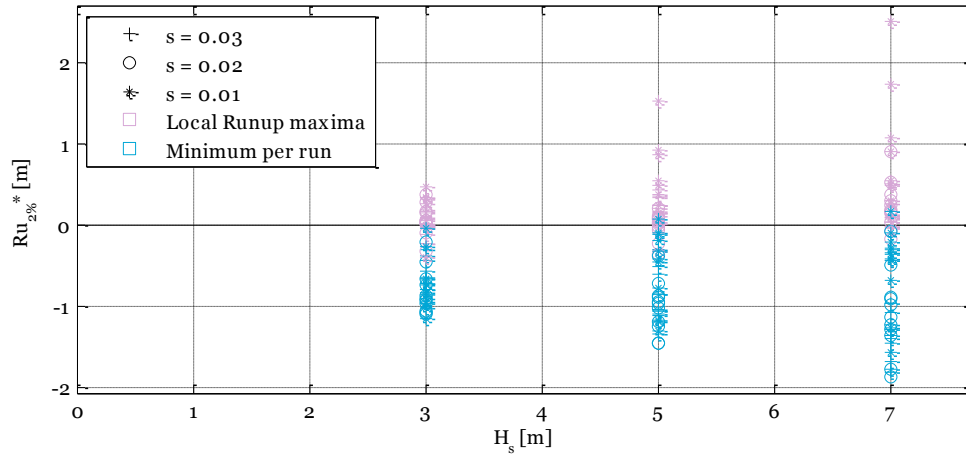


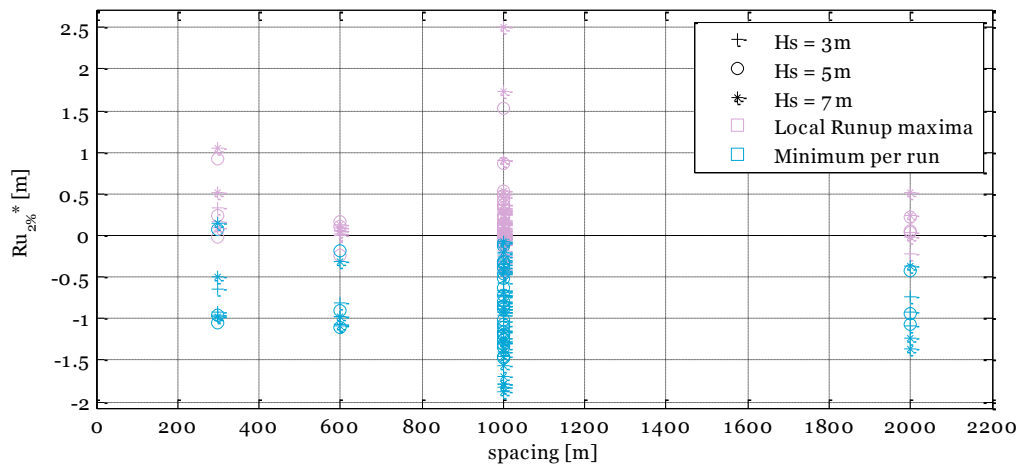
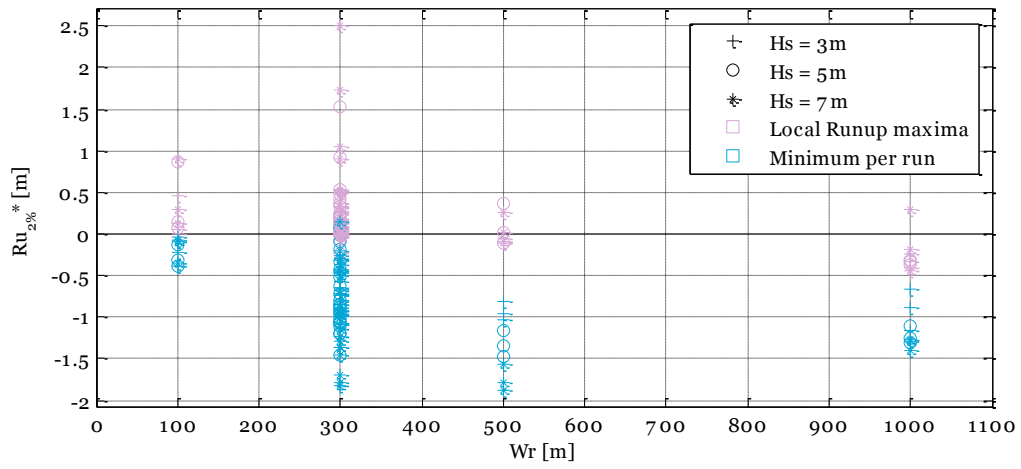
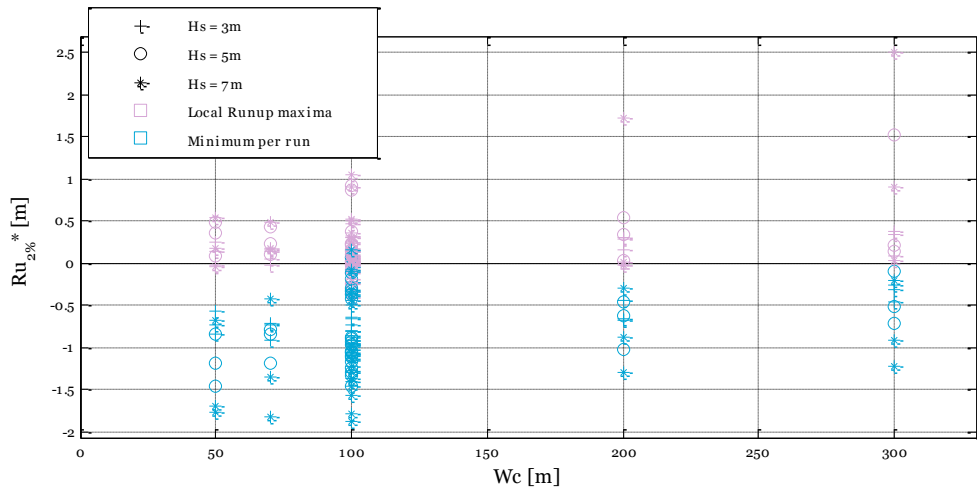
Overview of setup contribution to runup for variations in geometry and forcing



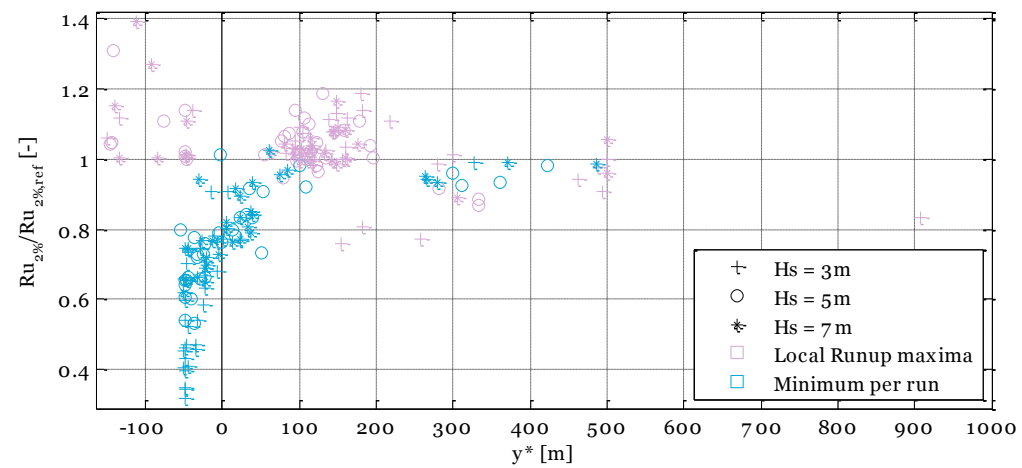
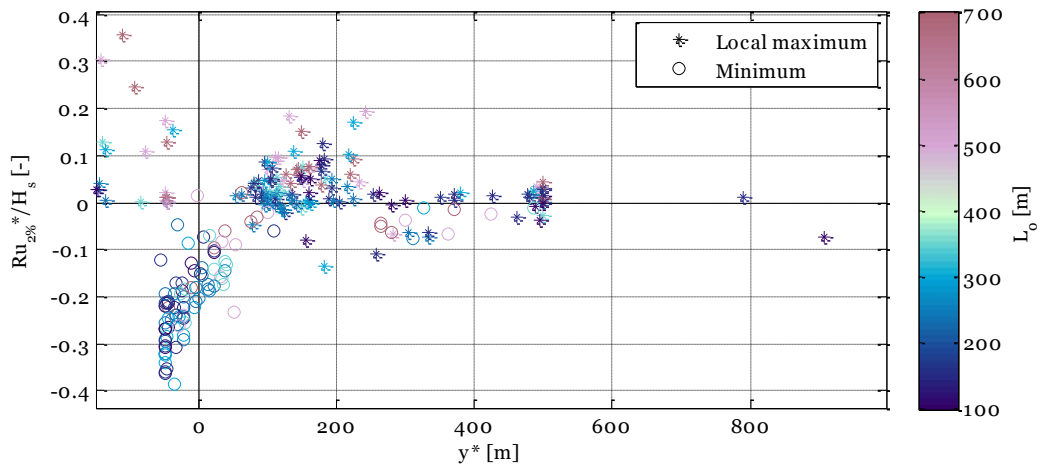
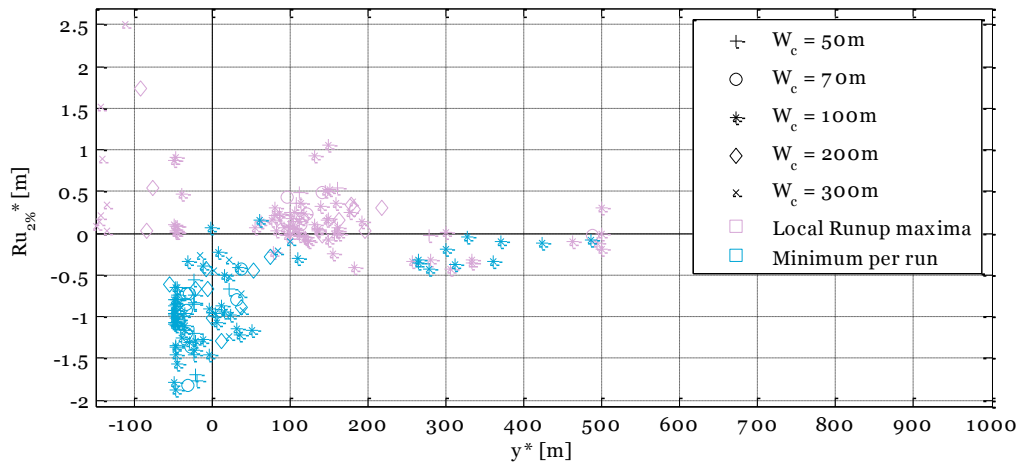
Appendix H. RUNUP SCATTERPLOTS

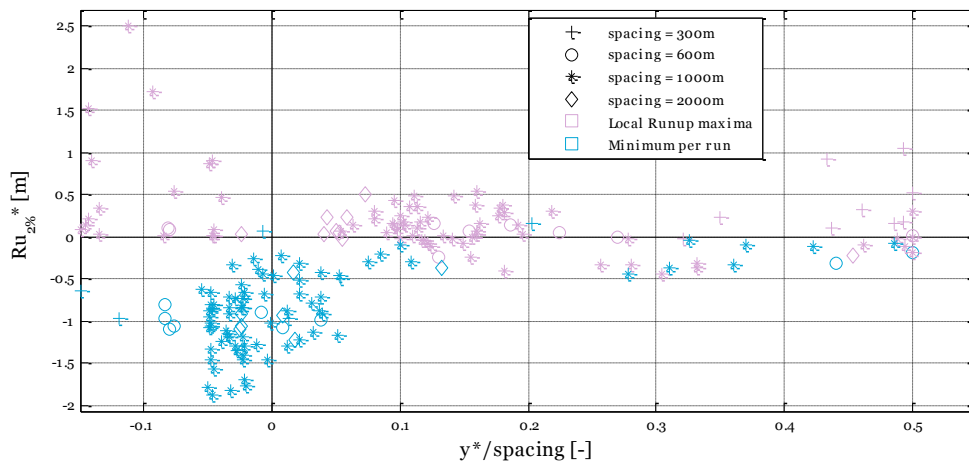
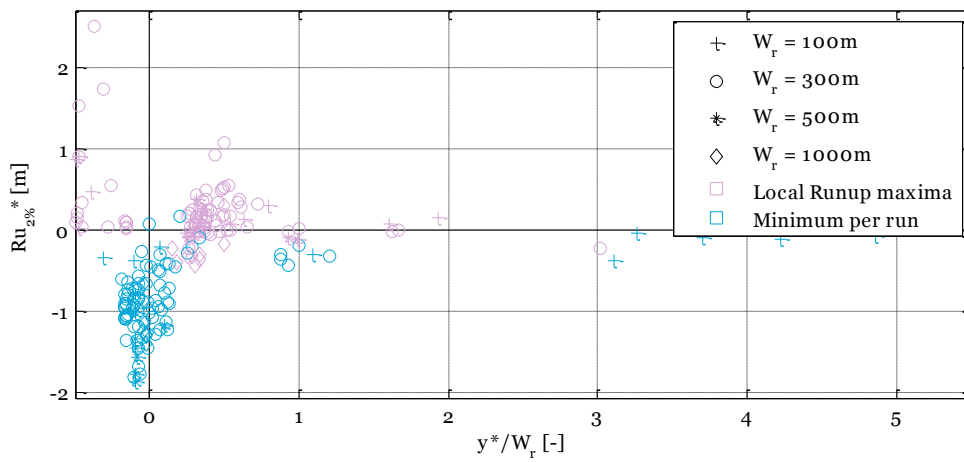
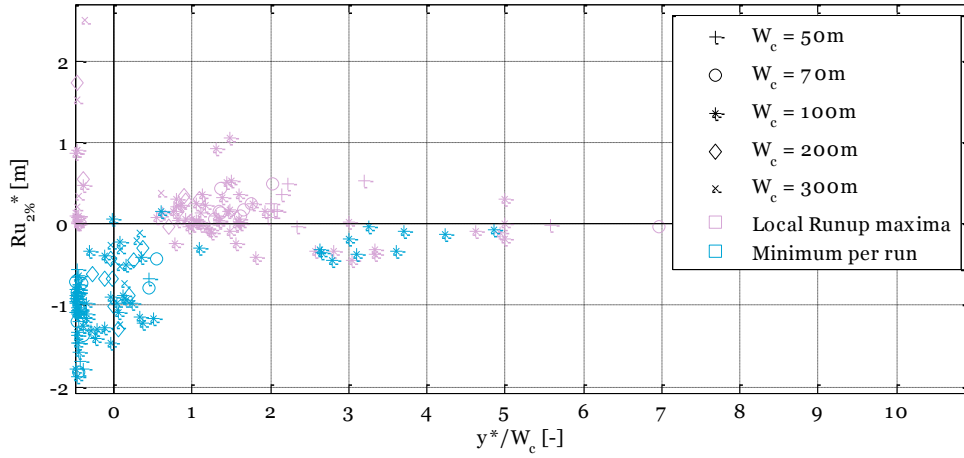
Runup versus input parameters

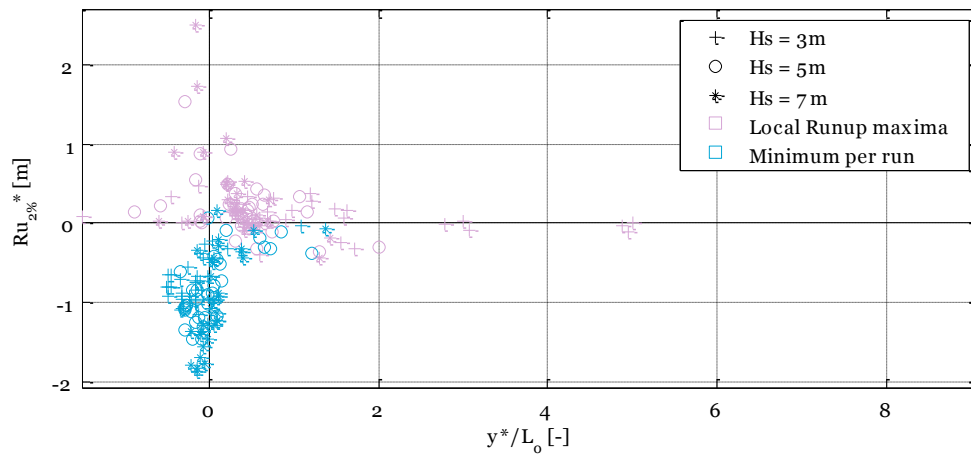




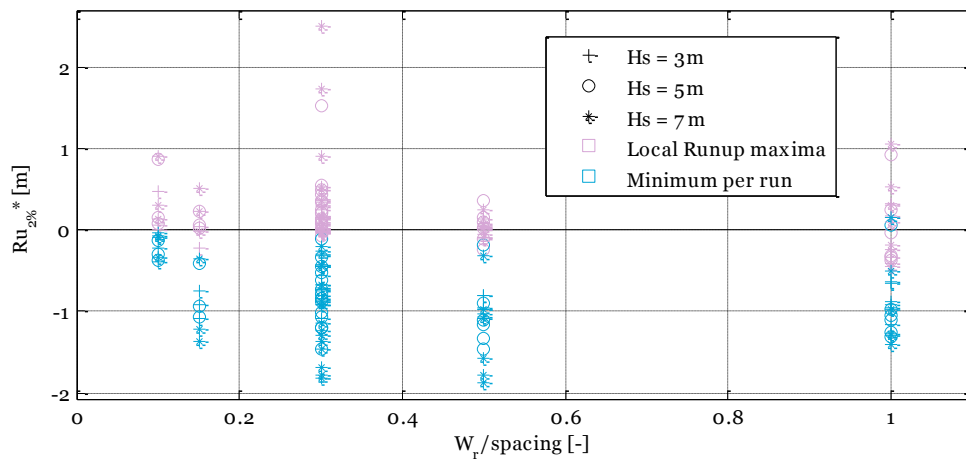
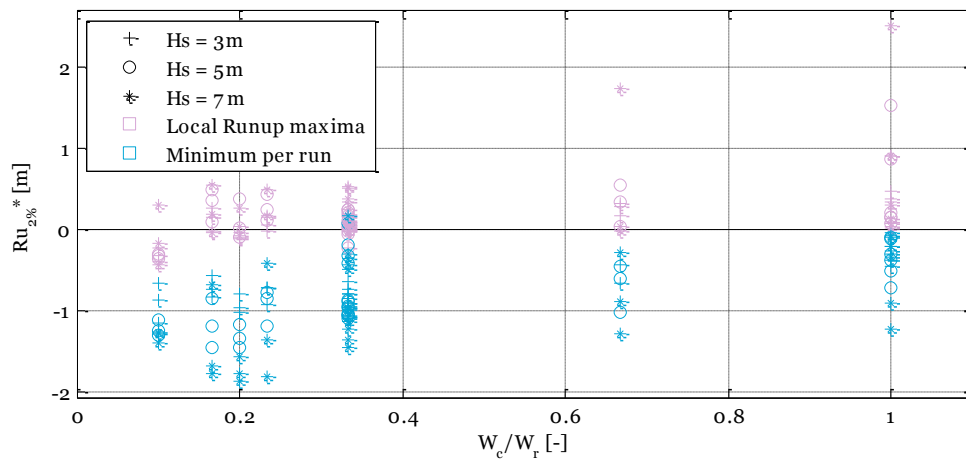
Runup versus (dimensionless) location

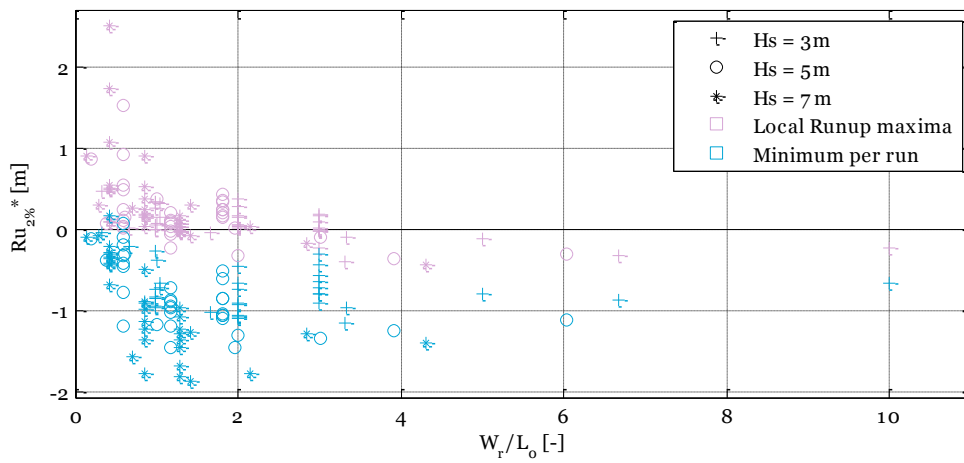
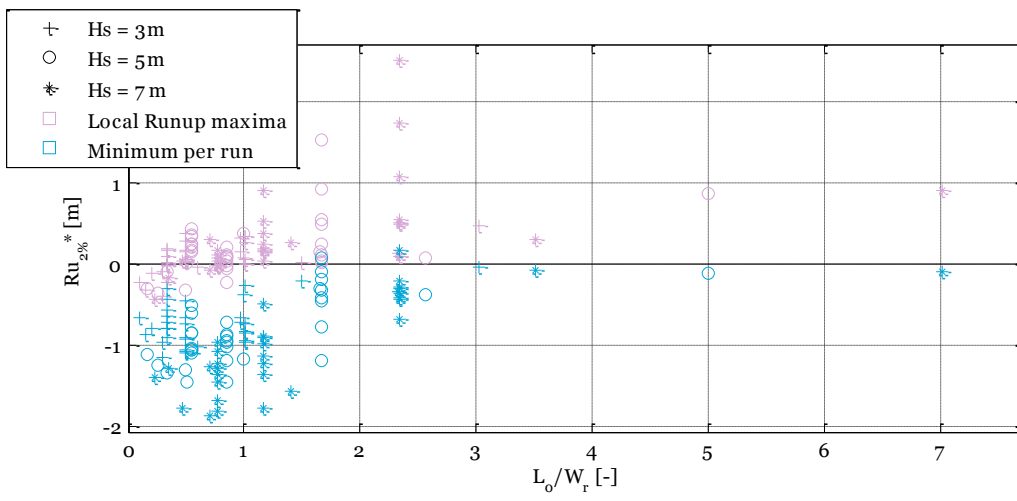
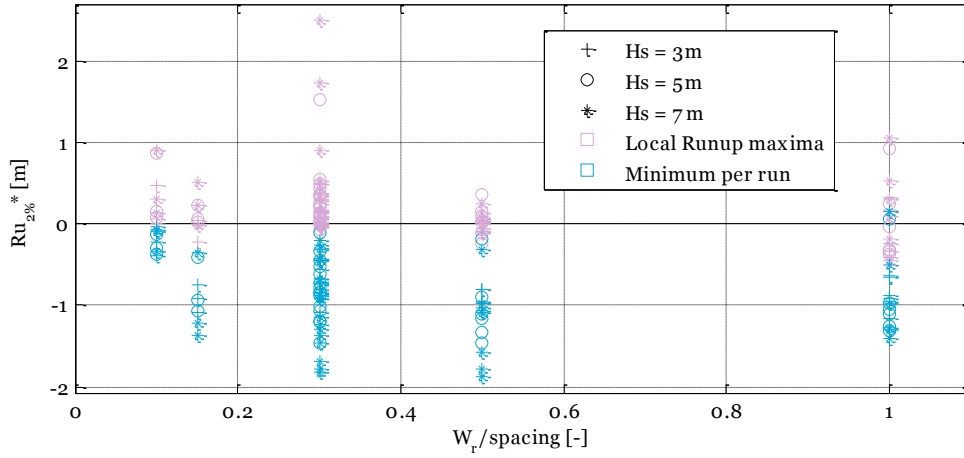


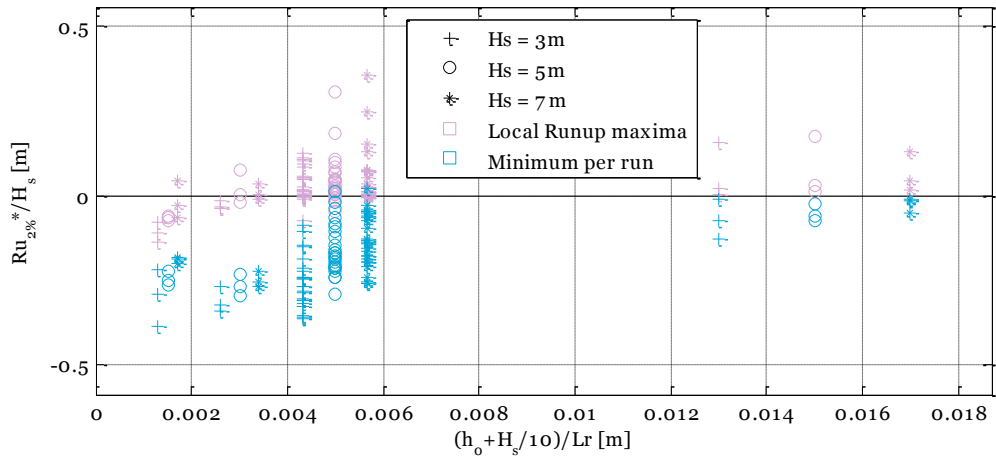




Runup versus other dimensionless parameters







Ru_{2%}* at mid reef for all input parameters

Ru_{2%}* at mid reef for different input parameters

